Functional and evolutionary constraints of *wtf* killer meiotic drivers

Authors:
Ananya Nidamangala Srinivasa[1,2], Samuel Campbell[1], Shriram Venkatesan[1], Nicole L. Nuckolls[1], Jeffrey J. Lange[1], Randal Halfmann[1,2], SaraH Zanders*[1,2]

[1]Stowers Institute for Medical Research, Kansas City, Missouri, United States of America
[2]Department of Cell Biology and Physiology, University of Kansas Medical Center, Kansas City, Kansas, United States of America

*Corresponding Author
Email: sez@stowers.org

Abstract

Killer meiotic drivers are selfish DNA loci that sabotage the gametes that do not inherit them from a driver+/driver- heterozygote. These drivers often employ toxic proteins that target essential cellular functions to cause the destruction of driver- gametes. Identifying the mechanisms of drivers can expand our understanding of infertility and reveal novel insights about the cellular functions targeted by drivers. In this work, we explore the molecular mechanisms underlying the *wtf* family of killer meiotic drivers found in fission yeasts. Each *wtf* killer acts using a toxic Wtf^{poison} protein that can be neutralized by a corresponding $Wtf^{antidote}$ protein. The *wtf* genes are rapidly evolving and extremely diverse. Here we found that self-assembly of Wtf^{poison} proteins is broadly conserved and associated with toxicity across the gene family, despite minimal amino acid conservation. In addition, we found the toxicity of Wtf^{poison} assemblies can be modulated by protein tags designed to increase or decrease the extent of the Wtf^{poison} assembly, implicating assembly size in toxicity. We also identified a conserved, critical role for the specific co-assembly of the Wtf^{poison} and $Wtf^{antidote}$ proteins in promoting effective neutralization of Wtf^{poison} toxicity. Finally, we engineered *wtf* alleles that encode toxic Wtf^{poison} proteins that are not effectively neutralized by their corresponding $Wtf^{antidote}$ proteins. The possibility of such self-destructive alleles reveals functional constraints on *wtf* evolution and suggests similar alleles could be cryptic contributors to infertility in fission yeast populations. As rapidly evolving killer meiotic drivers are widespread in eukaryotes, analogous self-killing drive alleles could contribute to sporadic infertility in many lineages.

Introduction

Genomes often contain selfish DNA sequences that persist by promoting their own propagation into the next generation without providing an overall fitness benefit to the organism [1,2]. Killer meiotic drivers are one such class of selfish sequences that act by preferentially destroying gametes that do not inherit the driver from a heterozygote [3]. This gamete destruction leads to biased, or sometimes, complete transmission of the driver+ genotype from driver+/driver-

heterozygotes. Killer meiotic drive systems generally decrease the fitness of the organism carrying the driver, both through their killing activities and through indirect mechanisms [4].

Distinct killer meiotic drive systems have repeatedly evolved in eukaryotes and drivers found in distinct species are generally not homologous [3,5–12]. Despite this, killer meiotic drivers fall into a limited number of mechanistic classes with shared themes [3,13,14]. Additionally, unrelated killer meiotic drivers have recurrently exploited conserved facets of cell physiology. This has enabled study of the killing and/or rescue activities of drive proteins outside of their endogenous species [5,11,15,16]. Overall, drivers represent unique tools that can be used to discover novel, unexpected insights into the exploited biological processes.

The *wtf* genes are a family of extremely diverse, rapidly evolving killer meiotic drivers found in multiple copies in most *Schizosaccharomyces* (fission yeast) species [17–22]. The *wtf* driver genes each produce a Wtf^{poison} and a $Wtf^{antidote}$ protein using distinct transcripts with overlapping coding sequences (Fig 1A) [15,17,23]. The amino acid sequences of the two proteins are largely identical, except the $Wtf^{antidote}$ proteins have an additional N-terminal domain of about 45 amino acids not found in the Wtf^{poison} (Fig 1A). All four developing spores (products of meiosis) are exposed to the Wtf^{poison}, but spores that inherit a compatible $Wtf^{antidote}$ can neutralize the poison and survive [22].

Little is known about the mechanism of toxicity of the Wtf^{poison} proteins. The general mechanism used by $Wtf^{antidote}$ proteins is better understood. The antidote-specific N-terminal domain is the most conserved region and includes targeting motifs (PY motifs) that are recognized by Rsp5/NEDD4 ubiquitin ligases which route the protein through the trans Golgi network to endosomes and, ultimately, to the vacuole (fungal lysosome; Fig 1B-C) [15,24]. When both proteins are present, the $Wtf^{antidote}$ co-assembles with the Wtf^{poison}, and the $Wtf^{antidote}$ thereby traffics the Wtf^{poison} to the vacuole [15,24]. This mechanism is similar to a non-homologous drive system recently described in rice, where an antidote protein rescues the driver+ gametes from a toxic poison protein by co-trafficking the poison to the autophagosome [5].

In general, the poison protein encoded by one *wtf* gene is not compatible with (i.e., neutralized by) the antidotes of widely diverged *wtf* genes [17,19,25]. However, Wtf^{poison} proteins can be neutralized by $Wtf^{antidote}$ proteins encoded at different loci if the sequences are identical or highly similar (outside of the antidote-specific N-terminal domain; Fig 1A) [17,22,24,26]. Although the

examples are limited, similarity at the C-termini of the Wtf poison and antidote proteins may be particularly important for compatibility [15,25,26]. For example, the *wtf18-2* allele encodes an antidote protein that neutralizes the poison produced by the *wtf13* driver. The Wtf18-2^{antidote} and Wtf13^{antidote} proteins are highly similar overall (82% amino acid identity) and identical at their C-termini. Interestingly, the antidote encoded by the reference allele of *wtf18* is not identical to Wtf13^{poison} at the C-terminus and does not neutralize it. In addition, changing two amino acids in the C-terminus of Wtf18-2^{antidote} (D366NN mutation) to make it more like the reference Wtf18^{antidote} abolishes the protein's ability to neutralize Wtf13^{poison} (Bravo Núñez et al., 2018). Still, the rules governing poison and antidote compatibility are largely unknown.

While it is clear that a functional *wtf* driver kills about half the spores produced by *wtf*+/*wtf*- heterozygotes, the full impacts of *wtf* gene evolution on the fitness of populations is not clear. Because the *wtf* genes encode the poison and antidote proteins on overlapping coding sequences (Fig 1A), novel poisons can emerge simultaneously with their corresponding antidotes via mutation. This has been observed with a limited number of engineered *wtf* alleles, and one can observe evidence of this divergence in the diversity of extant *wtf* alleles in natural populations [15,19–21,26]. The natural alleles, however, represent a selected population. Novel alleles that generate functional drivers are predicted to be favored by the self-selection enabled by drive, whereas alleles that generate a toxic poison without a compatible antidote would be expected to be self-killing and removed by natural selection.

Major questions remain about the mechanism(s) of Wtf^{poison} toxicity and about the rules of Wtf^{poison} and Wtf^{antidote} compatibility. Our working model is that the toxicity of Wtf^{poison} proteins is tied to their self-assembly [15]. This assembly, however, has only been conclusively demonstrated for the Wtf4 proteins, encoded by the *wtf4* gene from the isolate of *S. pombe* known as *kambucha*. For Wtf^{antidote} function, a working model is that a similar homotypic assembly with the Wtf^{poison} is required to establish a physical connection between the proteins so that the poison is shuttled to the vacuole along with a ubiquitinated antidote [15,24]. The ubiquitination and trafficking of the Wtf antidotes to the vacuole has been demonstrated to be conserved between widely diverged Wtf^{antidote} proteins [19,24]. However, it is not clear if antidote co-assembly with a poison has a functional role in poison neutralization, or if it merely provides a physical link between the proteins to facilitate co-trafficking. It is also unclear if changes in the coding sequence shared by the poison and antidote proteins of a given *wtf* can generate an

incompatible set of proteins, or if poisons will always be neutralized by sequence-matched antidotes.

To test these models and to better understand the amino acid sequences that support the Wtf protein functions, we analyzed a panel of natural and engineered Wtf proteins. We found that both well conserved and poorly conserved amino acid sequences can contribute to protein self-assembly and function. Our analyses revealed broad conservation of Wtf^{poison} self-assembly and suggest that assembly size can affect Wtf^{poison} toxicity, analogous to several other self-assembling toxic proteins [27–29]. In addition, we found that the specific co-assembly of the Wtf^{antidote} is required for efficient Wtf^{poison} neutralization via trafficking to the vacuole. Finally, our analyses identified multiple *wtf* alleles that generate poison proteins that are not neutralized by their corresponding antidotes. Such alleles would be self-destructive if they arose in nature. This work refines our understanding of Wtf protein functions with important evolutionary implications. More broadly, our observations offer insight into how functional conservation can be maintained despite extreme amino acid sequence divergence and extends our understanding of the limits of protein assembly trafficking mechanisms.

Results

Broad conservation of Wtf^{poison} protein self-assembly.

To test the models of Wtf protein functions and to understand how these functions could be supported by extremely diverse protein sequences (e.g., <20% amino acid identity), we generated a large panel of *wtf* variants that represent over 100 million years of divergence [19]. Twelve variants are wild-type or mutant alleles of *wtf* genes found in *S. octosporus*, *S. osmophilus* or *S. cryophilus* (S1 Fig A-D). One of these genes, *S. octosporus wtf25*, has been previously characterized and found to encode a functional meiotic driver in its endogenous species ([19]; S1 Table). Four additional genes (*S. cryophilus wtf1*, *S. osmophilus wtf19* and *wtf41*, and *S. octosporus wtf61*) have been shown to encode functional Wtf^{poison} and Wtf^{antidote} proteins in an ectopic *Saccharomyces cerevisiae* assay system ([19]; S1 Table). Finally, we assay a panel of new mutant alleles of the previously characterized *wtf4* gene from the *S. kambucha* isolate of *S. pombe* [15,22,23] (n=21; Fig 1 D).

Our model, based on Wtf4^{poison}, is that Wtf^{poison} toxicity is linked to the ability of a Wtf^{poison} to self-assemble [15]. To test this idea, we wanted to assay if Wtf^{poison} proteins that have greatly diverged from Wtf4 also self-assemble. To do this, we used the Distributed Amphifluoric FRET (DAmFRET) [15,30] approach, in which proteins are tagged with the photoconvertible mEos3.1 fluorophore (referred to as mEos hereafter) and expressed in *S. cerevisiae*. A uniform fraction of the green mEos population is photoconverted to its red form, and protein-protein interactions are then detected as FRET (Fluorescence Resonance Energy Transfer) between the green and red fluorophores within single cells. Monomeric mEos exhibits negligeble FRET and is used as a negative control (Fig 2A, B) [15,30]. The *S. cerevisiae* system used to study Wtf proteins is well established and reflects phenotypes observed in the endogenous fission yeast species [15,19,24]. We first tagged four toxic (*S. cryophilus* Wtf1^{poison}, *S. osmophilus* Wtf41^{poison}, and *S. octosporus* Wtf25^{poison} and Wtf61^{poison}) and one non-toxic (*S. osmophilus* Wtf19^{poison}) Wtf^{poison} protein at the C-terminus with mEos. The tagged proteins retained their toxic/non-toxic phenotypes when expressed in *S. cerevisiae* using a galactose-inducible expression system (Fig 2C). The assayed proteins all share less than 20% amino acid identity with Wtf4^{poison}, which we use as a positive control (S1 Fig B). We found that all five newly tested Wtf^{poison}-mEos proteins, including the nontoxic Wtf19^{poison}-mEos, exhibited self-assembly (Fig 2B). It is important to note, however, that the data reported for Wtf25^{poison}-mEos are limited and we could not reliably assay that protein via DAmFRET due to the high toxicity of the protein.

We also assayed DAmFRET in mutant alleles of *wtf4^{poison}-mEos* (S2 Fig, S3 Fig). The two toxic mutant proteins tested in this subset, Wtf4-14^{poison}-mEos (S2 Fig A, D-F) and Wtf4-18^{poison}-mEos (S3 Fig A-E) exhibited self-assembly. Of these two proteins, Wtf4-18-mEos is more like wild-type Wtf4^{poison}-mEos, in both toxicity and degree of assembly (S2 Fig D-F; S3 Fig B-E). Most non-toxic Wtf4 mutants (Wtf4-8^{poison}-mEos, Wtf4-12^{poison}-mEos, Wtf4-13^{poison}-mEos, Wtf4-15^{poison}-mEos and Wtf4-16^{poison}-mEos) exhibited reduced assembly compared to the wild-type (S2 Fig A-E, S3 Fig A-D). However, the non-toxic Wtf4-17^{poison}-mEos showed similar assembly to the wild-type (S3 Fig A-D). We could not reliably assay the assembly of Wtf4-9^{poison}-mEos, Wtf4-10^{poison}-mEos and Wtf4-11^{poison}-mEos due to low fluorescence signal (S2 Fig A-B, S6 Fig B).

These results show that Wtf^{poison} self-assembly is broadly conserved (over 100 million years) and can be supported by a wide range of amino acid sequences (e.g., proteins sharing <20% amino acid identity, S1 Fig B). Given the broad conservation of self-assembly, that all the toxic alleles exhibited assembly, and that mutant alleles with reduced toxicity also exhibited reduced

assembly, our results are consistent with an association between self-assembly and toxicity. However, our results demonstrate that assembly alone is insufficient for Wtf^{poison} toxicity, as we found several Wtf^{poison} proteins that assemble but are not toxic.

Intracellular localization of mutant Wtf^{poison} proteins is an imperfect predictor of toxicity.

We previously imaged the toxic *S. octosporus* Wtf25^{poison}-mCherry in *S. cerevisiae* cells and found that the localization was similar to the more extensively characterized toxic Wtf4^{poison} [19]. Specifically, the poisons show small puncta broadly distributed in the cytoplasm, with some localization to what appears to be the endoplasmic reticulum (ER; [15,19]). All functionally confirmed Wtf driver proteins have four to eight predicted transmembrane domains (S5 Table) and hence, this localization pattern may reflect the poison being trafficked from the ER through the secretory pathway, through the Golgi and trans-Golgi network [24].

The shared localization pattern of toxic Wtf^{poison} proteins suggested there may be a link between the intracellular distribution and toxicity of Wtf^{poison} proteins. To test this hypothesis, we imaged the wild-type Wtf^{poison}-mEos proteins described above in *S. cerevisiae* cells. The localization of the *S. octosporus* Wtf25^{poison}-mEos was similar to the previously described Wtf25^{poison}-mCherry described above (Fig 2D). The additional toxic Wtf^{poison} proteins from *S. octosporus*, *S. osmophilus* and *S. cryophilus*, also exhibited dispersed puncta, like the toxic Wtf4^{poison}-mEos control cells (Fig 2D). The nontoxic *S. osmophilus* Wtf19^{poison}-mEos, however, showed a strong signal enrichment in what appears to be the ER (Fig 2D).

We also assayed the localization of the mutant Wtf4^{poison} proteins mentioned above (S2 Fig F, S3 Fig E). The most toxic mutant protein, Wtf4-18^{poison}-mEos, localized in distributed puncta like wild-type (S3 Fig A-C, E). The slightly less toxic Wtf4-14^{poison}-mEos protein also formed distributed puncta, but also exhibited more ER-like localization than wild-type (S2 Fig A, D, F). Most of the non-toxic mutant Wtf4^{poison} proteins (Wtf4-8^{poison}-mEos, Wtf4-9^{poison}-mEos, Wtf4-11^{poison}-mEos, Wtf4-12^{poison}-mEos, Wtf4-13^{poison}-mEos, Wtf4-16^{poison}-mEos) were less dispersed and exhibited a largely ER-like localization in *S. cerevisiae* cells, similar to the non-toxic *S. osmophilus* Wtf19^{poison}-mEos (S2 Fig A-D, F, Fig 2C-D). One additional non-toxic mutant, Wtf4-10^{poison}-mEos, localized to the vacuole, reminiscent of Wtf^{antidote} protein localization (S2 Fig B, D, F). The non-toxic Wtf4-15^{poison}-mEos had a unique localization pattern that combined a diffuse distributed signal with some larger protein assemblies (S3 Fig A-C, E). Finally, the non-toxic

Wtf4-17^{poison}-mEos localization was indistinguishable from wild-type Wtf4^{poison}-mEos (S3 Fig A-C, E).

Together our results show that Wtf^{poison} self-assembly (assayed by DAmFRET) combined with cellular localization patterns are good, but imperfect predictors of toxicity. All the toxic proteins show both self-assembly in the DAmFRET assay and Wtf4^{poison}-like distributed protein localization in *S. cerevisiae* cells. Except for Wtf4-17^{poison}, the nontoxic proteins show reduced or lack of assembly (assayed by DAmFRET) and altered Wtf^{poison} protein localization (assayed by microscopy) in cells.

Altering assembly properties of Wtf^{poison} proteins affects toxicity.

To further explore a potential functional connection between the assembly of Wtf^{poison} proteins and their toxicity, we sought to alter the assembly properties of Wtf4^{poison} using tags. We first aimed to increase the overall size of the Wtf4^{poison} assemblies. To do this, we employed a recently described construct that contains the human ferritin heavy chain protein (FTH1) fused to a nanobody that recognizes mEos (mEosNB) (Kimbrough et al. forthcoming). The FTH1 domain self assembles to form a 24-mer core and can form supramolecular clusters when fused to self-assembling proteins [31,32]. In our assay, we expressed Wtf4^{poison}-mEos from a galactose inducible promoter and the mEosNB-FTH1 from a doxycycline repressible promoter (Fig 3A, B). As expected, we found that Wtf4^{poison}-mEos formed fewer and larger puncta inside cells in the presence of mEosNB-FTH1 (i.e., -Dox panels, Fig 3C). Expression of the mEosNB-FTH1 alone had no effect on yeast growth (Fig 3D, panel (i)). While expression of the Wtf4^{poison}-mEos alone was toxic, co-expression of the mEosNB-FTH1 and Wtf4^{poison}-mEos markedly suppressed the toxicity of the Wtf4^{poison}-mEos (Fig 3D, compare panel (ii) to panel (iii)). We also observed the same phenotypes with four additional toxic Wtf^{poison}-mEos proteins in the presence of the mEosNB-FTH1, indicating the effect was not specific to Wtf4^{poison} (Fig 3C-D).

We next attempted to increase the solubility Wtf4^{poison} assemblies using a modified N-terminal domain (NT*) tag derived from spidroins, a principal component of spider silk [33]. The NT* tag can decrease protein aggregation, which is the role of the native domain in spiders [34–38]. We added NT* to the N-terminus of the *wtf4^{poison}-mEos* allele to generate *wtf4-20^{poison}-mEos* (Fig 4A). We found that this protein had a novel combination of assembly and localization not represented in any of our other alleles. Specifically, the Wtf4-20^{poison}-mEos protein showed less

self-assembly than Wtf4^{poison}-mEos (Fig 4C), but the NT* tag did not visibly alter the localization of the protein within cells (Fig 4E). In addition, the Wtf4-20^{poison}-mEos protein showed increased toxicity in cells (Fig 4B). To test if the effects of the NT* tag were specific to Wtf4^{poison} or more general, we also tagged *S. octosporus* Wtf25^{poison} with NT* to generate Wtf25-4^{poison}-mEos (S4 Fig A). As with Wtf4-20^{poison}-mEos, we observed unaltered localization and increased toxicity of the Wtf25-4^{poison}-mEos protein, relative to wild-type Wtf25^{poison}-mEos (S4 Fig B, D). We could not, however, quantify Wtf25-4^{poison}-mEos assembly by DAmFRET as the protein was too toxic to cells (S6 Fig E).

We also assayed the how another solubility tag, the *E. coli* Maltose Binding Protein (MBP), affected Wtf^{poison} toxicity [39–41]. The MBP-tagged Wtf4^{poison} (Wtf4-21^{poison}-mEos) had the same phenotype as the NT*-tagged allele: decreased assembly, increased toxicity, unaltered localization, relative to the wild-type protein (S5 Fig). The phenotype of the MBP-tagged Wtf25^{poison} (Wtf25-5^{poison}-mEos) however, did not mirror that of the NT*-tagged allele. Instead, we found that the Wtf25-5^{poison}-mEos allele showed reduced toxicity and an altered, stronger endoplasmic reticulum-like localization, as compared to the wild-type protein (S5 Fig A-C). The Wtf25-5^{poison}-mEos protein did exhibit self-assembly, but we could unfortunately not compare it the wild-type protein as we failed to obtain sufficient viable cells to assay via DAmFRET (S5 Fig D, S6 Fig F).

The bulk of our experiments are consistent with a model where the assembly properties and the distribution of Wtf^{poison} proteins within cells affects toxicity, with distributed, punctate assemblies exhibiting more toxicity. The non-toxic Wtf4-17^{poison} protein that forms distributed assemblies, however, undermines this simple model or at least indicates that there are additional unidentified features that are essential for toxicity.

An additional possibility that we considered was that the expression levels of the Wtf^{poison} proteins likely contributes to the phenotypes we observed, despite expressing all alleles from a common vector backbone using a common promoter. To assay expression levels, we quantified fluorescence of the mEos tags shared by all alleles. We did not use western blots as that approach is challenging to apply to Wtf^{poison} proteins as they are toxic and highly hydrophobic [15,23]. Instead, we looked at the acceptor (red form of mEos) fluorescence in live cells analyzed in the DAmFRET experiments (S6 Fig; Data from Fig 2B, S2 Fig E, S3 Fig D, Fig 4C,). As expected, based on other studies [42–45], we observed significant fluorescent protein signal

heterogeneity within cells expressing the monomer mEos control and each Wtf^{poison} protein tested (S6 Fig). We did not, however, find increased fluorescent signal in cells expressing the most toxic proteins (as determined by growth assays). On the contrary, we tended to observe less signal in the cells expressing the most toxic proteins (e.g., Wtf4^{poison} and Wtf4-20^{poison}). These data support a model in which cells expressing the higher levels of toxic proteins are more likely to be removed by death and are not quantified. As mentioned above, however, we also observed low signal in the cells expressing the non-toxic Wtf4-11^{poison}, Wtf4-9^{poison}, and Wtf4-10^{poison} alleles (S6 Fig). The low levels of Wtf4-10^{poison} could be due to its degradation in the vacuole (S2 Fig F). For the other two alleles, it is formally possible the low levels of these proteins in cells could contribute to their lack of toxicity.

Limited modularity of the Wtf^{antidote}-specific domain.

We next wanted to test what protein features affect Wtf4^{antidote} function (Fig 1A-B). To do this, we first tested if the N-terminal antidote-specific domain encoded by exon 1 could act independently of the rest of the protein (S7 Fig A). We hypothesized that the amino acids encoded by exons 2-6 would be required for protein self-assembly as they comprise the poison protein, which self-assembles [15]. As expected, we found that a protein consisting of the exon 1-encoded residues linked to a mEos tag (Wtf4-exon1-mEos) could not self-assemble (S7 Fig B). The Wtf4-exon1-mEos protein was also not trafficked to the vacuole, despite this protein harboring two PY motifs that promote ubiquitin-mediated trafficking of wild-type Wtf^{antidote} proteins [24] (S7 Fig F). Finally, the Wtf4-exon1-mEos protein could not rescue Wtf4^{poison} toxicity, which parallels recent results using distinct Wtf proteins ((S7 Fig C) [24]). These results demonstrate that the antidote-specific domain encoded by exon 1 is insufficient for function.

In addition to self-assembly, the full length Wtf4^{antidote} also co-assembles with the Wtf4^{poison} ([15,22], S7 Fig G). The co-assembled Wtf4^{poison} and Wtf4^{antidote} proteins are co-trafficked to the vacuole and the toxicity of Wtf4^{poison} is neutralized [15,24]. We previously demonstrated that a mismatch in the copy number of coding sequence repeats found in exon 6 could disrupt Wtf^{poison} and Wtf^{antidote} interaction and compatibility [15,26]. We were curious if extensive shared sequence identity between Wtf4^{poison} and Wtf4^{antidote} proteins was important for co-assembly, or if identity between the two proteins at the C-terminus was sufficient. To test this idea, we generated a Wtf4 allele (*wtf4-6*) that moved the antidote-specific domain to the center of the protein, where it would interrupt the extensive shared amino acid identity with Wtf4^{poison} (S7 Fig

A). We also generated a control allele (*wtf4-7*) in which the antidote-specific domain was moved to the C-terminus of the protein where it should not interrupt the shared amino acid identity with Wtf4^{poison} but would control for the modularity of the exon 1 encoded domain (S7 Fig A). We found that mEos tagged versions of both Wtf4-6 and Wtf4-7 proteins were both non-toxic and trafficked to the vacuole (S7 Fig D, G). The Wtf4-7-mEos, with the antidote specific domain at the C-terminus, could also co-assemble with Wtf4^{poison}-mCherry and promote the poison's trafficking to the vacuole and neutralization (S7 Fig D, G).

The Wtf4-6-mEos protein with the antidote specific domain in the center, however, could not co-assemble with or neutralize wild-type Wtf4^{poison}-mCherry (S7 Fig D, G). This suggested that shared amino acid identity at the C-terminus is insufficient for Wtf4^{poison} and Wtf4^{antidote} co-assembly and function. However, this result could also mean that the Wtf4-6 protein is incapable of acting as an antidote. To try and distinguish these possibilities, we attempted to make a 'poison' protein (Wtf4-19) compatible with the Wtf4-6 protein by mutating the PY motifs required for ubiquitination and vacuole trafficking (PY mutated to PA; S7 Fig A)[24]. Analogous changes in bona fide antidote proteins turn them into toxic poison-like proteins [24]. As expected, the Wtf4-19-mCherry protein was toxic, but unexpectedly, it localized to the vacuole (S7 Fig E, H). In addition, the toxicity of Wtf4-19-mCherry was not neutralized by the Wtf4-6-mEos allele, despite sharing end-to-end amino acid identity, outside of the PY motifs, and despite both proteins being trafficked to the vacuole (S7 Fig E, H). This persistent toxicity was unexpected but suggests that shared amino acid identity can be insufficient for Wtf^{poison} and Wtf^{antidote} compatibility.

Protein co-assembly is important for Wtf^{antidote} function beyond linkage to the Wtf^{poison}.

We next wanted to know if co-assembly serves merely to link poison and antidote proteins to allow for co-trafficking, or if co-assembly serves a more nuanced role. To test this, we artificially tethered Wtf^{poison} proteins with diverged Wtf^{antidote} proteins with which they cannot co-assemble using a combination of GFP and GFP-binding (GBP) tags (Fig 5A, B; S8 Fig A, B).

We first tested if tethering Wtf4^{poison} to *S. octosporus* Wtf61^{antidote} could neutralize the toxic Wtf4^{poison}. We generated Wtf4^{poison}-GBP-mCherry and Wtf61^{antidote}-GFP proteins and found the tags did not disrupt protein function. Specifically, the Wtf4^{poison}-GBP-mCherry protein was toxic, and could be rescued by Wtf4^{antidote} proteins, including Wtf4^{antidote}-GFP. Similarly, the

Wtf61^{antidote}-GFP protein was able to rescue Wtf61^{poison}-mCherry (Fig 5C). However, Wtf61^{antidote}-GFP was not able to efficiently rescue Wtf4^{poison}-GBP-mCherry (Fig 5C, in bold). We found that the Wtf61^{antidote}-GFP and Wtf4^{poison}-GBP-mCherry proteins largely co-localized, but were not effectively transported into the vacuole (Fig 5D). We saw the same results when we analyzed a widely diverged, independent pair of Wtf proteins (*S. octosporus* Wtf25^{poison} and *S. cryophilus* Wtf1^{antidote}), suggesting that specific antidote-poison co-assembly generally promotes proper antidote function (S8 Fig).

Given that the Wtf61^{antidote}-GFP and Wtf4^{poison}-GBP-mCherry were often adjacent to vacuoles and not totally distributed in cells, as occurs when trafficking of Wtf proteins is disrupted [15], we suspected that the vacuolar targeting was still occurring, but blocked at a late step in the process (e.g., vacuole entry). Consistent with this notion, the assemblies often co-localized with the Rnq-1mCardinal protein, which is a prion protein that marks the insoluble protein deposit (IPOD) [46–48] (Fig 5E). This result was surprising to us because with a different expression system (β-estradiol induction) a considerable amount of the Wtf4^{poison}/Wtf4^{antidote} co-assemblies accumulate at the IPOD are not toxic to cells [15]. It is unclear why GFP/GBP mediated assemblies, but not Wtf/Wtf mediated co-assemblies, would be toxic at the IPOD, and we speculate about this in the discussion.

Beyond the GFP/GBP tethering experiments, we made additional observations suggesting that a specific nature of co-assembly with Wtf^{poison} is required for Wtf^{antidote} function when characterizing the *wtf4-20* allele (with the NT* domain that increases solubility) introduced earlier. The Wtf4-20^{poison}-mEos is toxic, as mentioned above, but we found that it could not be effectively rescued by wild-type Wtf4^{antidote}-mCherry (Fig 4D). This drastic reduction in rescue is striking given that the interaction (i.e., colocalization) of Wtf4-20^{poison}-mEos with Wtf4^{antidote}-mCherry appears only mildly disrupted relative to that observed between wild-type Wtf4 proteins (Figure 4E, F). The Wtf4-20^{poison}-mEos and Wtf4^{antidote}-mCherry proteins are not efficiently trafficked to the vacuole (Fig 4E). This effect was not, however, universal. We did not observe strong disruption of poison/antidote compatibility caused by the NT* tag on *S. octosporus* Wtf25^{poison} (Wtf25-4^{poison} allele, S4 Fig). If anything, the tag caused a mild decrease in rescue by the Wtf25^{antidote} (S4 Fig C). This suggests that the factors affecting poison/antidote compatibility can be complex or context dependent.

C-terminal domains support Wtf^{antidote} rescue.

Because Wtf proteins are encoded on largely overlapping coding sequence, a change in the shared coding sequence can simultaneously create a novel Wtf^{poison} protein and a matching novel Wtf^{antidote} protein. Our engineered mutant alleles offered the opportunity to explore if matching proteins are always compatible (i.e., if a novel toxic Wtf^{poison} protein is always neutralized by its corresponding Wtf^{antidote} protein).

We described above how the Wtf4-6 protein could not neutralize the toxicity of the largely identical Wtf4-19 protein, but it is unlikely an allele like this (with exon 1 moved after exon 3) would arise spontaneously (S7 Fig). We therefore explored poison and antidote compatibility more broadly within the alleles we generated. In many cases, the Wtf^{antidote} proteins were able to rescue their matching Wtf^{poison} alleles (S1 Table). One class of mutants, however, created toxic Wtf^{poison} proteins that were not rescued by the matching Wtf^{antidote}. In *wtf4*, these mutants changed a region of exon 6 that encodes a 7 amino acid repeat found in variable numbers (0-84 base pairs of repeat sequence) within *S. pombe wtf* genes (Figure 6A, B) [20]. The repeat region in *wtf4* encodes one complete repeat plus three additional amino acids of the repeat (Figure 6C). We found that mutating this region in *wtf4* by either scrambling the amino acid order (*wtf4-4* allele) or by replacing the ten amino acids with alanine (*wtf4-5* allele) generated toxic Wtf^{poison} proteins that were not neutralized by their matching Wtf^{antidote} proteins (Figure 6D). The Wtf4-4^{antidote} and Wtf4-5^{antidote} proteins were both trafficked to the vacuole when expressed alone but did not effectively co-traffic their corresponding Wtf^{poison} proteins (Figure 6E). The Wtf4-4 poison, and antidote proteins showed decreased co-localization, relative to wild-type proteins, suggesting the proteins failed to co-assemble (Figure 6E-F). Alternatively, the Wtf4-5 proteins colocalized (Fig 6F), but remained more distributed within cells relative to wild-type (Figure 6E). The incompatibility of the Wtf4-5 proteins further supports that a particular form of association is required between Wtf^{antidote} and Wtf^{poison} proteins to ensure the poison is trafficked to the vacuole and neutralized.

We also assayed the effects of deleting the repeat region of *wtf4* exon 6 alone (*wtf4-2* allele), or in combination with deleting another repetitive region found in exon 3 (*wtf4-3* allele; S9 Fig A) [20]. We found that the Wtf4-2^{poison}-mEos protein is toxic but is only partially rescued by Wtf4-2^{antidote}-mCherry, relative to the rescue observed between wild-type Wtf4 poison and antidote proteins (S9 Fig D). We found that the two Wtf4-2 proteins exhibit decreased colocalization, relative to wild-type proteins, suggesting the limited rescue is due to disrupted poison-antidote

interaction (S9 Fig E-F). Interestingly, we found that the defect in poison-antidote compatibility conferred by the deletion of the exon 6 repeats in the *wtf4-2* allele is partially suppressed by also deleting the repetitive region found in exon 3. Specifically, the proteins encoded by the *wtf4-3* allele, with both regions deleted, have near wild-type phenotypes (S9 Fig A-F). We observed no defects associated with an allele (*wtf4-1*) lacking only the repetitive region in exon 3 (S9 Fig A-B, D-E).

Finally, we also tested if the novel mutations we made in this study in the exon 3 or C-terminal repeats affected compatibility with wild-type Wtf proteins. In all cases tested, the repeat mutant Wtf^{poison} proteins were not neutralized by their wild-type Wtf^{antidote} counterparts and vice versa (S10 Fig A-H). For example, Wtf4-1^{poison} is not neutralized by Wtf4^{antidote} and Wtf4^{poison} is not neutralized by Wtf4-1^{antidote} (S10 Fig B).

The repeats in exon 6, but not in exon 3, are broadly conserved in the *wtf* gene family [19]. We also mutated the homologous region in *S. octosporus wtf25* and found analogous phenotypes as those described above in *wtf4* (S11 Fig). Like *wtf4*, *S. octosporus wtf25* also encodes 10 amino acids in this C-terminal region (S11 Fig A-C). We generated the *S. octosporus wtf25-2* allele by swapping the endogenous codons for those of *wtf4*. We found that this allele encoded an incompatible Wtf25-2^{poison} and Wtf25-2^{antidote} pair (S11 Fig D). Surprisingly, the individual Wtf25-2 proteins were compatible with Wtf25 proteins (e.g., Wtf25-2^{poison}-mCherry was rescued by Wtf25^{antidote}-mEos). We also deleted the repeat region of *S. octosporus wtf25* (to generate the *wtf25-1* allele) and again found phenotypes similar to those observed in the analogous *wtf4* mutant (*wtf4-2*) (S12 Fig A-D). Specifically, the Wtf25-1^{antidote}-mCherry showed reduced rescue of the Wtf25-1^{poison}-mEos toxicity, relative to the wild-type Wtf25 protein pair (S12 Fig C). Altogether, our results further support a critical role for the repeats in Wtf^{poison} and Wtf^{antidote} compatibility and reveal that mutants in this domain can encode Wtf^{poison} proteins not neutralized by the matching Wtf^{antidote} proteins.

C-terminal truncations reveal idiosyncrasy of Wtf protein functional domains.

An additional set of mutants we characterized followed up on an observation by Hu et al in one of the inaugural papers describing *wtf* drivers [17]. In that work, Hu et al described 10 amino acid C-terminal truncations of two *wtf* genes known as *cw9* and *cw27*. These mutant alleles both

exhibited disrupted Wtf^{poison}, but not Wtf^{antidote} activity. These proteins share 62% amino acid identity in the C-terminal exon 6 with each other and, at most, 70% with Wtf4. We tested if a similar 10 amino acid truncation of *wtf4* would specifically disrupt Wtf4^{poison} activity. This mutation gave us the exceptional *wtf4-17* allele described above that encodes a non-toxic Wtf4-17^{poison}, that surprisingly exhibits wild-type self-assembly and wild-type protein localization in cells (S3 Fig A-E). The disrupted Wtf4-17^{poison} toxicity is consistent with the phenotypes of the *cw9* and *cw27* truncations, but unlike those alleles, Wtf4-17^{antidote}-mCherry was not able to rescue the toxicity of a wild-type Wtf4^{poison}-mEos (S13 Fig A-B). Though we could not detect Wtf4-17^{antidote}-mCherry signal in cells, we infer it is expressed as it confers a phenotype, described below.

We also generated a larger truncation allele that deleted all 29 amino acids found in exon 6 of *wtf4*. This *wtf4-15* allele, also mentioned above, encodes a non-toxic Wtf4-15^{poison}-mEos, which has slightly reduced self-assembly, and shows diffused localization, with some larger assemblies (S3 Fig A-E). The Wtf4-15^{antidote}-mCherry is also unable to neutralize Wtf4^{poison}-mEos (S13 Fig B). Imaging of the proteins shows a lack of colocalization between Wtf4-15^{antidote}-mCherry and Wtf4^{poison}-mEos, suggesting that failed co-assembly underlies the failed compatibility (S13 Fig C).

Given that the 10 and 29 amino acid C-terminal truncation mutants both make non-toxic Wtf4^{poison} proteins and Wtf4^{antidote} proteins that do not rescue wild-type Wtf4^{poison}, we were surprised to find that a 20 amino acid C-terminal truncation generated a more functional *wtf* allele, *wtf4-18*, which was mentioned above (S3 Fig A-E). The 20 amino acid truncation extends into the exon 6 repeats, deleting the last two amino acids of the repeat (S3 Fig B). The Wtf4-18^{poison} is slightly less toxic than wild-type Wtf4^{poison} (S3 Figure C) but can be neutralized by the wild-type Wtf4^{antidote} and, to a lesser extent by the Wtf4-18^{antidote} (S13 Fig B). The Wtf-18^{antidote} can also partially rescue the toxicity of wild-type Wtf4^{poison} (S13 Fig B). Finally, we were also surprised to find that the Wtf4-18^{poison} could be partially rescued by the antidotes encoded by the other truncation mutants Wtf4-17^{antidote} and Wtf4-15^{antidote}, despite those antidotes being ineffective against wild-type Wtf4^{poison} (S13 Fig B). This reveals that the truncated Wtf4-15 and Wtf4-17 antidotes are at least partially functional.

Finally, to expand our analyses beyond *wtf4*, we also made 10 amino acid C-terminal truncations of *S. cryophilus wtf1, S. osmophilus wtf41, S. octosporus wtf61* and *wtf25*. We found

these truncations all retained toxicity and were rescuable by the corresponding wildtype antidotes (S3 Fig F-G; S14 Fig A-D). In the case of *S. osmophilus wtf41*, the rescue of Wtf41-1^{poison}-mEos by Wtf41^{antidote}-mEos was better than that of the wild-type Wtf41^{poison}-mEos (S14 Fig C). This uncovers another idiosyncratic pair, where the wild-type antidote rescued the mutant poison better than the wild-type poison. Overall, our C-terminal truncations reveal that the C-terminus sequences affect the protein function in a context dependent, sometimes idiosyncratic, manner.

Discussion

Protein assembly plays conserved roles in Wtf protein function.

The mutant analyses provided in this work expands and supports a working model in which 1) Wtf^{poison} toxicity is tied to the homotypic assembly of the proteins [15], 2) Wtf^{antidote} proteins are ubiquitinated and trafficked to the vacuole [15,24] and, 3) Wtf^{antidote} proteins co-assemble with their matching Wtf^{poison} proteins and co-traffic them to the vacuole [15,26]. Recent work has established that ubiquitin-mediated Wtf^{antidote} trafficking and co-trafficking with their corresponding Wtf^{poison} proteins are conserved within the extremely diverse gene family [24]. It was unclear, however, if homotypic protein assembly is a conserved feature of Wtf^{poison} or Wtf^{antidote} protein function.

The results of this study support the model that homotypic protein assembly plays critical roles in the function of Wtf^{poison} proteins. First, we observed that the ability to self-assemble was conserved amongst functional (i.e., toxic) wild-type Wtf^{poison} proteins from four *Schizosaccharomyces* species (Fig 2). Given that the functional proteins share as little as 20% amino acid identity, these observations likely reflect conserved functional importance of self-assembly. Our mutant analyses of Wtf4^{poison} proteins provided additional support for this model in that all toxic mutant proteins self-assembled (S2 Fig, S3 Fig). Furthermore, we found that the Wtf^{poison} toxicity could be modulated by altering the assembly properties of the protein with tags (Fig 3, Fig 4, S4 Fig, S5 Fig). Together, our data suggest that Wtf^{poison} toxicity is tied to protein assembly with distributed, small assemblies showing greater toxicity than localized, larger assemblies (Fig 2-4, S2-5 Fig). The recent work of Zheng et al. (2023) suggests the distributed assemblies represent localization to the trans-Golgi network.

Still, it is important to note that the Wtf4-17^{poison} allele was non-toxic, despite assembling into small, distributed assemblies indistinguishable from those generated by the wild-type protein (S3 Fig). This exceptional protein highlights that even if self-assembly is critical for Wtf^{poison} toxicity, it is not the only factor required. In addition, this allele offers an opportunity for future work to explore features that distinguish toxic from nontoxic protein assemblies.

Our results also support an expanded, more nuanced role for homotypic protein assembly and trafficking in Wtf^{antidote} function. First, we found that the antidote-specific domain that contains the PY motifs is insufficient to promote vacuole trafficking, suggesting some other features of Wtf proteins are also required (S7 Fig). We posit protein self-assembly could contribute to this function. For Wtf^{antidote} neutralization of a Wtf^{poison}, we initially assumed that co-assembly of Wtf^{antidote} with Wtf^{poison} proteins served only to physically link the proteins, thus enabling the Wtf^{antdiote} to traffic the Wtf^{poison} to the vacuole [24]. We found, however, that physical linkage between a Wtf^{poison} and Wtf^{antidote} can be insufficient to ensure their co-trafficking to the vacuole and neutralization of the Wtf^{poison}'s toxicity. We observed this insufficiency in experiments linking non-matching Wtf^{poison} and Wtf^{antidote} proteins using physical tags (Fig 5, S8 Fig). In addition, we found that the *wtf4-5* and *wtf4-20* alleles encode protein pairs in which poison-antidote interaction appeared largely intact, but trafficking into the vacuole and poison neutralization was disrupted (Fig 4, Fig 6). These experiments suggest that efficient co-trafficking of Wtf^{poison}/ Wtf^{antidote} protein assemblies requires a particular conformation or strong affinity between the interacting proteins not replicated in the ineffective Wtf^{poison}/Wtf^{antidote} combinations mentioned above.

Moreover, our experiments surprisingly revealed that trafficking toxic Wtf assemblies to the proper destination may not always be sufficient to ensure their neutralization. In previous work using a different induction system than that employed here, we found that much of the trafficked Wtf4^{poison}/Wtf4^{antidote} assemblies accumulated at the insoluble protein deposit (IPOD), in addition to the vacuole [15] and the cells were viable. Similar, but generally smaller, assemblies can be seen accumulating outside of the vacuole (likely the IPOD) in many of the viable cells we image expressing Wtf^{antidote} proteins or compatible Wtf^{poison}/Wtf^{antidote} assemblies using the GAL induction system employed in this study (e.g., Fig 6E panels expressing Wtf4^{antidote} and Wtf4^{antidote}/Wtf4^{poison}). Similarly, Zheng et al found that vacuole localization was not essential for Wtf^{poison} neutralization as they observed that trafficking to the endosome can be sufficient [24]. Here, however, we observed that Wtf4^{poison}-GBP/Wtf61^{antidote}-GFP assemblies (and likely the

Wtf25^{poison}-GBP/Wtf1^{antidote}-GFP assemblies) were trafficked to the IPOD, but were still toxic (Fig 5 and S8 Fig). Finally, we found that the *wtf4-19* allele encoded a protein that was toxic, despite its localization to the vacuole (S7 Fig). These results suggest that factors beyond localization, perhaps assembly conformation, can also affect the toxicity of Wtf proteins.

Commonalities between Wtf proteins and other self-assembling proteins.

The Wtf proteins share broad parallels with other nonhomologous proteins that form assemblies. For example, a sequence-independent common oligomeric property may underly the toxicity of unrelated amyloid proteins [49]. While Wtf^{poison} proteins are related to each other, their sequences are extremely diverged. We propose a common feature of their assembled forms is likely responsible for their shared toxicity. Another feature Wtf proteins share with several unrelated proteins is the capacity to form functional assemblies. Multiple amyloidogenic proteins form functional amyloids that perform diverse biological functions, including long term memory in flies [50], epigenetic inheritance in yeast [51] and biofilm formation in bacteria [52–54]. Some functionally aggregating amyloids have also shown to be toxic at intermediate stages of assembly, suggesting that protein toxicity could pose a risk in certain instances [55]. The co-expression of Wtf^{antidote} with the toxic Wtf^{poison} results in a change in its localization and the assembly properties of the Wtf^{poison}-Wtf^{antidote} complex. This suggests that protein-protein interaction within a pair of corresponding Wtf proteins is similar to functional aggregation. While the outcome of functional Wtf protein assembly is different (i.e., successful drive), the delicate interplay between toxic and non-toxic protein assemblies is similar to functionally aggregating amyloids.

The use of E3 ubiquitin ligases to direct protein trafficking is an additional theme Wtf proteins share with other self-assembling proteins acting in diverse cell signaling processes, including immune response [56,57], prion disease [58] and other neurodegenerative disorders [59–65]. In multiple cases, ubiquitination of a key protein results in its aggregation, differential trafficking to specific intracellular locations or degradation, suggesting that this is a common mechanism for enabling downstream signaling processes. Additionally, a lack of ubiquitination by the ligase often results in toxic aggregates [58,61,64] or reduced functionality of the key protein [56,57], which are very reminiscent of the Wtf^{poison} + Wtf^{antidote} assemblies discussed above.

Rapidly evolving coding sequence repeats can affect Wtf^{poison}-Wtf^{antidote} compatibility.

Most *S. pombe wtf* genes contain varying copy numbers of a sequence repeat in exon 3 [20]. The potential role of the exon 3 repeats was unclear, but all functionally validated *S. pombe wtf* drivers contain the exon 3 repeats (S5 Table). One *wtf* gene (*wtf23* from the CBS5557 strain) that lacks the exon 3 repeats has been tested in *S. pombe* and failed to cause drive in two strain backgrounds, although it was not determined if the encoded proteins were non-functional or if the driver was effectively suppressed [20,25]. Previous work also found that a mismatch of repeat numbers in exon 3 between a Wtf13^{poison} (five repeats) and Wtf18-2^{antidote} (four repeats) could still produce a compatible poison + antidote pair. In this work, we found that deleting the exon 3 repeats in *wtf4* (*wtf4-1* allele) produced a functional, compatible Wtf^{poison} and Wtf^{antidote} pair. The Wtf4-1^{poison}, however, was not neutralized by the wild-type Wtf4^{antidote}, which has two repeats (S10 Fig B). This indicates that the exon 3 repeats can affect Wtf^{poison} and Wtf^{antidote} compatibility.

Many *S. pombe wtf* genes also contain a sequence repeat in exon 6 [20]. Repeats homologous to those found in *S. pombe* exon 6 can also be found in the C-termini of many genes in *S. octosporus* and *S. osmophilus* [19]. All functionally validated drivers contain repeats in *S. octosporus*, but one functional *S. pombe* driver (*wtf35* from FY29033) lacks the repeats (S5 Table) [19,25]. Previous work demonstrated that a mismatch in the number of exon 6 repeats could affect Wtf^{poison} and Wtf^{antidote} compatibility in *S. pombe* Wtf proteins [15,26]. This current work extends previous work by showing with additional alleles of *wtf4* and novel alleles of *S. octosporus wtf25* that copy number mismatches in this region disrupt Wtf^{poison} and Wtf^{antidote} compatibility.

Overall, our results support the model that the rapid copy number evolution of the repeats found in *wtf* genes contributes to rapid innovation of novel Wtf^{poison} and Wtf^{antidote} pairs [19,20]. These highly evolvable sequences have likely contributed to the long-term evolutionary success of *wtf* drivers, as generating novel alleles allows frequent generation of novel drivers likely to be heterozygous (and thus drive) in crosses. Frequent driver turnover may also complicate the evolution of drive suppressors that are not other *wtf* genes. Still, this work reveals that these hypermutable regions come with a burden as they contain the potential to generate self-killing alleles, which are discussed below.

Wtf fitness landscape likely includes self-killing alleles.

Our analyses of mutations in the repeats found in exon 6 of *S. pombe* genes revealed a novel self-killing phenotype in which a *wtf* allele can encode a toxic Wtf^{poison} that is not effectively neutralized by its corresponding $Wtf^{antidote}$. Such an allele is expected to lead to a dominant loss of fertility, analogous to mutations where the antidote protein expression or function is disrupted [17,22,24]. This phenotype was strongest in mutants that changed the sequence of the repeats (i.e. *wtf4-4*, *wtf4-5* and *wtf25-2*). These mutations are rather dramatic and have a low probability of arising spontaneously in nature.

A weaker version of the self-killing phenotype was, however, also observed in mutations that deleted the repeats. Interestingly, the deleterious effects of removing the exon 6 repeats in *wtf4* (*wtf4-2* allele) could be suppressed by also deleting the exon 3 repeats (*wtf4-3* allele) (S9 Fig D). This suppression, in addition to the one functional driver known to lack the exon 6 repeats, shows that changes in other regions of the protein can compensate for the missing repeats. Still, the existence of *wtf* genes without the repeats, and extensive gene conversion within the family, suggests that novel deleterious repeat deletion mutations are likely to arise recurrently in natural populations [19–21].

We may have also fortuitously sampled one largely self-killing allele from a natural population that did not have disrupted repeats, suggesting there are multiple paths to generating such alleles. The *wtf41* gene from *S. octosporus* encodes a toxic $Wtf41^{poison}$ that is not efficiently neutralized by the corresponding $Wtf41^{antidote}$ protein (S14 Fig, [19]). All together, we propose self-killing *wtf* alleles could contribute to recurrent, spontaneous sub-fertility or infertility. We propose this spontaneous sub-fertility could be a persistent burden on the population fitness of all *Schizosaccharomyces* species carrying *wtf* drivers.

Rapid evolution and the risk of self-killing alleles.

Beyond *wtf* genes, there are many known killer meiotic drivers [3,5,6,8,9,11]. There are also likely many more yet to be discovered, given their accelerated pace of discovery in recent years. Although the genes causing drive in different systems are not homologous, they often share mechanistic and evolutionary themes [13,14,66]. Those themes include production of poisons/killer elements and rapid evolution. The *wtf* genes have illustrated that high evolvability, via nonallelic gene conversion and mutable coding sequence repeats, can facilitate the

evolutionary success of meiotic drivers [19,21,67]. This work has illustrated that rapid evolution of killer elements also presents the risk of generating self-killing alleles. There is no reason to suppose such risks would be specific to the *wtf* killers. Instead, we posit that such self-killing alleles may be a widespread source of recurrent, spontaneous infertility in eukaryotes.

Materials and Methods

Cloning

We confirmed all the vectors described in this study by Sanger sequencing or by Nanopore sequencing via Plasmidsaurus. Find the specifics for the yeast strains used in this study are listed in S2 Table, plasmids are in S3 Table and the oligos are in S4 Table.

***S. cerevisiae* vectors:**

Generation of a Gal-inducible GFP vector to tag alleles: We amplified GFP-ADH1 terminator from a previously published plasmid, pSZB464 [15] with oligos 3744+3743. We digested this product with SacI and SpeI and cloned it into pDK20 [68] to generate pSZB1528. We then isolated the Gal promoter-GFP-ADH1T after digestion with SacI and KpnI, and cloned it into a SacI-KpnI digested pRS316 [69] to generate pSZB1540.

Generation of a Gal-inducible mCherry vector to tag alleles: We amplified mCherry-ADH1 terminator from pFA6a-mCherry-kanMX6 [70] with oligos 3745+3743. We digested this product with SacI and SpeI and cloned it into pDK20 [68] to generate pSZB1526. We then isolated the Gal promoter-mCherry-ADH1T after digestion with SacI and KpnI, and cloned it into a SacI-KpnI digested pRS314 [69] to generate pSZB1537.

Generation of a Gal-inducible mEos3.1 vector to tag alleles: We digested V08 [30] with SacI and KpnI to release the fragment with Gal promoter- 4x(EAAAR) linker-mEos3.1. We then cloned this into SacI-KpnI digested pRS316 [69] to generate pSZB1460.

Generation of a monomer mEos3.1 in an ARS/CEN plasmid: We cut out Gal-monomer mEos3.1-cyc1T from RHX0935 [30] with SacI and KpnI, and cloned into SacI, KpnI cut pRS316 [69] to generate pSZB1514.

Generation of Gal-inducible wtf alleles:

S. kambucha wtf4 exon 1: The gene consisting of 136 base pairs that makes up exon 1 of *S. kambucha wtf4* was synthesized and cloned into pSZB1460 by IDT to generate pSZB1552.

S. kambucha wtf4-1: We deleted 66 base pairs (bases 313-378 of poison coding sequence) that make up the exon 3 coding sequence repeats in *S. kambucha wtf4*^{poison} and cloned it into pSZB1460 to generate pSZB1565. We repeated the same deletion in *S. kambucha wtf4*^{antidote} (bases 439-504 of antidote coding sequence) and this construct was synthesized and cloned it into pSZB1537 by IDT to generate pSZB1736.

S. kambucha wtf4-2: We deleted 30 base pairs (bases 802-831 of poison coding sequence) that make up the exon 6 repeats in *S. kambucha wtf4* and this construct was synthesized and cloned it into pSZB1460 to generate pSZB1566 by IDT. To construct the mutant antidote, we deleted bases 928-957 of the antidote coding sequence and this construct was synthesized and cloned it into pSZB1537 by IDT generate pSZB1737.

S. kambucha wtf4-3: We deleted 66 base pairs (bases 313-378 of poison coding sequence) and 30 base pairs (bases 802-831 of poison coding sequence) to delete both the exon 3 and 6 coding sequence repeats in *S. kambucha wtf4.* This construct was then synthesized and cloned into pSZB1460 to generate pSZB1670. To construct the mutant antidote, we deleted 66 base pairs (bases 439-504 of antidote coding sequence) and 33 base pairs (bases 928-957 of antidote coding sequence) and this construct was synthesized and cloned it into pSZB1537 by IDT generate pSZB1738.

S. kambucha wtf4-4: We randomly scrambled the 10 amino acids that make up the exon 6 coding sequence repeats in *S. kambucha wtf4*^{poison}, and then reordered the codons to match the amino acids. We then replaced the wild-type 30 base pairs with the scrambled 30 base pairs (TTTGGGAGAGCGAGAGGGATAGGTAATATA) and this construct was synthesized and cloned into pSZB1460 to generate pSZB1742. To construct the mutant antidote, we replaced the exon 6 coding sequence repeats with the same scrambled 30 base pairs, and this construct was synthesized and cloned into pSZB1537 by IDT to generate pSZB1740.

S. kambucha wtf4-5: We replaced the 30 base pairs that make up the exon 6 coding sequence repeats with alanine codons (GCAGCGGCTGCCGCTGCAGCTGCCGCAGCG) in *S. kambucha wtf4*^{poison} and this construct was synthesized and was cloned into pSZB1460 to generate pSZB1743. To construct the mutant antidote, we replaced the exon 6 coding sequence repeats with the same alanine codons, and this construct was synthesized and cloned into pSZB1537 by IDT to generate pSZB1741.

S. kambucha wtf4-6: We inserted exon 1 in between exons 3 and 4 of *S. kambucha wtf4*^{poison} and this construct was synthesized and cloned into pSZB1460 by IDT to generate pSZB1616. To maintain the in-frame codons, we inserted exon 1 at 541 base pairs of the poison coding sequence, which is one base pair before exon 3 ends.

S. kambucha wtf4-19: We mutated the two PY motifs within exon 1 in *S. kambucha wtf4-6* to PA (637-670 base pairs mutated from TAC to GCC; 670-673 base pairs mutated from TAC to GCC) and this construct was synthesized and cloned into pSZB1460 by IDT to generate pSZB1922.

S. kambucha wtf4-7: We inserted exon 1 before the stop codon of *S. kambucha wtf4*^{poison} coding sequence and this construct was synthesized and cloned into pSZB1460 by IDT to generate pSZB1555.

S. kambucha wtf4-8: We used TMHMM2.0 [71,72] to predict transmembrane topology (see S6 Table for a detailed description). With these predictions as guidance, we deleted the first predicted transmembrane domain (bases 121-186 of poison coding sequence) from in *S. kambucha wtf4*^{poison} and this construct was synthesized and cloned into pSZB1460 by IDT to generate pSZB1561.

S. kambucha wtf4-9: We deleted the second predicted transmembrane domain (bases 232-291 of poison coding sequence) of *S. kambucha wtf4*^{poison} coding sequence and this construct was synthesized and cloned into pSZB1460 by IDT to generate pSZB1562.

S. kambucha wtf4-10: We deleted the sixth predicted transmembrane domain (bases 580-648 of poison coding sequence) of *S. kambucha wtf4*^{poison} coding sequence and this construct was synthesized and cloned into pSZB1460 by IDT to generate pSZB1563.

S. kambucha wtf4-11: We deleted exon 2 (bases 11-283) of *S. kambucha wtf4^{poison}* coding sequence and this construct was synthesized and cloned into pSZB1460 by IDT to generate pSZB1556.

S. kambucha wtf4-12: We deleted exon 3 (bases 284-541) of *S. kambucha wtf4^{poison}* coding sequence and this construct was synthesized and cloned into pSZB1460 by IDT to generate pSZB1557.

S. kambucha wtf4-13: We deleted exon 4 (bases 542-733) of *S. kambucha wtf4^{poison}* coding sequence and this construct was synthesized and cloned into pSZB1460 by IDT to generate pSZB1558.

S. kambucha wtf4-14: We deleted exon 5 (bases 734-796) of *S. kambucha wtf4^{poison}* coding sequence and this construct was synthesized and cloned into pSZB1460 by IDT to generate pSZB1559.

S. kambucha wtf4-15: We deleted exon 6 (bases 797-885) of *S. kambucha wtf4^{poison}* coding sequence and this construct was synthesized and cloned into pSZB1460 by IDT to generate pSZB1560. To construct the mutant antidote, we deleted exon 6 and this construct was synthesized and cloned into pSZB1537 by IDT to generate pSZB1899.

S. kambucha wtf4-16: From previous analysis of *S. pombe wtf* genes, a conserved region within exon 3 was identified [20]. This conserved region within exon 3 was 29 base pairs long (bases 284-312) in *S. kambucha wtf4^{poison}* coding sequence. To maintain in-frame codons, we included one base pair upstream the conserved region, and made a 30 base pairs deletion (bases 283-312) in *S. kambucha wtf4^{poison}* coding sequence and this construct was synthesized and cloned into pSZB1460 by IDT to generate pSZB1617.

S. kambucha wtf4-17^{poison}-mEos: We amplified a 10 amino acid truncated poison from pSZB464 [15] with oligos 3183+3186 and cloned this into V08 [30] via Golden Gate assembly (New England Biolabs) to generate pSZB1402. We digested this with SacI and KpnI and cloned the insert into SacI, KpnI digested pRS316 [69] to generate pSZB1505.

S. kambucha wtf4-17^{antidote}-mCherry: We amplified 10 amino acid truncated antidote from pSZB708 [15] with oligos 1402+3138, and mCherry-cyc1T from pSZB708 [15] with oligos 3139+2170. We then stitched these pieces with oligos 1402+2170. We cut this fragment with XhoI, BamHI and cloned this into XhoI, BamHI cut pDK20 [68] to generate pSZB1416. We cut this plasmid with KpnI and XhoI and cloned the insert into KpnI, XhoI cut pRS314 [69] to generate pSZB1550.

S. kambucha wtf4-18^{poison}-mEos: We amplified 20 amino acid truncated poison from pSZB464 [15] with oligos 3183+3282 and cloned this into V08 [30][30] via Golden Gate assembly (New England Biolabs) to generate pSZB1444. We digested this with SacI and KpnI and cloned the insert into SacI, KpnI digested pRS316 [69] to generate pSZB1507.

S. kambucha wtf4-18^{antidote}-mCherry: We amplified 20 amino acid truncated antidote from pSZB708 [15] with oligos 1402+3829. We digested this fragment with XhoI and BamHI and cloned the insert into XhoI, BamHI cut pSZB1537 to generate pSZB1567.

S. kambucha wtf4^{poison}-mCherry: We amplified *S. kambucha wtf4^{poison}-mCherry-cyc1T* from pSZB708 [15] with oligos 2625+964. This product was cut with BamHI and XhoI and cloned into BamHI, XhoI cut pDK20 [68] to generate pSZB1374. We cut this plasmid with KpnI and XhoI and cloned the insert into KpnI, XhoI cut pRS314 [69] to generate pSZB1381.

S. kambucha wtf4^{poison}-mEos: We digested RHX1389 [15] with KpnI, SacI and ligated the insert with KpnI, SacI cut pRS316 [69] to generate pSZB1455. This plasmid had the start site of the poison mutated to TAG, which was then corrected to ATG by GenScript to generate pSZB1476.

S. kambucha wtf4^{poison}-GBP-mCherry: We added the GFP-binding protein sequence from Addgene plasmid #89068 [73] at the end of *S. kambucha wtf4^{poison}* and this construct was synthesized and cloned into pSZB1537 by IDT to generate pSZB1748.

S. kambucha wtf4-20^{poison}-mEos: We added the mutated N-terminal domain (D40K, K65D) from the flagelliform spidroin 1A variant 1 from *Trichonephila clavipes*, NT* [33,34], followed by a TEV cleavage site (ENLYFQS) [74] at the N-terminus of *S. kambucha wtf4^{poison}* coding sequence, which was synthesized and cloned into pSZB1460 by IDT to generate pSZB1900.

S. kambucha wtf4-21^{poison}-mEos: We added the *S. cerevisiae* codon-optimized *E. coli* Maltose Binding Protein (MBP) coding sequence [75,76] followed by a 4X(GGGS)-GG linker to the N-terminus of *S. kambucha wtf4^{poison}* coding sequence, which was synthesized and cloned into pSZB1460 by IDT to generate pSZB1949.

S. kambucha wtf4^{antidote}-GFP: We ordered *S. kambucha wtf4^{antidote}* which was synthesized and cloned into pSZB1540 by IDT to generate pSZB1874.

S. kambucha wtf4^{antidote}-mCherry: We amplified *S. kambucha wtf4^{antidote}-mCherry-cyc1T* from pSZB1005 [15] with oligos 1402+2170. This product was digested with BamHI and XhoI and cloned into BamHI, XhoI cut pDK20 [68] to generate pSZB1699. This plasmid was digested with KpnI, XhoI and ligated with KpnI, XhoI cut pRS314 [69] to generate pSZB1774.

S. kambucha wtf4^{antidote}-mEos: We digested pSZB1120 (7) with KpnI, SacI and ligated the insert into KpnI, SacI cut pRS316 [69] to generate pSZB1453. This plasmid had the start site of the antidote mutated to TAG, which was then corrected to ATG by GenScript to generate pSZB1477.

S. octosporus wtf25^{poison}-mEos: We amplified *S. octosporus wtf25^{poison}* from pSZB1353 [19] with oligos 3841+3840 and cloned this into V08 [30] via Golden Gate assembly (New England Biolabs) to generate pSZB1548. We digested this with SacI and KpnI and cloned the insert into SacI, KpnI digested pRS316 [69] to generate pSZB1585.

S. octosporus wtf25^{poison}-mCherry: We ordered *S. octosporus wtf25^{poison}* coding sequence was synthesized and cloned into pSZB1537 by IDT to generate pSZB1807.

S. octosporus wtf25^{poison}-GBP-mCherry: We added the GFP-binding protein sequence from Addgene plasmid #89068 [73] at the end of *S. octosporus wtf25^{poison}* coding sequence and this construct was synthesized and cloned into pSZB1537 by IDT to generate pSZB1868.

S. octosporus wtf25^{antidote}-mCherry: We ordered *S. octosporus wtf25^{antidote}* coding sequence was synthesized and cloned into pSZB1537 by IDT to generate pSZB1746.

S. octosporus wtf25^{antidote}-mEos: We ordered *S. octosporus wtf25^{antidote}* coding sequence was synthesized and cloned into pSZB1460 by IDT to generate pSZB1806.

S. octosporus wtf25^{antidote}-mEos in pRS314: We amplified *S. octosporus wtf25^{antidote}* from pSZB1347 [19] with oligos 3839+3840. This insert was cloned into V08 [30] via Golden Gate cloning (New England Biolabs) to generate pSZB1593. We digested this with KpnI, SacI and cloned the insert into pRS314 [69] to generate pSZB1598.

S. octosporus wtf25^{antidote}-GFP: We ordered *S. octosporus wtf25^{antidote}* coding sequence was synthesized and cloned into pSZB1540 by IDT to generate pSZB1869.

S. octosporus wtf25-1: We deleted 30 base pairs (bases 505-534) that make up the exon 4 repeats in *S. octosporus wtf25^{poison}* and was synthesized and cloned into pSZB1460 by IDT to generate pSZB1687. To construct the mutant antidote, we deleted bases 640-669 of the antidote coding sequence and this construct was synthesized and cloned it into pSZB1540 by IDT generate pSZB1739.

S. octosporus wtf25-2: To swap the coding sequence repeats between *S. kambucha wtf4* exon 6 and *S. octosporus wtf25* exon 4, we replaced the 30 base pairs from *wtf25* (ATAGGAAACGGTGCACGGCATAGGAAAT) with 30 base pairs from *wtf4* (ATAGGGAATATAGGGAGAGCGTTTAGAGGT) in *S. octosporus wtf25*. The mutant poison was synthesized and cloned into pSZB1537 by IDT to generate pSZB1732. The mutant antidote was synthesized and cloned into pSZB1460 by IDT to generate pSZB1731.

S. octosporus wtf25-3^{poison}-mEos: We amplified a 10 amino acid C-terminal truncated *wtf25^{poison}* from pSZB1353 [19] with oligos 4173+4174 and cloned this into V08 [30] via Golden Gate assembly (New England Biolabs) to generate pSZB1675. We then cut out the tagged poison with SacI and KpnI, and ligated it with cut pRS316 [69] to generate pSZB1694.

S. octosporus wtf25-4^{poison}: We added the mutated N-terminal domain (D40K, K65D) from the flagelliform spidroin 1A variant 1 from *Trichonephila clavipes*, NT* [33,34], followed by a TEV cleavage site (ENLYFQS) [74] at the N-terminus of *S. octosporus wtf25^{poison}* coding sequence, which was synthesized and cloned into pSZB1460 by IDT to generate pSZB1927.

S. octosporus wtf25-5^{poison}-mEos: We added the *S. cerevisiae* codon-optimized *E. coli* Maltose Binding Protein (MBP) coding sequence [75,76] followed by a 4X(GGGS)-GG linker to the N-terminus of *S. octosporus wtf25^{poison}* coding sequence, which was synthesized and cloned into pSZB1460 by IDT to generate pSZB1950.

S. octosporus wtf61^{poison}-mEos: We amplified *S. osmophilus wtf61^{poison}* from pSZB1040 [19] with oligos 3837+3838 and cloned this into V08 [30] via Golden Gate assembly (New England Biolabs) to generate pSZB1569. We digested this with SacI and KpnI and cloned the insert into SacI, KpnI digested pRS314 [69] to generate pSZB1583.

S. octosporus wtf61^{poison}-mCherry: We amplified *S. osmophilus wtf61^{poison}* from pSZB1040 [19] with oligos 4193+4194. We digested this product with XhoI, BamHI and cloned this into XhoI, BamHI cut pSZB1537 to generate pSZB1706.

S. octosporus wtf61^{antidote}-GFP: We amplified *S. osmophilus wtf61^{antidote}* from pSZB1095 [19] with oligos 4192+4194. We digested this product with XhoI, BamHI and cloned this into with XhoI, BamHI cut pSZB1540 to generate pSZB1708.

S. octosporus wtf61^{antidote}-mEos: We amplified *S. osmophilus wtf61^{antidote}* from pSZB1095 [19] with oligos 3836+3837 and cloned into V08 [30] via Golden Gate assembly (New England Biolabs) to generate pSZB1645. We then digested pSZB1645 with KpnI and SacI and ligated it with KpnI, BamHI cut pRS314 to generate pSZB1647.

S. cryophilus wtf1^{poison}-mEos: We amplified *S. cryophilus wtf1^{poison}* from pSZB1122 [19] with oligos 3844+3843 and cloned this into V08 [30] via Golden Gate assembly (New England Biolabs) to generate pSZB1544. We digested this with SacI and KpnI and cloned the insert into SacI, KpnI digested pRS316 [69] to generate pSZB1575.

S. cryophilus wtf1^{poison}-mCherry: We ordered *S. cryophilus wtf1^{poison}* which was synthesized and cloned into pSZB1537 by IDT to generate pSZB1870.

S. cryophilus wtf1^{antidote}-mEos: We amplified *S. cryophilus wtf1^{antidote}* from pSZB1192 [19] with oligos 3843+3842 and cloned this into V08 [30] via Golden Gate assembly (New England

Biolabs) to generate pSZB1605. We digested this with SacI and KpnI and cloned the insert into SacI, KpnI digested pRS314 [69] to generate pSZB1612.

S. cryophilus wtf1^{antidote}-GFP: We ordered *S. cryophilus wtf1^{antidote}* which was synthesized and cloned into pSZB1540 by IDT to generate pSZB1871.

S. cryophilus wtf1-1^{poison}: We amplified a 10 amino acid C-terminal truncated *wtf1^{poison}* from pSZB1122 [19] and oligos 4177+4178 and cloned this into V08 [30] via Golden Gate assembly (New England Biolabs) to generate pSZB1673. We then cut out the tagged poison with SacI, KpnI and cloned into cut pRS316 [69] to generate pSZB1692.

S. osmophilus wtf41^{poison}-mEos: We cloned *S. osmophilus wtf41^{poison}* from pSZB1327 [19] with oligos 3361+3362 and cloned this into V08 [30] via Golden Gate assembly (New England Biolabs) to generate pSZB1533. We then cut out the tagged poison with SacI, KpnI and cloned into cut pRS316 [69] to generate pSZB1581.

S. osmophilus wtf41-1^{poison}-mEos: We cloned C-terminus 10 amino acid truncated *S. osmophilus wtf41^{poison}* from pSZB1325 [19] with oligos 4175+4176 and cloned this into V08 [30] via Golden Gate assembly (New England Biolabs) to generate pSZB1676. We then cut out the tagged poison with SacI, KpnI and cloned into cut pRS316 [69] to generate pSZB1696.

S. osmophilus wtf41^{antidote}-mEos: We amplified *S. osmophilus wtf41^{antidote}* from pSZB1325 [19] with oligos 3832+3362 and cloned this into V08 [30] via Golden Gate assembly (New England Biolabs) to generate pSZB1599. We then cut out the tagged poison with SacI, KpnI and cloned into cut pRS314 [69] to generate pSZB1607.

S. osmophilus wtf19^{poison}-mEos: We amplified *S. osmophilus wtf19^{poison}* from pSZB1324 [19] with oligos 3835+3834 and cloned this into V08 [30] via Golden Gate assembly (New England Biolabs) to generate pSZB1546. We then cut out the tagged poison with SacI, KpnI and cloned into cut pRS316 [69] to generate pSZB1579.

Strain construction

S. cerevisiae strains with Galactose and β-estradiol inducible systems:

We used the previously published strain, SZY1637 [15] and an independently constructed isolate of SZY1637, SZY1639 or SZY5807, to construct the strains in this study by transforming in the appropriate vectors. These strains have the lexA-ER-haB42 transcription factor integrated at *HIS3* [77]. In general, we used a protocol, modified from [78], to transform the vectors into these strains. Briefly, we incubated a mixture of 266μL of PLATE solution, 50μL of boiled salmon sperm DNA, 30μL of water, 1-4μL of vector DNA and a match-head sized amount of yeast at 30°C overnight and plated on selective media on the following day to select for transformants. We used Synthetic Complete (SC) media (Yeast Nitrogen Base from VWR #291940 and SC Supplement mix from SunSci) with the appropriate dropouts of the selective components to maintain vectors in the strains as in [15]. In some cases, transformants did not express the construct when induced. To ensure proper testing of genotypes, we screened multiple transformants via cytometry or microscopy to ensure that strains express the fluorescently tagged construct(s).

Construction of S. cerevisiae strain with mEosNB-FTH1:

We mated RHY3171 (Kimbrough et al, forthcoming) to BY4741 [79] to obtain progeny that did not have the *pGal-WHI5::hphMX* construct, which resulted in the generation of SZY6594. This strain had the *hoΔ::natMX::tTa{Off}tet07^mEosNB-(G4s)3-FTH1* construct, and did not undergo cell cycle arrest when induced with Galactose.

Spot assays

For spot assays, we first grew the strains for each experiment in the appropriate SC dropout media overnight at 30°C. The next day, we measured the OD600 of each strain, and normalized the OD of all the strains to an OD of ~1. We then serially diluted these normalized cultures 10-fold (up to the dilution of 10^{-5}) in water and plated 5μL of each dilution on both SC dropout media and SC Galactose dropout media. We imaged the plates post 72h of growth at 30°C, except in the case of Fig 4B and S4 Fig B C, where plates were grown for an additional day at 30°C to clearly visualize differences in poison toxicity.

For the spot assays presented in Fig 3D, we first grew the strains in 5mL SC-URA (uracil) media overnight at 30°C. The next day, we pelleted overnight cultures and resuspended in 1mL of sterile water. We then used 100μL of this as the first in the dilution series. This was diluted 5-fold, up to eleven dilutions in order to observe the toxicity/suppression clearly. We plated 5μL of each dilution on SC-URA media, SC Galactose-URA media and SC Galactose-URA media with 40mg/L Doxycycline (Calbiochem #324385). We imaged the plates post 72h of growth at 30°C.

For the spot assays presented in S5 Fig B, we first grew the strains in 5mL SC-TRP-URA media overnight at 30°C. The next day, we pelleted overnight cultures and resuspended in 1mL of sterile water. We then used 100μL of this as the first in the dilution series. This was diluted 5-fold, up to 11 dilutions in order to observe the toxicity/suppression clearly. We plated 5μL of each dilution on SC-TRP-URA media and SC Galactose-TRP-URA media. We imaged the plates post 72h of growth at 30°C.

Microscopy

The appropriate strains for each experiment were first grown in 5mL of the appropriate SC dropout media overnight at 30°C. The next day, we inoculated 3mL of SC Raffinose dropout media with 1mL of the saturated overnight cultures and let them grow overnight at 30°C. On the following day, we pelleted the cultures and resuspended the cells in 3mL SC Galactose dropout media and incubated at 30°C. Cells were induced for 4-6 hours on SC Galactose dropout media, and then imaged on a Zeiss LSM 980 confocal microscope which consisted of an Axio Observer Z1 base, through a 40x C-Apochromat (NA = 1.2) water immersion objective. The GFP and mCherry tagged proteins were excited at 488 and 561 nm, respectively. Emission was collected in channel mode onto a GaAsP detector in photon counting mode through a 491-544 nm bandpass for GFP and a 570-632 nm bandpass for mCherry. Transmitted light was also collected. Image fields of view were zoomed optically to a ~26 µm square with 512 pixels in each dimension.

For imaging cells expressing *S. octosporus* Wtf61^{antidote}-GFP, *S. kambucha* Wtf4^{poison}-GBP-mCh and Rnq1-mCardinal, we first grew cells in SC-Trp-Ura-Leu media. The next day, we inoculated 3mL of SC Raffinose-Trp-Ura-Leu media with 1mL of the saturated overnight cultures and let them grow overnight at 30°C. The following day, we pelleted the cultures and resuspended the

cells in 3mL SC Galactose-Trp-Ura-Leu + 500nM β-estradiol (VWR, # #AAAL03801-03) media and incubated at 30°C. Cells were induced for 4 hours and then imaged as described above, except that we also excited mCardinal tagged proteins at 640nm and collected the emission on channel mode onto a 650-700 nm bandpass detector of the Zeiss LSM 980 confocal microscope.

Spectral unmixing for mEosNB-FTH1 strains

For imaging the mEosNB-FTH1 strains, we first grew the strains in 5mL SC-URA+40mg/L Doxycycline. The next day, we inoculated 3mL of both SC Raffinose-URA and SC Raffinose-URA+40mg/L Doxycycline media with 1mL of the saturated overnight cultures and let them grow overnight at 30°C. The following day, we pelleted the cultures and resuspended the cells in 3mL of both SC Galactose-URA and SC Galactose-URA+40mg/L Doxycycline and incubated at 30°C. The rest of the methodology was as described in the section above.

The background fluorescence for strains constructed with SZY6594 had high autofluorescence in the GFP channel. To distinguish autofluorescence from true mEos signal, we spectrally unmixed the images. First, we captured spectral images with the lambda mode on the dectector of the Zeiss LSM 980 confocal microscope (same settings as above), exciting the cells at 488 nm and collecting emission over the entire visual spectrum, We then made reference spectra for mEos and autofluorescence from control cells, and then spectrally unmixed images using an in-house written plugin on ImageJ (https://research.stowers.org/imagejplugins/). The data presented in Figure 3C has transmitted light images collected on the channel mode with GFP excitation, and the spectrally unmixed images collected on lambda mode.

Image analysis to quantify colocalization of mEos and mCherry signals in tagged constructs

Cell regions of interest (ROIs) were found based on the transmitted light only using Cellpose (https://www.cellpose.org/) in Python using the “cyto” model and a diameter of 200. Pixels from these ROIs were then background subtracted using an average background signal from an ROI placed away from any cell. The Scipy Pearson Correlation for each cell ROI was then calculated for all pixels in each cell. Dead cells and aberrant ROIs were hand filtered out using Fiji (https://fiji.sc/). Find the raw data for these analyses in S1 Data.

DAmFRET

We performed the analysis similar to the methods in [15], with a few exceptions. We grew the strains in the same method described for microscopy, however, we induced the cells for 5-6 hours. We then photoconverted the cells post induction for 5 minutes, using the OmniCure S2000 Elite UV lamp for photoconversion. The total power over 5 minutes of exposure amounts to 12.048 J/cm^2. The sample collection and data analysis were similar to methods described in [15] with a few exceptions. We included an empty vector strain in each experiment to effectively exclude auto fluorescent cell populations. All the cells for each experiment were induced at the same time, for the same amount of time, and were grown in the same 96-well plate. Three technical replicates were included for each sample.

There was only one fluorescent population that was independent of expression level for each construct analyzed. In order to clearly visualize AmFRET values across the cells expressing different constructs, we analyzed cells above a certain Acceptor fluorescence intensity threshold set for each experiment. For each set of experimental data, the median of the poison AmFRET values was calculated. The difference of this median value from 1 was then added to all the datasets within an experiment. For visualizing the results of the DAmFRET experiments, plots of AmFRET values were generated using GraphPad Prism 10 (Version 10.2.3 (347)).

Statistical analysis for the DAmFRET experiments involved pooling the technical replicates and performing pairwise t-tests comparing these values to either the wild-type Wtf4^{poison}-mEos dataset, or the monomer dataset. For each DAmFRET experiment, we then did a multiple sampling correction (Bonferroni correction) by dividing the p value cutoff (0.05) by the number of tests performed. Find the raw data and statistical analysis for each DAmFRET experiment in S2 Data.

We used GraphPad Prism 10 (Version 10.2.3 (347)) to visualize acceptor fluorescence intensity values of live cells expressing the relevant Wtf^{poison} constructs. Three technical replicates of each isolate were plotted, with the median included. Find the raw data for this analysis in S2 Data.

Figure legends

Figure 1. Features of *wtf4* and mutant alleles.

A. A cartoon of *S. kambucha wtf4* coding sequence (CDS). Wtf4^{antidote} coding sequence is shown in magenta, which includes exons 1-6. The Wtf4^{poison} coding sequence is shown in cyan, which includes 21 base pairs from intron 1 (in grey), and exons 2-6. **B.** Features of Wtf4^{antidote} and Wtf4^{poison} proteins. Row 1 shows predicted secondary structure domains and functional motifs, including PY motifs (in mustard) and predicted transmembrane domains (in red). Row 2 shows the coding sequence repeats in exon 3 and exon 6. Row 3 highlights a well-conserved region 9 amino acids long. Row 4 is the normalized hydrophobicity of the Wtf4 proteins from ProtScale, with the Kyle and Doolittle Hydropathy scale [80]. The higher the number on the scale, the higher the hydrophobicity of the amino acid. See S5 and S6 Tables for detailed descriptions. **C.** Percentage amino acid identity of Wtf^{antidotes} from 33 *wtf* driver genes from four isolates of *S. pombe* [20]. The antidote sequences were aligned using Geneious Prime (2023.0.4) and the percentage amino acid identity is depicted as a heatmap, with yellow being 100% identity. *S. kambucha wtf4* CDS is shown below for comparison, with the exons labeled corresponding to the consensus. Labeled areas within exons 3 and 6, where identity is low, represent the expansion and contraction of the coding sequence repeats of different *wtf* genes. **D.** Cartoon of *wtf4* mutants constructed in this study. Each mutant category was constructed based on a specific feature mentioned above. The categories are depicted with a wild type *wtf4* allele at the top. Each mutant allele is represented by *wtf-'x,'* where 'x' is the mutant allele number. See S1 Table for a comprehensive overview of the alleles and their phenotypes.

Figure 2. Extremely diverged toxic Wtf^{poison} proteins exhibit similar self-assembly and intracellular localization.

A. Cartoon illustrating the Distributed Amphifluoric FRET (DAmFRET) assay (modified from [30]). AmFRET values for individual cells were calculated by dividing the acceptor fluorescence by the FRET fluorescence, both measured via cytometry. **B.** Combined AmFRET values for three technical replicates of the specified Wtf^{poison}-mEos proteins and monomer-mEos (negative control). X^{P} represents the WtfX poison proteins tested here. The median is indicated with a solid line and the bars represent the interquartile range. For easier comparison, the values were normalized so that Wtf4^{poison} had a median of 1 in each experiment. Statistical significance: ns $p>0.01$, *$p<0.01$; t-tests with Bonferroni correction. See S2 Data for p-values. **C.** A spot assay of cells serially diluted and plated on SC-Trp-Ura and SC Gal-Trp-Ura plates. Each strain carries an empty [*TRP1*] plasmid, and either an empty [*URA3*] plasmid (EV) or the indicated *wtf^{poison}-mEos* allele under the control of a galactose-inducible promoter. The plates were grown at 30•C

for 3 days. **D.** Representative images of the same strains depicted in C were induced in galactose media for 4 hours at 30•C to express the indicated mEos-tagged proteins. The images are not at the same brightness and contrast settings to clearly show localization of tagged proteins. TL is transmitted light, and the scale bar is 4 µm.

Figure 3. Increasing poison assembly with tags suppresses Wtf^{poison} toxicity.

A. A cartoon of the constructs used in this experiment (C-D). The mEosNB-FTH1 construct was integrated into the genome and is under the control of a doxycycline-repressible promoter. mEosNB is a nanobody that binds mEos. The *wtf^{poison}* alleles are carried on a [*URA3*] plasmid and are under the control of a galactose-inducible promoter. **B.** Cartoon of the constructs expressed on each medium used: SC-Ura, SC Galactose-Ura + 40 mg/L doxycycline, and SC Galactose-Ura. FTH1 is a 24-mer, but is depicted as an 8-mer core. **C.** Representative images of cells induced with galactose media (with or without 40mg/L Doxycycline) for 4 hours at 30•C to express the indicated Wtf^{poison}mEos proteins. The cells induced without Doxycycline (-Dox) also express mEosNB-FTH1. This strain background exhibits high autofluorescence, so we spectrally unmixed the signal to remove autofluorescence (See Methods). The images are not at the same brightness and contrast settings to clearly show localization of tagged proteins. TL is transmitted light, and the scale bar is 4 µm. **D.** A spot assay of cells carrying the constructs illustrated in A-C serially diluted on SC-Ura, SC Galactose-Ura + 40mg/L Doxycycline and SC Galactose-Ura plates and grown at 30•C for 3 days. Each strain carries either an empty [*URA3*] plasmid (EV) or the indicated *wtf^{poison}-mEos* allele. These media induce the expression of mEosNB-FTH1 (i), the indicated Wtf^{poison}-mEos protein (ii), or both (iii), respectively. The horizontal break in the image of each plate is due to rearrangements of the images to facilitate easy comparison. All strains within a panel were grown on the same plates (i.e., one SC-Trp-Ura or SC Gal-Trp-Ura or SC Gal-Trp-Ura + 40mg/L Doxycycline plate).

Figure 4. Reducing Wtf4^{poison} assembly with NT* tag increases toxicity and affects its rescue by Wtf4^{antidote}.

A. Cartoon of alleles used in this experiment (B-F). The NT* tag has a general anti-aggregation property [33]. **B.** A spot assay of cells serially diluted and plated on SC-Trp-Ura and SC Gal-Trp-Ura plates and grown at 30•C for 4 days. Each strain carries both a [*URA3*] and a [*TRP1*] plasmid. The plasmids are either empty (EV) or carry the indicated *wtf4* alleles under the control of galactose-inducible promoters. The horizontal break in the image for each plate is due to a rearrangement of the image to facilitate easy comparison. All strains were grown on the same

plates (i.e., one SC-Trp-Ura or SC Gal-Trp-Ura plate). **C.** AmFRET values for three technical replicates of the specified Wtf4^{poison}-mEos alleles and monomer-mEos (negative control). The median is indicated with a solid line and the bars represent the interquartile range. For easier comparison, the values were normalized so that Wtf4^{poison} had a median of 1 in each experiment. Since Wtf4-20^{poison}-mEos cells were very low in number, we pooled two biological replicates (n=6 technical replicates). Statistical significance: ns $p>0.025$, *$p<0.025$, t-tests with Bonferroni correction. Find the p-values in S2 Data. **D.** A spot assay of cells serially diluted and plated on SC-Trp-Ura and SC Gal-Trp-Ura plates and grown at 30•C for 3 days. Each strain carries both a [*URA3*] and a [*TRP1*] plasmid. The plasmids are either empty (EV) or carry the indicated *wtf4* alleles under the control of galactose-inducible promoters. The horizontal break in the image for each plate is due to a rearrangement of the image to facilitate easy comparison. All strains were grown on the same plates (i.e., one SC-Trp-Ura or SC Gal-Trp-Ura plate). **E.** Representative images of the same strains depicted in D were induced with galactose media for 4 hours at 30•C to express the indicated Wtf4^{poison}-mEos proteins and/or Wtf4^{antidote}-mCherry. The images are not at the same brightness and contrast settings to clearly show localization of tagged proteins. 4^{P} indicates Wtf4^{poison}, 4^{A} indicates Wtf4^{antidote}, TL is transmitted light, and the scale bar is 4 µm. **F**. Pearson's Correlation between mCherry and mEos signal in cells from E expressing the specified proteins. N>100, *** $p<0.001$, t-test.

Figure 5. Effective neutralization of Wtf4^{poison} requires more than a physical connection to a Wtf^{antidote}.

A. Cartoon of constructs used in this experiment. *S. kambucha wtf4^{poison}* was tagged at the C-terminus with either mCherry or GBP-mCherry (GBP: GFP-binding protein). *S. kambucha wtf4^{antidote}* was tagged with mEos or GFP. *S. octosporus wtf61^{antidote}* was tagged with GFP. *S. octosporus wtf61^{poison}* was tagged with mCherry. **B.** Experimental set up and summary of the results shown in C and D. In a matching Wtf protein pair (top), poison-antidote interaction and rescue of poison toxicity is observed. In the mismatched pair (bottom), interaction between GFP and GBP results in a forced interaction between the poison and the antidote (shown in D). This interaction is insufficient to rescue the mismatched poison (shown in C). **C.** Spot assay of cells serially diluted and plated on SC-Trp-Ura and SC Gal-Trp-Ura plates and grown at 30•C for 3 days. Each strain carries both a [*URA3*] and a [*TRP1*] plasmid. The plasmids are either empty (EV) or carry the indicated *wtf* alleles under the control of galactose-inducible promoters. The horizontal break in the image of each plate is due to rearrangements of the images to facilitate easy comparison. All strains within a panel were grown on the same plates (i.e., one SC-Trp-

Ura or SC Gal-Trp-Ura plate). **D.** Representative images of the same strains shown in C were induced in galactose for 4 hours at 30•C to express the indicated Wtf proteins. **E.** Representative images of cells induced with galactose and 500 nM β-estradiol for 4 hours at 30•C to produce the indicated proteins. Rnq1-mCardinal marks the insoluble protein deposit (IPOD) that is associated with the vacuole [46–48]. In D-E, the images are not at the same brightness and contrast settings to clearly show localization of tagged proteins. 4^{P} indicates $Wtf4^{poison}$, 4^{A} indicates $Wtf4^{antidote}$, 61^{P} indicates $Wtf61^{poison}$, 61^{A} indicates $Wtf61^{antidote}$, TL is transmitted light, and the scale bar is 4 µm.

Figure 6. Modification of *wtf4* exon 6 CDS repeats can disrupt antidote rescue.
A. Cartoon of two coding sequence repeat mutants of *S. kambucha wtf4*. **B**. Logo representing the amino acids encoded by the repeats found in exon 6 of *S. pombe wtf* genes from [20]. **C.** The amino acids encoded by the exon 6 repeats in *S. kambucha wtf4* and the *wtf4-4* and *wtf4-5* mutant alleles. **D.** Spot assay of cells serially diluted and plated on SC-Trp-Ura and SC Gal-Trp-Ura plates and grown at 30•C for 3 days. Each strain carries both a [*URA3*] and a [*TRP1*] plasmid. The plasmids are either empty (EV) or carry the indicated *wtf4* alleles under the control of galactose-inducible promoters. The horizontal breaks in the image of each plate are due to rearrangements of the images to facilitate easy comparison. All strains within a panel were grown on the same plates (i.e., one SC-Trp-Ura or SC Gal-Trp-Ura plate). **E.** Representative images the same strains depicted in D were induced in galactose for 4 hours at 30•C to express the indicated Wtf proteins. The images are not at the same brightness and contrast settings to clearly show localization of tagged proteins. The arrows in the TL panels highlight vacuoles. 4^{P} indicates $Wtf4^{poison}$, 4^{A} indicates $Wtf4^{antidote}$, TL indicates transmitted light, and the scale bar is 4 µm. **F**. Pearson's Correlation between mEos and mCherry signal in cells expressing the specified constructs from E. N>100, n.s. p>0.05, ***p<0.001, t-test.

Supplemental Information

S1 Figure. Wtf proteins share limited amino acid identity but have common features
A. A cartoon of *S. octosporus wtf25* coding sequence (CDS). $Wtf25^{antidote}$ coding sequence is shown in purple, which includes exons 1-5. The $Wtf4^{poison}$ coding sequence is shown in navy, which begins at the 27th base pair of exon 2 and extends through exon 5. Row 4 depicts the predicted transmembrane domains (in red) and PY motif (in mustard). Row 5 depicts the CDS repeats found in exon 4 (in cobalt). Row 6 depicts the normalized hydrophobicity of Wtf25

proteins from ProtScale, with the Kyle and Doolittle Hydropathy scale [80]. The higher the number on the scale, the higher the hydrophobicity of the amino acid. See S5 and S6 Tables for more detailed descriptions. **B.** Pairwise amino acid identity of the 6 Wtf^{antidote} proteins shown. The amino acid sequences were aligned using Geneious Prime (2023.0.4), and the percentage amino acid identity is depicted as a heatmap, with yellow being 100% identity. **C.** Depiction of CDS repeats and lengths of 6 *wtf^{antidote}* CDSs. The CDS repeats found in exon 6 of *S. kambucha wtf4* are homologous to those found in exon 4 of the other *wtf* genes [19]. The scale bar represents 108 base pairs (bp). **D-E.** *S. octosporus wtf25* (**D**), *S. cryophilus wtf1*, and *S. osmophilus wtf41* (**E**) mutants constructed in this study. The categories have their respective wild type allele shown on top. Each mutant allele is represented by *wtf-'x',* where 'x' is the mutant allele number. See S1 Table for a comprehensive overview of the alleles and their phenotypes.

S2 Figure. Deletion mutants affect Wtf4^{poison} toxicity, self-assembly and localization. Cartoon of *S. kambucha wtf4* exon deletion mutants (**A**), predicted transmembrane domain (TMD) deletion mutants (**B**) and a mutant that deletes a 9 amino acid conserved region encoded in exon 3 (**C**). **D.** A spot assay of cells serially diluted and plated on SC-Ura and SC Gal-Ura plates and grown at 30•C for 3 days. Each strain carries an empty [*LEU2*] plasmid, and either an empty [*URA3*] plasmid (EV) or the indicated *wtf4^{poison}-mEos* alleles under the control of a galactose-inducible promoter. The horizontal break in the image for each plate is due to rearrangement of the image to facilitate easy comparison. All strains were grown on the same plates (i.e., one SC-Leu-Ura or SC Gal-Leu-Ura plate). **E.** AmFRET values for three technical replicates of the specified Wtf4^{poison}-mEos proteins and monomer-mEos (negative control). The median is indicated with a solid line and the bars represent the interquartile range. For easier comparison, the values were normalized so that Wtf4^{poison} had a median of 1 in each experiment. Statistical significance: ns $p>0.008$, *$p<0.008$, **$p<0.0008$, t-tests between the means of each replicate, with Bonferroni correction. **F.** Representative images of the same strains depicted in D were induced in galactose media for 4 hours at 30•C to express the indicated mEos-tagged proteins. The images are not at the same brightness and contrast settings to clearly show localization of tagged proteins. 4^{P} indicates Wtf4^{poison}, TL is transmitted light, and the scale bar is 4 µm.

S3 Figure. C-terminal truncations have inconsistent effects on Wtf^{poison} protein toxicity.

A. Cartoon of C-terminal truncation mutants of *S. kambucha wtf4*. **B.** Cartoon illustrating the amino acids lost with the C-terminal truncation alleles of *wtf4*. The amino acids comprising the exon 6 coding sequence repeats are highlighted in pink. **C.** A spot assay of cells serially diluted and plated on SC-TRP-URA and SC Gal-TRP-URA plates and grown at 30•C for 3 days. Each strain carries both an empty [*TRP1*] plasmid (EV) and a [*URA3*] plasmid that is either empty or carries the indicated *wtf4^{poison}-mEos* allele under the control of a galactose inducible promoter. **D.** AmFRET values for three technical replicates of the specified Wtf4^{poison}-mEos alleles and monomer-mEos (negative control). The median is indicated with a solid line and the bars represent the interquartile range. For easier comparison, the values were normalized so that Wtf4^{poison} had a median of 1 in each experiment. Statistical significance: ns $p>0.0125$, *$p<0.0125$, t-test with Bonferroni correction. Find p-values in S2 Data. **E.** Representative images of the same strains depicted in C were induced with galactose media for 4 hours at 30•C to express the indicated mEos-tagged proteins. The images are not at the same brightness and contrast settings to clearly show localization of tagged proteins. 4^{P} indicates Wtf4^{poison}, TL is transmitted light, and the scale bar is 4 µm. **F.** Cartoons of C-terminal truncation mutants of *S. cryophilus wtf1* (*wtf1-1*), *S. osmophilus wtf41* (*wtf41-1*), and *S. octosporus wtf25* (*wtf25-3*). **G.** Spot assays of cells serially diluted and plated on SC-URA and SC Gal-URA plates and grown at 30•C for 3 days. Each strain carries either an empty [*URA3*] plasmid (EV), or the indicated *wtf^{poison}-mEos* allele under the control of a galactose-inducible promoter. The horizontal breaks in the images for each plate are due to rearrangements of the image to facilitate easy comparison. All strains were grown on the same plates (i.e., one SC-Ura or SC Gal-Ura plate).

S4 Figure. **Reducing assembly with NT* tag increases Wtf25^{poison} toxicity.**
A. Cartoon of alleles used in this experiment (B-E). The NT* tag has a general anti-aggregation property [33]. **B-C.** Spot assays of cells serially diluted on SC-Trp-Ura and SC Gal-Trp-Ura plates and grown at 30•C for 4 days. Each strain carries both a [*URA3*] and a [*TRP1*] plasmid. The plasmids are either empty (EV) or carry the indicated *wtf25* alleles under the control of galactose-inducible promoters. In B, the horizontal break in the image of each plate is due to a rearrangement of the image to facilitate easy comparison. All strains within a panel were grown on the same plates (i.e., one SC-Trp-Ura or SC Gal-Trp-Ura plate for panel B). **D.** Representative images of the same strains shown in C were induced with galactose media for 4 hours at 30•C to express the indicated Wtf25^{poison}-mEos proteins and/or Wtf25^{antidote}-mCherry. The images are not at the same brightness and contrast settings to clearly show localization of tagged proteins. 25^{P} indicates Wtf25^{poison}, 25^{A} indicates Wtf25^{antidote}, TL is transmitted light, and

the scale bar is 4 µm. **E**. Pearson's Correlation between mCherry and mEos signal in cells from D expressing the specified proteins. N>100, p>0.05, t-test.

S5 Figure. Reducing Wtf^{poison} assembly with MBP tag affects toxicity.

A. Cartoon of alleles used in this experiment (B-C). MBP is the *E. coli* Maltose Binding Protein [75]. **B.** Spot assay of cells serially diluted and plated on SC-Trp-Ura and SC Gal-Trp-Ura plates and grown at 30•C for 4 days. Each strain carries both an empty [*TRP1*] plasmid and a [*URA3*] plasmid that is either empty (EV) or carries the indicated *wtf^{poison}-mEos* allele under the control of a galactose-inducible promoter. The horizontal break in the image of each plate is due to rearrangement of the image to facilitate easy comparison. All strains were grown on the same plates (i.e., one SC Gal-Trp-Ura plate or SC-Trp-Ura). **C.** Representative images of the same strains depicted in B induced with galactose media for 4 hours at 30•C to express the indicated mEos-tagged proteins. The images are not at the same brightness and contrast settings to clearly show localization of tagged proteins. 4^{P} indicates Wtf4^{poison}, 25^{P} indicates Wtf25^{poison}, TL is transmitted light, and the scale bar is 4 µm. **D.** AmFRET values for three technical replicates of the specified Wtf^{poison}-mEos alleles and monomer-mEos (negative control). The median is indicated with a solid line and the bars represent the interquartile range. For easier comparison, the values were normalized so that Wtf4^{poison} had a median of 1 in each experiment. Statistical significance: ns p>0.016, *p<0.016, t-test with Bonferroni correction. Find p-values in S2 Data.

S6 Figure. The fluorescence signal intensity of expressed Wtf^{poison} proteins does not correlate with toxicity.

A-F Acceptor fluorescence intensity (in arbitrary units, a.u.) of similarly sized live cells across all Wtf DAmFRET experiments in this study, with the line indicating the median of the population. Data represented here is from the following experiments: A corresponds to Fig 2B, B corresponds to S3 Fig E, C corresponds to S4 Fig D, D corresponds to Fig 4C, E corresponds alleles in S4 Fig, and F corresponds to S5 Fig D respectively. The Y-axis is scaled to a log10 scale. The data are color coded, with toxic poisons in teal, and non-toxic alleles in orange.

S7 Figure. Limited modularity of the Wtf4^{antidote}-specific domain.

A. Cartoon of *wtf4^{antidote}* exon 1 and mutants that relocate, or both relocate and mutate the exon. Wild-type PY motifs are shown in orange and mutated (PY to PA) motifs are in red. **B.** AmFRET values for three technical replicates of the specified mEos-tagged proteins and monomer-mEos (negative control). The median is indicated with a solid line and the bars represent 1.5 times the

interquartile range. For easier comparison, the values were normalized so that Wtf4^{poison} had a median of 1 in each experiment. Statistical significance: ns p>0.0125, *p<0.0125, t-tests with Bonferroni correction. Find p-values in S2 Data. **C-E.** Spot assays of cells serially diluted on SC-Trp-Ura and SC Gal-Trp-Ura plates and grown at 30•C for 3 days. Each strain carries both a [*URA3*] and a [*TRP1*] plasmid. The plasmids are either empty (EV) or carry the indicated *wtf4* alleles under the control of galactose-inducible promoters. The horizontal breaks in the images of each plate in panels C and E are due to rearrangements of the images to facilitate easy comparison. All strains within a panel were grown on the same plates (i.e., one SC-Trp-Ura or SC Gal-Trp-Ura plate for panel C). **F.** Representative images of the same strains shown in C induced with galactose media for 4 hours at 30•C to express the Wtf4^{poison}-mEos, Wtf4 exon1-mCherry, or both proteins. **G.** Representative images of the same strains shown in D were induced with galactose media for 4 hours at 30•C to the indicated *wtf4* alleles. **H.** Representative images of the same strains shown in E induced with galactose media for 4 hours at 30•C to express the indicated *wtf4* alleles. In F-H, arrows in the transmitted light images indicate vacuoles. The images are not at the same brightness and contrast settings to clearly show localization of the tagged proteins. 4^{P} indicates Wtf4^{poison}, 4^{A} indicates Wtf4^{antidote}, Ex1 is Wtf4 exon1, TL is transmitted light, and the scale bar is 4 µm.

S8 Figure. Effective neutralization of Wtf25^{poison} requires more than a physical connection to a Wtf^{antidote}.

A. Cartoon of constructs used in this experiment. *S. octosporus* Wtf25^{poison} was tagged at the C-terminus with either mCherry or GBP-mCherry (GBP: GFP-binding protein). *S. octosporus* Wtf25^{antidote} was tagged with mEos or GFP. *S. cryophilus* Wtf1^{antidote} was tagged with GFP. *S. cryophilus* Wtf1^{poison} was tagged with mCherry. **B.** Experimental set up and summary of the results shown in C and D. In a matching Wtf protein pair (top), poison-antidote interaction and rescue of poison toxicity is observed. In the mismatched pair (bottom), interaction between GFP and GBP results in a forced interaction between the poison and the antidote (shown in D). This interaction is insufficient to rescue the mismatched poison (shown in C). **C.** Spot assay of cells serially diluted and plated on SC-Trp-Ura and SC Gal-Trp-Ura plates and grown at 30•C for 3 days. Each strain carries both a [*URA3*] and a [*TRP1*] plasmid. The plasmids are either empty (EV) or carry the indicated *wtf* alleles under the control of galactose-inducible promoters. The horizontal breaks in the images of each plate are due to rearrangements of the image to facilitate easy comparison. All strains within a panel were grown on the same plates (i.e., one SC-Trp-Ura or SC Gal-Trp-Ura plate). **D.** Representative images the strains depicted in C were

induced in galactose for 4 hours at 30•C to express the indicated Wtf proteins. The images are not at the same brightness and contrast settings to clearly show localization of tagged proteins. 25^{P} indicates $Wtf25^{poison}$, 25^{A}- indicates $Wtf25^{antidote}$, 1^{P} indicates $Wtf1^{poison}$, 1^{A} indicates $Wtf1^{antidote}$, TL indicates transmitted light, and the scale bar is 4 µm.

S9 Figure. *wtf4* coding sequence repeats are dispensable, but can affect antidote rescue. **A.** Cartoon of exon 3 and exon 6 coding sequence repeat deletion mutants of *S. kambucha wtf4*. **B-C.** Logo for amino acids encoded by the repeats found in exon 3 (B) and exon 6 (C) of *S. pombe wtf* genes from [20]. The sequence of the amino acids encoded in each repeat region in *S. kambucha wtf4* is shown below each logo. **D.** Spot assay of cells serially diluted and plated on SC-Trp-Ura and SC Gal-Trp-Ura plates and grown at 30•C for 3 days. Each strain carries both a [*URA3*] and a [*TRP1*] plasmid. The plasmids are either empty (EV) or carry the indicated *wtf4* alleles under the control of galactose-inducible promoters. The horizontal break in the image of each plate is due to rearrangements of the images to facilitate easy comparison. All strains within a panel were grown on the same plates (i.e., one SC-Trp-Ura or SC Gal-Trp-Ura plate). **E.** Representative images of the same strains as depicted in D were induced in galactose for 4 hours at 30•C to express the indicated Wtf4 proteins. The images are not at the same brightness and contrast settings to clearly show localization of tagged proteins. The arrows in the TL panels highlight vacuoles. 4^{P} indicates $Wtf4^{poison}$, 4^{A} indicates $Wtf4^{antidote}$, TL indicates transmitted light, and the scale bar is 4 µm. **F**. Pearson's Correlation between mEos and mCherry signal in cells expressing the specified constructs from E. N>100, n.s. p>0.05, ***p<0.001, t-test.

S10 Figure. Coding sequence repeat mutants do not interact with wildtype Wtf4 proteins functionally.
A. Cartoon of coding sequence repeat mutants of *S. kambucha wtf4.* **B-E.** Spot assays of cells serially diluted on SC-Trp-Ura and SC Gal-Trp-Ura plates and grown at 30•C for 3 days. Each strain carries both a [*URA3*] and a [*TRP1*] plasmid. The plasmids are either empty (EV) or carry the indicated *wtf4* alleles under the control of galactose-inducible promoters. The horizontal breaks in the images in within a panel are due to rearrangements of the images to facilitate easy comparison. All strains within a panel were grown on the same plates (i.e., one SC-Trp-Ura or SC Gal-Trp-Ura plate in panel B).

S11 Figure. Swapping *wtf* CDS repeats across species affects Wtf25 antidote rescue.

A. Cartoon of a coding sequence repeat mutant of *S. octosporus wtf25*. **B**. Logo representing the amino acids encoded by the repeats found in exon 4 of *S. octosporus wtf* genes from [19]. **C.** The amino acids encoded by the exon 4 repeats of *S. octosporus wtf25* and by the 6 repeats of *S. kambucha wtf4*. **D.** Spot assay of cells serially diluted and plated on SC-Trp-Ura and SC Gal-Trp-Ura plates and grown at 30•C for 3 days. Each strain carries both a [*URA3*] and a [*TRP1*] plasmid. The plasmids are either empty (EV) or carry the indicated *wtf25* alleles under the control of galactose-inducible promoters. The horizontal breaks in the images are due to rearrangements of the images to facilitate easy comparison. All strains within a panel were grown on the same plates (i.e., one SC-Trp-Ura or SC Gal-Trp-Ura plate). **E.** Representative images of the same strains depicted in D were induced in galactose for 4 hours at 30•C to express the indicated Wtf25 proteins. The images are not at the same brightness and contrast settings to clearly show localization of tagged proteins. The arrows in the TL panel highlight vacuoles. 25^{P} indicates $Wtf25^{poison}$, 25^{A} indicates $Wtf25^{antidote}$, TL indicates transmitted light, and the scale bar is 4 µm.

S12 Figure. *S. octosporus wtf25* coding sequence repeats are functionally dispensable for poison toxicity but promote antidote rescue.

A. Cartoon of *S. octosporus wtf25* exon 4 coding sequence repeat deletion mutant. **B.** Logo for the amino acids encoded by the repeats found in exon 4 of *S. octosporus wtf* genes from [19] **C.** Spot assay of cells serially diluted and plated on SC-Trp-Ura and SC Gal-Trp-Ura plates and grown at 30•C for 4 days. Each strain carries both a [*URA3*] and a [*TRP1*] plasmid. The plasmids are either empty (EV) or carry the indicated *wtf25* alleles under the control of galactose-inducible promoters. The horizontal breaks in the images are due to rearrangements of the images to facilitate easy comparison. All strains within a panel were grown on the same plates (i.e., one SC-Trp-Ura or SC Gal-Trp-Ura plate). **D.** Representative images the same strains depicted in C were induced in galactose for 4 hours at 30•C to express the indicated Wtf25 proteins. The images are not at the same brightness and contrast settings to clearly show localization of tagged proteins. The arrows in the TL panels highlight vacuoles. 25^{P} indicates $Wtf25^{poison}$, 25^{A} indicates $Wtf25^{antidote}$, TL indicates transmitted light, and the scale bar is 4 µm.

S13 Figure. Idiosyncratic poison and antidote compatibility between wild-type and truncation alleles of *wtf4*.

A. Cartoon of *S. kambucha wtf4* C-terminal truncation mutants. **B.** Spot assay of cells serially diluted and plated on SC-Trp-Ura and SC Gal-Trp-Ura plates and grown at 30•C for 3 days.

Each strain carries both a [*URA3*] and a [*TRP1*] plasmid. The plasmids are either empty (EV) or carry the indicated *wtf4* alleles under the control of galactose-inducible promoters. The horizontal breaks in the images are due to rearrangements of the images to facilitate easy comparison. All strains within a panel were grown on the same plates (i.e., one SC-Trp-Ura or SC Gal-Trp-Ura plate). **C.** Representative images the strains depicted in B were induced in galactose for 4 hours at 30•C to express the indicated Wtf4 proteins. The images are not at the same brightness and contrast settings to clearly show localization of tagged proteins. The arrows in the TL panels highlight vacuoles. 4^{P} indicates $Wtf4^{poison}$, 4^{A} indicates $Wtf4^{antidote}$, TL indicates transmitted light, and the scale bar is 4 µm.

S14 Figure. C-terminus truncation alleles of diverged Wtf^{poison}s are rescued by their corresponding wild-type $Wtf^{antidote}$s.

A. Cartoon of *S. cryophilus wtf1*, *S. osmophilus wtf41*, and *S. octosporus wtf25* C-terminal truncation mutants. **B-D.** Spot assays of cells serially diluted on SC-Trp-Ura and SC Gal-Trp-Ura plates and grown at 30•C for 3 days. Each strain carries both a [*URA3*] and a [*TRP1*] plasmid. The plasmids are either empty (EV) or carry the indicated *wtf* alleles under the control of galactose-inducible promoters. The horizontal breaks in the images within a panel are due to rearrangements of the images to facilitate easy comparison. All strains within a panel were grown on the same plates (i.e., one SC-Trp-Ura or SC Gal-Trp-Ura plate).

S1 Table. Overview of *wtf* alleles and their phenotypes in this study. Columns 1-2 describe the allele names and their construction. Columns 3-4 describe the toxicity of the poison and antidote proteins encoded by the corresponding allele. Column 5 notes if the mutant antidote can rescue the corresponding poison allele. Column 6-7 note if the specific antidote allele can rescue the wild-type poison (Column 6), or if the specific poison can be rescued by the wild-type antidote (Column 7). Column 9 notes if the corresponding antidote can rescue other poison alleles. Column 10 notes the AmFRET values are comparable to the wild-type $Wtf4^{poison}$-mEos or monomer-mEos. Finally, column 11 notes the figures/supplemental figures where these alleles can be found. Rows are separated based on the wild-type allele that the mutants were constructed from, where applicable. ND indicates that the specified experiment was not done.

S2 Table. Yeast strains used in this study. Column 1 is the figure where these strains were used, Column 2 is the name of the yeast strain and column 3 is the genotype of the strain. If the

strain was constructed in this study, column 4 has the details on how the strain was constructed. If the strain was constructed in another study, column 5 notes the references for the same.

S3 Table. Plasmids used in this study. Column 1 denotes if the plasmids were used for strain construction or cloning, and the specific wild-type alleles that the plasmids correspond to. Column 2 is the name of the plasmid and column 3 is a short description of the plasmid. If the plasmid was not constructed in this study, column 4 references the studies the plasmids were constructed in.

S4 Table. Oligos used in this study. Column 1 denotes the name of the oligo and column 2 has the sequence of the oligos. If the oligo was not constructed in this study, column 3 references the studies the oligos were used in.

S5 Table. Overview of features across *wtf* driver genes. Column 1 denotes the *wtf* driver gene, and columns 2-8 describe specific features of each gene and their encoded proteins. Column 2 notes if the gene has been shown to drive in fission yeast or been shown to encode for functional Wtf poison and antidote proteins in *S. cerevisiae*. Column 3 notes the number of exons in the gene, and column 4 notes the size of the $Wtf^{antidote}$ protein in amino acids. If the antidote sequence had a predicted coiled-coil domain, column 4 notes the size and location in the antidote protein as described in [15]. Column 5 notes the numbers of PY motifs (L/PPXY; [24]) in exon 1. While some $Wtf^{antidote}$ proteins also have an additional PY motif in exon 2, we didn't include that information here since those motifs are shared by the corresponding poison proteins as well. Column 6 notes the number of predicted transmembrane domains predicted by TMHMM2.0 [71,72]. Column 7 notes the length of the exon 3 coding sequence repeats (if present) in amino acids. Column 8 notes the length of the exon 4/6 coding sequence repeats (if present) in amino acids. NA (not applicable) here indicates that the repeats were not present in the Wtf protein. Column 8 mentions the reference(s) where these genes/encoded proteins were characterized.

S6 Table. Overview of predicted transmembrane domains of $Wtf^{antidote}$ proteins. The results from the TMHMM2.0 [71,72] analysis of $Wtf^{antidote}$ proteins encoded by *wtf* driver genes in S5 table are detailed here. Find the specific results of the analyses, including the number of amino acids in the predicted transmembrane domains, probability of the N-terminal being

internal to the membrane (N-in), the specific location and the length of the predicted transmembrane domains.

S1 Data. Raw Data for Pearson's Correlation tests performed in this study. Each sheet contains the raw data for the Pearson's Correlation tests and the statistical analysis corresponding to the tests performed in Fig 4F, S4 Fig E, Fig 6F and S9 Fig F respectively. See Methods for how this analysis was performed.

S2 Data. Raw Data for AmFRET plots presented in this study. Each sheet contains the raw data and the statistical analysis for the AmFRET plots of different Wtf^{poison}-mEos proteins, Wtf4^{antidote}-mEos, *S. kambucha wtf4* Exon1-mEos and monomer-mEos proteins in Fig 2B, S2 Fig E, S3 Fig D, Fig 4C, S5 Fig, S6 Fig D and S7 Fig B respectively. The corresponding raw data for the Acceptor fluorescence intensity presented in S6 Fig for each of these experiments are found next to the relevant AmFRET data. See Methods for how this analysis was performed.

Acknowledgements

We thank the members of the Zanders lab, the Halfmann lab and the Core facilities at Stowers Institute for their help and guidance throughout the stages of development of this paper.

Data Availability

All relevant data are within the manuscript and the Supporting Information Files. Additional raw data and images can be found at the Stowers Original Data Repository. Instructions for accessing data from the Stowers original data repository via FTP can be found at https://www.stowers.org/research/publications/odr#ftp.

Funding

This work was supported by The Stowers Institute for Medical Research (SEZ, RHN); National Institutes of Health (NIH) R35 GM151982-01 and DP2 GM132936 (SEZ); and the Eunice Kennedy Shriver National Institute of Child Health & Human Development of the NIH under Award Number F31HD097974 (NLN). The funders had no role in study design, data collection and analysis, or manuscript preparation. The content is solely the responsibility of the authors and does not necessarily represent the official views of the funders.

Competing interests

I have read the journal's policy, and the authors of this manuscript have the following competing interests: NLN, SEZ: Inventor on patent application based on *wtf* meiotic drivers. Patent application serial 62/491,107. The other authors declare that no competing interests exist.

References

[1] Burt A, Trivers R. Genes in Conflict. Harvard University Press; 2006. https://doi.org/10.2307/J.CTVJHZRC6.

[2] Sandler L, Novitski E. Meiotic Drive as an Evolutionary Force. Am Nat 1957;91:105–10.

[3] Bravo Núñez MA, Nuckolls NL, Zanders SE. Genetic Villains: Killer Meiotic Drivers. Trends in Genetics 2018;34:424–33. https://doi.org/10.1016/j.tig.2018.02.003.

[4] Zanders SE, Unckless RL. Fertility Costs of Meiotic Drivers. Current Biology 2019;29:R512–20. https://doi.org/10.1016/j.cub.2019.03.046.

[5] Wang C, Wang J, Lu J, Wang H, Wu C, Xiong Y, et al. A natural gene drive system confers reproductive isolation in rice. Cell 2023;186:3577–92. https://doi.org/10.1016/j.cell.2023.06.023.

[6] Xie Y, Shen R, Chen L, Liu YG. Molecular mechanisms of hybrid sterility in rice. Sci China Life Sci 2019;62:737–43. https://doi.org/10.1007/S11427-019-9531-7.

[7] Li J, Zhou J, Zhang Y, Yang Y, Pu Q, Tao D. New Insights into the Nature of Interspecific Hybrid Sterility in Rice. Front Plant Sci 2020;11. https://doi.org/10.3389/FPLS.2020.555572.

[8] Myint ZM, Koide Y, Takanishi W, Ikegaya T, Kwan C, Hikichi K, et al. OlCHR, encoding a chromatin remodeling factor, is a killer causing hybrid sterility between rice species *Oryza sativa* and *O. longistaminata*. IScience 2024;27. https://doi.org/10.1016/J.ISCI.2024.109761.

[9] Saupe SJ, Johannesson H. On the Mechanistic Basis of Killer Meiotic Drive in Fungi. Annu Rev Microbiol 2022; 76:305–23. https://doi.org/10.1146/ANNUREV-MICRO-041320-113730.

[10] Simon M, Durand S, Ricou A, Vrielynck N, Mayjonade B, Gouzy J, et al. APOK3, a pollen killer antidote in *Arabidopsis thaliana*. Genetics 2022;221. https://doi.org/10.1093/GENETICS/IYAC089.

[11] Wang D, Wang H, Xu X, Wang M, Wang Y, Chen H, et al. Two complementary genes in a presence-absence variation contribute to *indica-japonica* reproductive isolation in rice. Nat Commun 2023;14. https://doi.org/10.1038/S41467-023-40189-X.

[12] You S, Zhao Z, Yu X, Zhu S, Wang J, Lei D, et al. A toxin-antidote system contributes to interspecific reproductive isolation in rice. Nat Commun 2023;14. https://doi.org/10.1038/S41467-023-43015-6.

[13] Courret C, Wei X, Larracuente AM. New perspectives on the causes and consequences of male meiotic drive. Curr Opin Genet Dev 2023;83. https://doi.org/10.1016/J.GDE.2023.102111.

[14] Lai EC, Vogan AA. Proliferation and dissemination of killer meiotic drive loci. Curr Opin Genet Dev 2023;82. https://doi.org/10.1016/J.GDE.2023.102100.

[15] Nuckolls NL, Mok AC, Lange JJ, Yi K, Kandola TS, Hunn AM, et al. The *wtf4* meiotic driver utilizes controlled protein aggregation to generate selective cell death. Elife 2020; 9:1–35. https://doi.org/10.7554/eLife.55694.

[16] Urquhart AS, Gardiner DM. A Natural Fungal Gene Drive Enacts Killing via DNA Disruption. MBio 2023;14. https://doi.org/10.1128/MBIO.03173-22.

[17] Hu W, Jiang Z Di, Suo F, Zheng JX, He WZ, Du LL. A large gene family in fission yeast encodes spore killers that subvert Mendel's law. Elife 2017;6. https://doi.org/10.7554/ELIFE.26057.

[18] Brysch-Herzberg M, Jia GS, Sipiczki M, Seidel M, Li W, Assali I, et al. *Schizosaccharomyces lindneri* sp. nov., a fission yeast occurring in honey. Yeast 2023; 40:237–53. https://doi.org/10.1002/YEA.3857.

[19] De Carvalho M, Jia GS, Nidamangala Srinivasa A, Billmyre RB, Xu YH, Lange JJ, et al. The *wtf* meiotic driver gene family has unexpectedly persisted for over 100 million years. Elife 2022;11. https://doi.org/10.7554/eLife.81149.

[20] Eickbush MT, Young JM, Zanders SE. Killer meiotic drive and dynamic evolution of the *wtf* gene family. Mol Biol Evol 2019; 36:1201–14. https://doi.org/10.1093/molbev/msz052.

[21] Xu Y-H, Suo F, Zhang X-R, Du T-Y, Hua Y, Jia G-S, et al. Evolutionary modes of *wtf* meiotic driver genes in *Schizosaccharomyces pombe*. BioRxiv 2024:2024.05.30.596636. https://doi.org/10.1101/2024.05.30.596636.

[22] Nuckolls NL, Núñez MAB, Eickbush MT, Young JM, Lange JJ, Yu JS, et al. *wtf* genes are prolific dual poison-antidote meiotic drivers. Elife 2017;6. https://doi.org/10.7554/ELIFE.26033.

[23] Nuckolls NL, Nidamangala Srinivasa A, Mok AC, Helston RM, Núñez MAB, Lange JJ, et al. *S. pombe wtf* drivers use dual transcriptional regulation and selective protein exclusion from spores to cause meiotic drive. PLoS Genet 2022;18. https://doi.org/10.1371/JOURNAL.PGEN.1009847.

[24] Zheng JX, Du TY, Shao GC, Ma ZH, Jiang Z Di, Hu W, et al. Ubiquitination-mediated Golgi-to-endosome sorting determines the toxin-antidote duality of fission yeast *wtf* meiotic drivers. Nat Commun 2023;14. https://doi.org/10.1038/S41467-023-44151-9.

[25] Bravo Nuñez MA, Sabbarini IM, Eickbush MT, Liang Y, Lange JJ, Kent AM, et al. Dramatically diverse *Schizosaccharomyces pombe wtf* meiotic drivers all display high gamete-killing efficiency. PLoS Genet 2020;16. https://doi.org/10.1371/journal.pgen.1008350.

[26] Bravo Núñez MA, Lange JJ, Sarah ZE. A suppressor of a *wtf* poison-antidote meiotic driver acts via mimicry of the driver's antidote. PLoS Genet 2018;14. https://doi.org/10.1371/journal.pgen.1007836.

[27] Mannini B, Mulvihill E, Sgromo C, Cascella R, Khodarahmi R, Ramazzotti M, et al. Toxicity of protein oligomers is rationalized by a function combining size and surface hydrophobicity. ACS Chem Biol 2014; 9:2309–17. https://doi.org/10.1021/CB500505M/SUPPL_FILE/CB500505M_SI_001.PDF.

[28] Ries HM, Nussbaum-Krammer C. Shape matters: The complex relationship between aggregation and toxicity in protein-misfolding diseases. Essays Biochem 2016; 60:181–90. https://doi.org/10.1042/EBC20160008.

[29] Bucciantini M, Giannoni E, Chiti F, Baroni F, Taddei N, Ramponi G, et al. Inherent toxicity of aggregates implies a common mechanism for protein misfolding diseases. Nature 2002 416:6880 2002; 416:507–11. https://doi.org/10.1038/416507a.

[30] Khan T, Kandola TS, Wu J, Venkatesan S, Ketter E, Lange JJ, et al. Quantifying Nucleation In Vivo Reveals the Physical Basis of Prion-like Phase Behavior. Mol Cell 2018; 71:155-168.e7. https://doi.org/10.1016/j.molcel.2018.06.016.

[31] Bellapadrona G, Elbaum M. Supramolecular Protein Assemblies in the Nucleus of Human Cells. Angewandte Chemie International Edition 2014; 53:1534–7. https://doi.org/10.1002/ANIE.201309163.

[32] Bracha D, Walls MT, Wei MT, Zhu L, Kurian M, Avalos JL, et al. Mapping Local and Global Liquid Phase Behavior in Living Cells Using Photo-Oligomerizable Seeds. Cell 2018; 175:1467-1480.e13. https://doi.org/10.1016/J.CELL.2018.10.048.

[33] Schellhaus AK, Xu S, Gierisch ME, Vornberger J, Johansson J, Dantuma NP. A spider silk-derived solubility domain inhibits nuclear and cytosolic protein aggregation in human cells. Communications Biology 2022 5:1 2022; 5:1–8. https://doi.org/10.1038/s42003-022-03442-5.

[34] Kronqvist N, Sarr M, Lindqvist A, Nordling K, Otikovs M, Venturi L, et al. Efficient protein production inspired by how spiders make silk. Nat Commun 2017;8. https://doi.org/10.1038/NCOMMS15504.

[35] Askarieh G, Hedhammar M, Nordling K, Saenz A, Casals C, Rising A, et al. Self-assembly of spider silk proteins is controlled by a pH-sensitive relay. Nature 2010 465:7295 2010; 465:236–8. https://doi.org/10.1038/nature08962.

[36] Abelein A, Chen G, Kitoka K, Aleksis R, Oleskovs F, Sarr M, et al. High-yield Production of Amyloid-β Peptide Enabled by a Customized Spider Silk Domain. Scientific Reports 2020 10:1 2020; 10:1–10. https://doi.org/10.1038/s41598-019-57143-x.

[37] Jaudzems K, Askarieh G, Landreh M, Nordling K, Hedhammar M, Jörnvall H, et al. pH-Dependent Dimerization of Spider Silk N-Terminal Domain Requires Relocation of a Wedged Tryptophan Side Chain. J Mol Biol 2012; 422:477–87. https://doi.org/10.1016/J.JMB.2012.06.004.

[38] Andersson M, Chen G, Otikovs M, Landreh M, Nordling K, Kronqvist N, et al. Carbonic Anhydrase Generates CO2 and H+ That Drive Spider Silk Formation Via Opposite Effects on the Terminal Domains. PLoS Biol 2014;12: e1001921. https://doi.org/10.1371/JOURNAL.PBIO.1001921.

[39] Brumbaugh-Reed EH, Aoki K, Toettcher JE, Toettcher J. Rapid and reversible dissolution of biomolecular condensates using light-controlled recruitment of a solubility tag. BioRxiv 2024:2024.01.16.575860. https://doi.org/10.1101/2024.01.16.575860.

[40] Raran-Kurussi S, Keefe K, Waugh DS. Positional effects of fusion partners on the yield and solubility of MBP fusion proteins. Protein Expr Purif 2015; 110:159. https://doi.org/10.1016/J.PEP.2015.03.004.

[41] Raran-Kurussi S, Sharwanlal SB, Balasubramanian D, Mote KR. A comparison between MBP- and NT* as N-terminal fusion partner for recombinant protein production in E. coli. Protein Expr Purif 2022; 189:105991. https://doi.org/10.1016/J.PEP.2021.105991.

[42] Blake WJ, Kærn M, Cantor CR, Collins JJ. Noise in eukaryotic gene expression. Nature 2003 422:6932 2003; 422:633–7. https://doi.org/10.1038/nature01546.

[43] Elowitz MB, Levine AJ, Siggia ED, Swain PS. Stochastic gene expression in a single cell. Science (1979) 2002; 297:1183–6. https://doi.org/10.1126/SCIENCE.1070919/

[44] Ozbudak EM, Thattai M, Kurtser I, Grossman AD, Van Oudenaarden A. Regulation of noise in the expression of a single gene 2002. https://doi.org/10.1038/ng869.

[45] Nordholt N, Van Heerden J, Kort R, Bruggeman FJ. Effects of growth rate and promoter activity on single-cell protein expression. Scientific Reports 2017 7:1 2017; 7:1–11. https://doi.org/10.1038/s41598-017-05871-3.

[46] Rothe S, Prakash A, Tyedmers J. The Insoluble Protein Deposit (IPOD) in Yeast. Front Mol Neurosci 2018; 11:385163. https://doi.org/10.3389/FNMOL.2018.00237/

[47] Tyedmers J, Treusch S, Dong J, McCaffery JM, Bevis B, Lindquist S. Prion induction involves an ancient system for the sequestration of aggregated proteins and heritable changes in prion fragmentation. Proc Natl Acad Sci U S A 2010; 107:8633–8. https://doi.org/10.1073/PNAS.1003895107/

[48] Kaganovich D, Kopito R, Frydman J. Misfolded proteins partition between two distinct quality control compartments. Nature 2008 454:7208 2008; 454:1088–95. https://doi.org/10.1038/nature07195.

[49] Kayed R, Head E, Thompson JL, McIntire TM, Milton SC, Cotman CW, et al. Common structure of soluble amyloid oligomers implies common mechanism of pathogenesis. Science (1979) 2003; 300:486–9. https://doi.org/10.1126/SCIENCE.1079469/

[50] Majumdar A, Cesario WC, White-Grindley E, Jiang H, Ren F, Khan MR, et al. Critical role of amyloid-like oligomers of *Drosophila* Orb2 in the persistence of memory. Cell 2012; 148:515–29. https://doi.org/10.1016/J.CELL.2012.01.004.

[51] Alberti S, Halfmann R, King O, Kapila A, Lindquist S. A systematic survey identifies prions and illuminates sequence features of prionogenic proteins. Cell 2009; 137:146. https://doi.org/10.1016/J.CELL.2009.02.044.

[52] Perov S, Lidor O, Salinas N, Golan N, Tayeb-Fligelman E, Deshmukh M, et al. Structural Insights into Curli CsgA Cross-β Fibril Architecture Inspire Repurposing of Anti-amyloid Compounds as Anti-biofilm Agents. PLoS Pathog 2019;15. https://doi.org/10.1371/JOURNAL.PPAT.1007978.

[53] Yan Z, Yin M, Chen J, Li X. Assembly and substrate recognition of curli biogenesis system. Nature Communications 2020 11:1 2020; 11:1–10. https://doi.org/10.1038/s41467-019-14145-7.

[54] Sheng J, Olrichs NK, Gadella BM, Kaloyanova D V., Bernd Helms J. Regulation of Functional Protein Aggregation by Multiple Factors: Implications for the Amyloidogenic Behavior of the CAP Superfamily Proteins. Int J Mol Sci 2020; 21:1–23. https://doi.org/10.3390/IJMS21186530.

[55] Jackson MP, Hewitt EW. Why Are Functional Amyloids Non-Toxic in Humans? Biomolecules 2017;7. https://doi.org/10.3390/BIOM7040071.

[56] Kong L, Sui C, Chen T, Zhang L, Zhao W, Zheng Y, et al. The ubiquitin E3 ligase TRIM10 promotes STING aggregation and activation in the Golgi apparatus. Cell Rep 2023;42. https://doi.org/10.1016/j.celrep.2023.112306.

[57] Liu B, Zhang M, Chu H, Zhang H, Wu H, Song G, et al. The ubiquitin E3 ligase TRIM31 promotes aggregation and activation of the signaling adaptor MAVS through Lys63-linked polyubiquitination. Nat Immunol 2017; 18:214–24. https://doi.org/10.1038/ni.3641.

[58] Masperone L, Codrich M, Persichetti F, Gustincich S, Zucchelli S, Legname G. The E3 Ubiquitin Ligase TRAF6 Interacts with the Cellular Prion Protein and Modulates Its Solubility and Recruitment to Cytoplasmic p62/SQSTM1-Positive Aggresome-Like Structures. Mol Neurobiol 2022; 59:1577–88. https://doi.org/10.1007/S12035-021-02666-6/

[59] Zhang ZY, Harischandra DS, Wang R, Ghaisas S, Zhao JY, McMonagle TP, et al. TRIM11 protects against tauopathies and is down-regulated in Alzheimer's disease. Science (1979) 2023;381. https://doi.org/10.1126/science.add6696.

[60] Davidson JM, Wu SSL, Rayner SL, Cheng F, Duncan K, Russo C, et al. The E3 Ubiquitin Ligase SCF Cyclin F Promotes Sequestosome-1/p62 Insolubility and Foci Formation and is Dysregulated in ALS and FTD Pathogenesis. Mol Neurobiol 2023; 60:5034–54. https://doi.org/10.1007/s12035-023-03355-2.

[61] Watabe K, Kato Y, Sakuma M, Murata M, Niida-Kawaguchi M, Takemura T, et al. Praja1 RING-finger E3 ubiquitin ligase suppresses neuronal cytoplasmic TDP-43 aggregate formation. Neuropathology 2020; 40:570–86. https://doi.org/10.1111/neup.12694.

[62] Won SY, Park JJ, You ST, Hyeun JA, Kim HK, Jin BK, et al. p21-activated kinase 4 controls the aggregation of α-synuclein by reducing the monomeric and aggregated forms of α-synuclein: involvement of the E3 ubiquitin ligase NEDD4-1. Cell Death Dis 2022;13. https://doi.org/10.1038/s41419-022-05030-1.

[63] Watabe K, Niida-Kawaguchi M, Tada M, Kato Y, Murata M, Tanji K, et al. Praja1 RING-finger E3 ubiquitin ligase is a common suppressor of neurodegenerative disease-associated protein aggregation. Neuropathology 2022; 42:488–504. https://doi.org/10.1111/neup.12840.

[64] Nadel CM, Thwin AC, Callahan M, Lee K, Connelly E, Craik CS, et al. The E3 Ubiquitin Ligase, CHIP/STUB1, Inhibits Aggregation of Phosphorylated Proteoforms of Microtubule-associated Protein Tau (MAPT). J Mol Biol 2023;435. https://doi.org/10.1016/j.jmb.2023.168026.

[65] Yan C, Gong L, Chen L, Xu M, Abou-Hamdan H, Tang M, et al. PHB2 (prohibitin 2) promotes PINK1-PRKN/Parkin-dependent mitophagy by the PARL-PGAM5-PINK1 axis 2020. https://doi.org/10.1080/15548627.2019.1628520.

[66] Lindholm AK, Dyer KA, Firman RC, Fishman L, Forstmeier W, Holman L, et al. The Ecology and Evolutionary Dynamics of Meiotic Drive. Trends Ecol Evol 2016; 31:315–26. https://doi.org/10.1016/j.tree.2016.02.001.

[67] Hernández JFL, Rubinstein BY, Unckless RL, Zanders SE. Modeling the Evolution of Populations with Multiple Killer Meiotic Drivers. BioRxiv 2023:2023.09.28.560003. https://doi.org/10.1101/2023.09.28.560003.

[68] Dasgupta SK, Jain S, Kaushal D, Tyagi AK. Expression Systems for Study of Mycobacterial Gene Regulation and Development of Recombinant BCG Vaccines. Biochem Biophys Res Commun 1998; 246:797–804. https://doi.org/10.1006/BBRC.1998.8724.

[69] Sikorski RS, Hieter P. A system of shuttle vectors and yeast host strains designed for efficient manipulation of DNA in Saccharomyces cerevisiae. Genetics 1989; 122:19–27. https://doi.org/10.1093/GENETICS/122.1.19.

[70] Snaith HA, Samejima I, Sawin KE. Multistep and multimode cortical anchoring of tea1p at cell tips in fission yeast. EMBO J 2005; 24:3690. https://doi.org/10.1038/SJ.EMBOJ.7600838.

[71] Sonnhammer ELL, Von Heijne G, Krogh A. A hidden Markov model for predicting transmembrane helices in protein sequences. AAAI Press; 1998.

[72] Krogh A, Larsson B, Von Heijne G, Sonnhammer ELL. Predicting transmembrane protein topology with a hidden Markov model: Application to complete genomes. J Mol Biol 2001; 305:567–80. https://doi.org/10.1006/jmbi.2000.4315.

[73] Chen Y hui, Wang G yuan, Hao H chao, Chao C jiang, Wang Y, Jin Q wen. Facile manipulation of protein localization in fission yeast through binding of GFP-binding protein to GFP. J Cell Sci 2017; 130:1003–15. https://doi.org/10.1242/JCS.198457.

[74] Sanchez MI, Ting AY. Directed evolution improves the catalytic efficiency of TEV protease. Nature Methods 2019 17:2 2019; 17:167–74. https://doi.org/10.1038/s41592-019-0665-7.

[75] Kapust RB, Waugh DS. *Escherichia coli* maltose-binding protein is uncommonly effective at promoting the solubility of polypeptides to which it is fused. Protein Sci 1999; 8:1668. https://doi.org/10.1110/PS.8.8.1668.

[76] Fox JD, Routzahn KM, Bucher MH, Waugh DS. Maltodextrin-binding proteins from diverse bacteria and archaea are potent solubility enhancers. FEBS Lett 2003; 537:53–7. https://doi.org/10.1016/S0014-5793(03)00070-X.

[77] Ottoz DSM, Rudolf F, Stelling J. Inducible, tightly regulated and growth condition-independent transcription factor in *Saccharomyces cerevisiae*. Nucleic Acids Res 2014;42. https://doi.org/10.1093/nar/gku616.

[78] R Elble. A simple and efficient procedure for transformation of yeasts. Biotechniques 1992.

[79] Winston F, Dollard C, Ricupero-Hovasse SL. Construction of a set of convenient *Saccharomyces cerevisiae* strains that are isogenic to S288C. Yeast 1995;11:53–5. https://doi.org/10.1002/YEA.320110107.

[80] Gasteiger E, Hoogland C, Gattiker A, Duvaud S, Wilkins MR, Appel RD, et al. Protein Identification and Analysis Tools on the ExPASy Server. The Proteomics Protocols Handbook 2005:571–607. https://doi.org/10.1385/1-59259-890-0:571.

Figure 1

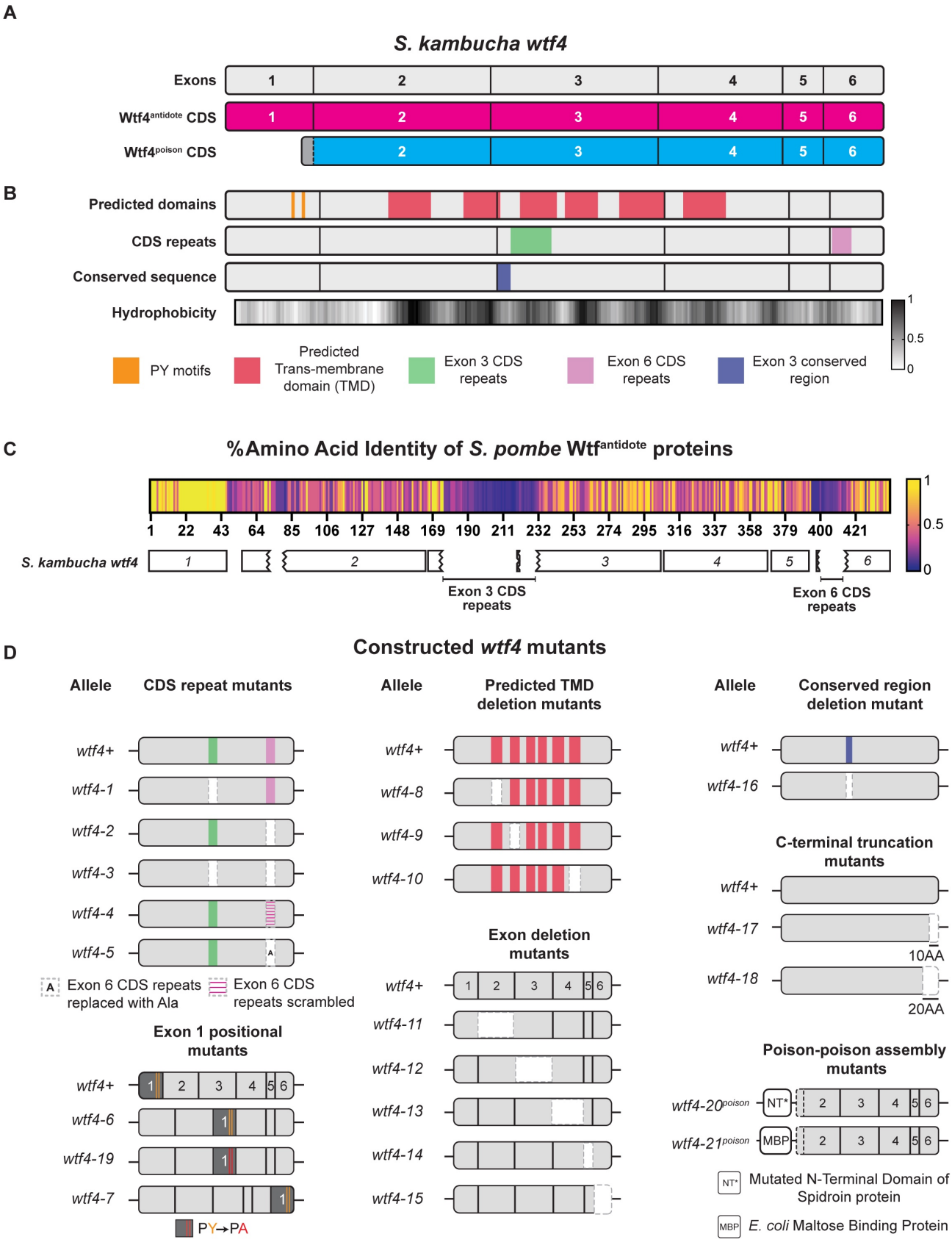
A
S. kambucha wtf4
Exons
1
2
3
4
5
6
Wtf4antidote CDS
Wtf4poison CDS
B
Predicted domains
CDS repeats
Conserved sequence
Hydrophobicity
1
0.5
0
PY motifs
Predicted Trans-membrane domain (TMD)
Exon 3 CDS repeats
Exon 6 CDS repeats
Exon 3 conserved region
C
%Amino Acid Identity of S. pombe Wtfantidote proteins
1 22 43 64 85 106 127 148 169 190 211 232 253 274 295 316 337 358 379 400 421
S. kambucha wtf4
Exon 3 CDS repeats
Exon 6 CDS repeats
D
Constructed wtf4 mutants
Allele
CDS repeat mutants
wtf4+
wtf4-1
wtf4-2
wtf4-3
wtf4-4
wtf4-5
Exon 6 CDS repeats replaced with Ala
Exon 6 CDS repeats scrambled
Exon 1 positional mutants
wtf4-6
wtf4-19
wtf4-7
PY→PA
Predicted TMD deletion mutants
wtf4-8
wtf4-9
wtf4-10
Exon deletion mutants
wtf4-11
wtf4-12
wtf4-13
wtf4-14
wtf4-15
Conserved region deletion mutant
wtf4-16
C-terminal truncation mutants
wtf4-17
10AA
wtf4-18
20AA
Poison-poison assembly mutants
wtf4-20poison
wtf4-21poison
NT*
MBP
Mutated N-Terminal Domain of Spidroin protein
E. coli Maltose Binding Protein

Figure 2

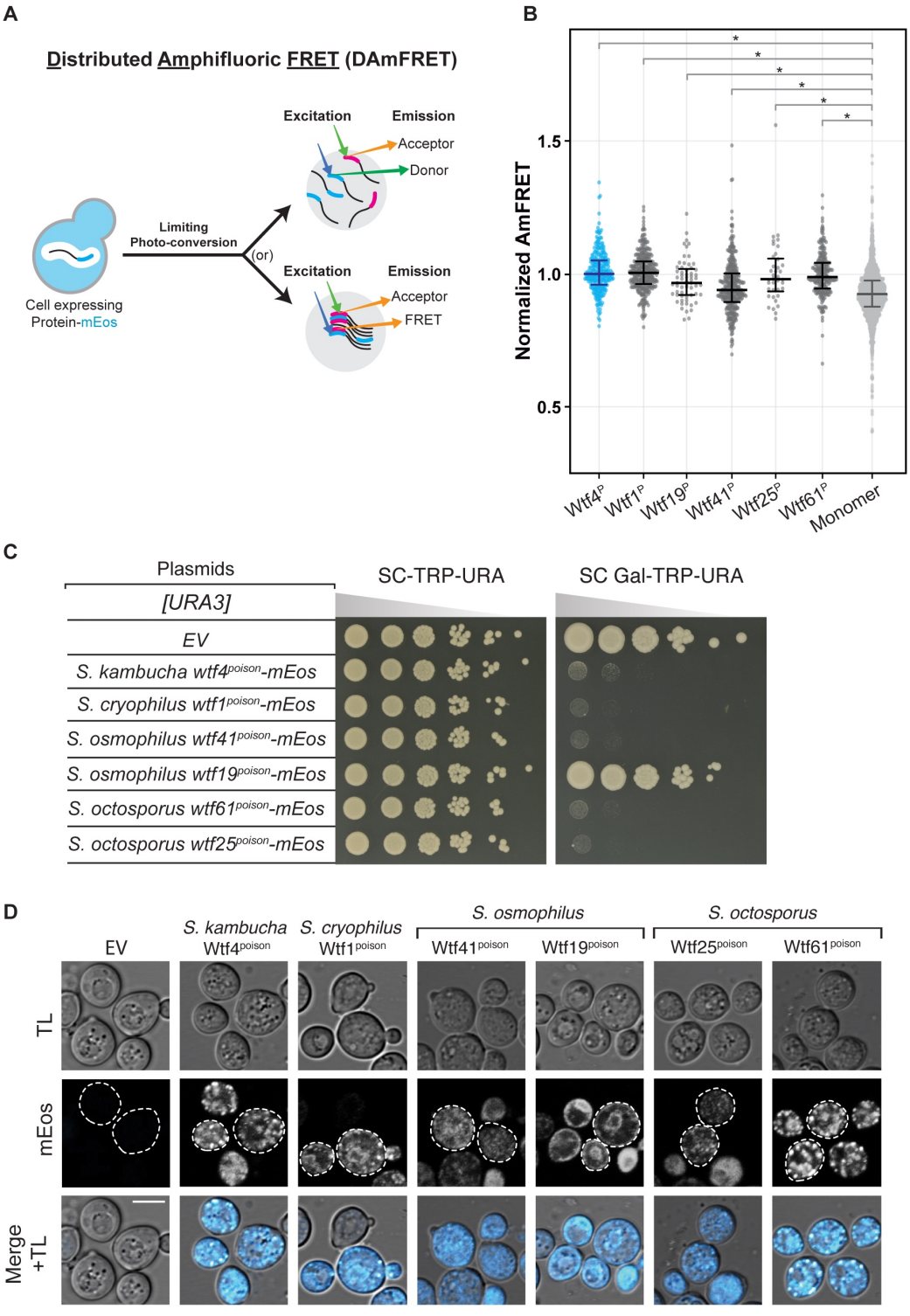
A
Distributed Amphifluoric FRET (DAmFRET)
Excitation
Emission
Acceptor
Donor
Limiting
Photo-conversion
(or)
Excitation
Emission
Acceptor
FRET
Cell expressing
Protein-mEos
B
Normalized AmFRET
1.5
1.0
0.5
Wtf4P
Wtf1P
Wtf19P
Wtf41P
Wtf25P
Wtf61P
Monomer
C
Plasmids
SC-TRP-URA
SC Gal-TRP-URA
[URA3]
EV
S. kambucha wtf4poison-mEos
S. cryophilus wtf1poison-mEos
S. osmophilus wtf41poison-mEos
S. osmophilus wtf19poison-mEos
S. octosporus wtf61poison-mEos
S. octosporus wtf25poison-mEos
D
EV
S. kambucha Wtf4poison
S. cryophilus Wtf1poison
S. osmophilus
Wtf41poison
Wtf19poison
S. octosporus
Wtf25poison
Wtf61poison
TL
mEos
Merge +TL

Figure 3

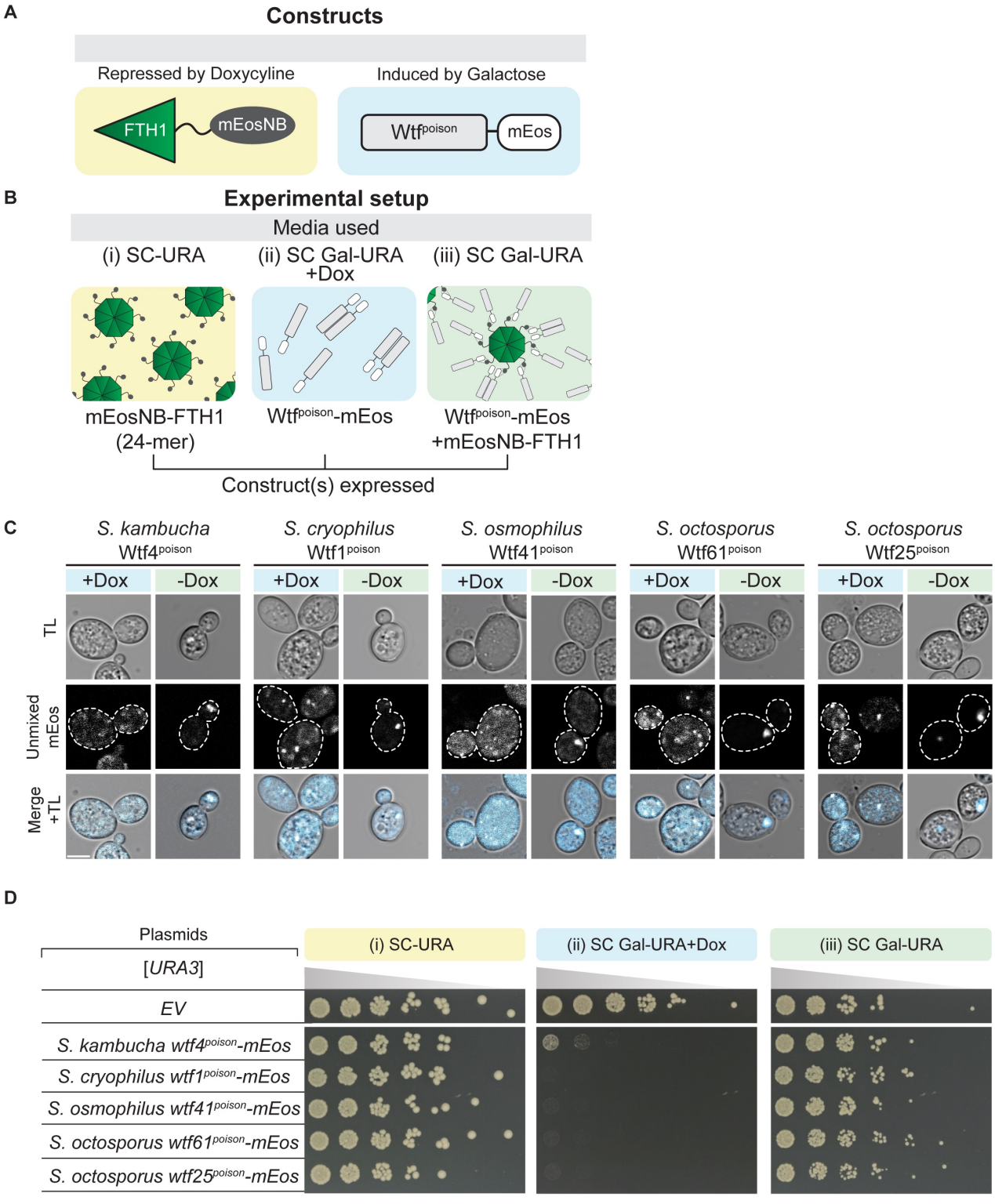
A
Constructs
Repressed by Doxycyline
Induced by Galactose
FTH1
mEosNB
Wtf poison
mEos
B
Experimental setup
Media used
(i) SC-URA
(ii) SC Gal-URA +Dox
(iii) SC Gal-URA
mEosNB-FTH1 (24-mer)
Wtf poison-mEos
Wtf poison-mEos +mEosNB-FTH1
Construct(s) expressed
C
S. kambucha Wtf4 poison
S. cryophilus Wtf1 poison
S. osmophilus Wtf41 poison
S. octosporus Wtf61 poison
S. octosporus Wtf25 poison
+Dox
-Dox
TL
Unmixed mEos
Merge +TL
D
Plasmids
[URA3]
EV
S. kambucha wtf4 poison-mEos
S. cryophilus wtf1 poison-mEos
S. osmophilus wtf41 poison-mEos
S. octosporus wtf61 poison-mEos
S. octosporus wtf25 poison-mEos
(i) SC-URA
(ii) SC Gal-URA+Dox
(iii) SC Gal-URA

Figure 4

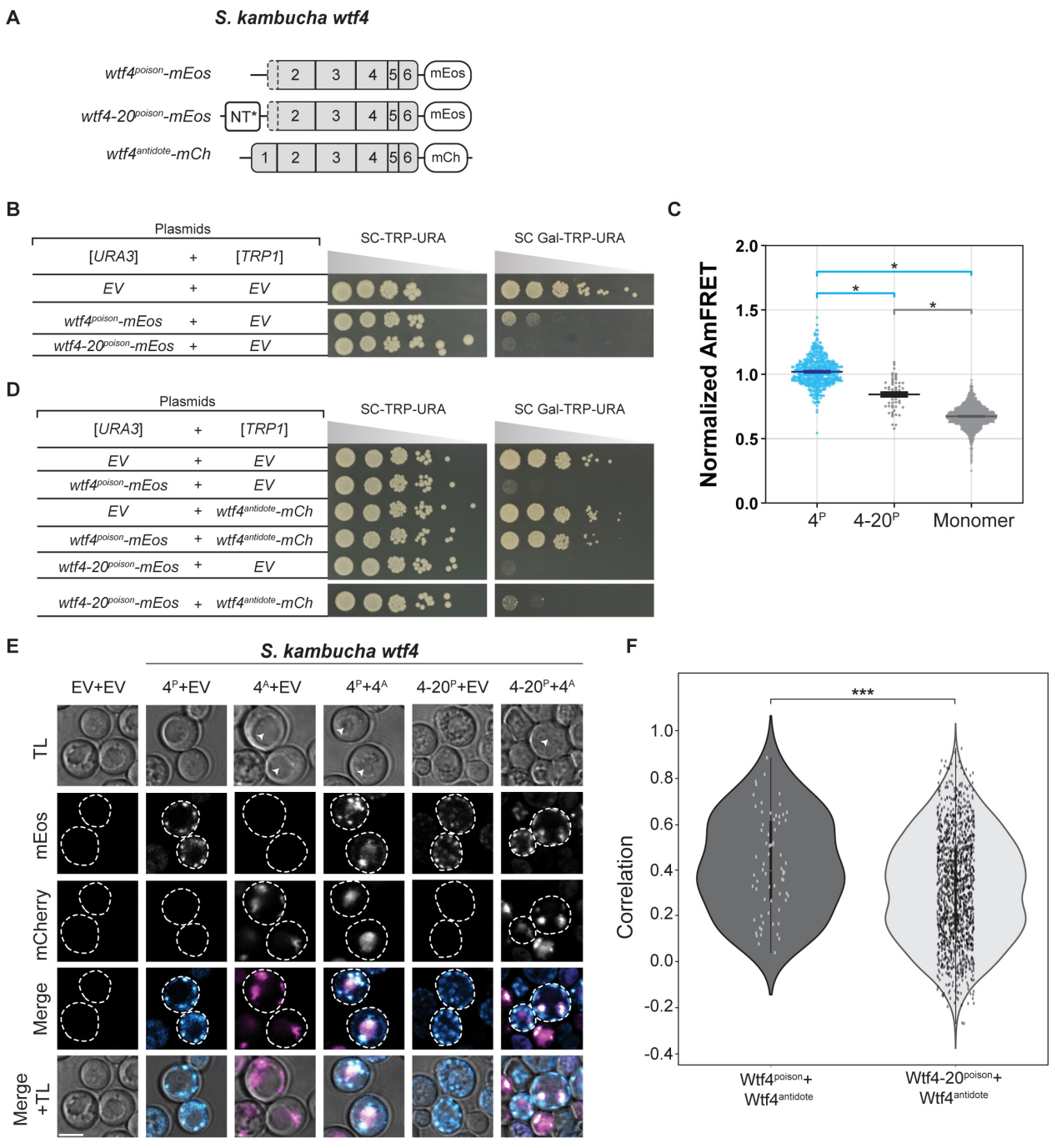
A
S. kambucha wtf4
wtf4poison-mEos
wtf4-20poison-mEos
wtf4antidote-mCh
NT*
mEos
mCh
B
Plasmids
[URA3] + [TRP1]
EV + EV
wtf4poison-mEos + EV
wtf4-20poison-mEos + EV
SC-TRP-URA
SC Gal-TRP-URA
C
Normalized AmFRET
4P
4-20P
Monomer
D
wtf4antidote-mCh
E
S. kambucha wtf4
EV+EV
4P+EV
4A+EV
4P+4A
4-20P+EV
4-20P+4A
TL
mEos
mCherry
Merge
Merge +TL
F
Correlation
Wtf4poison+ Wtf4antidote
Wtf4-20poison+ Wtf4antidote

Figure 5

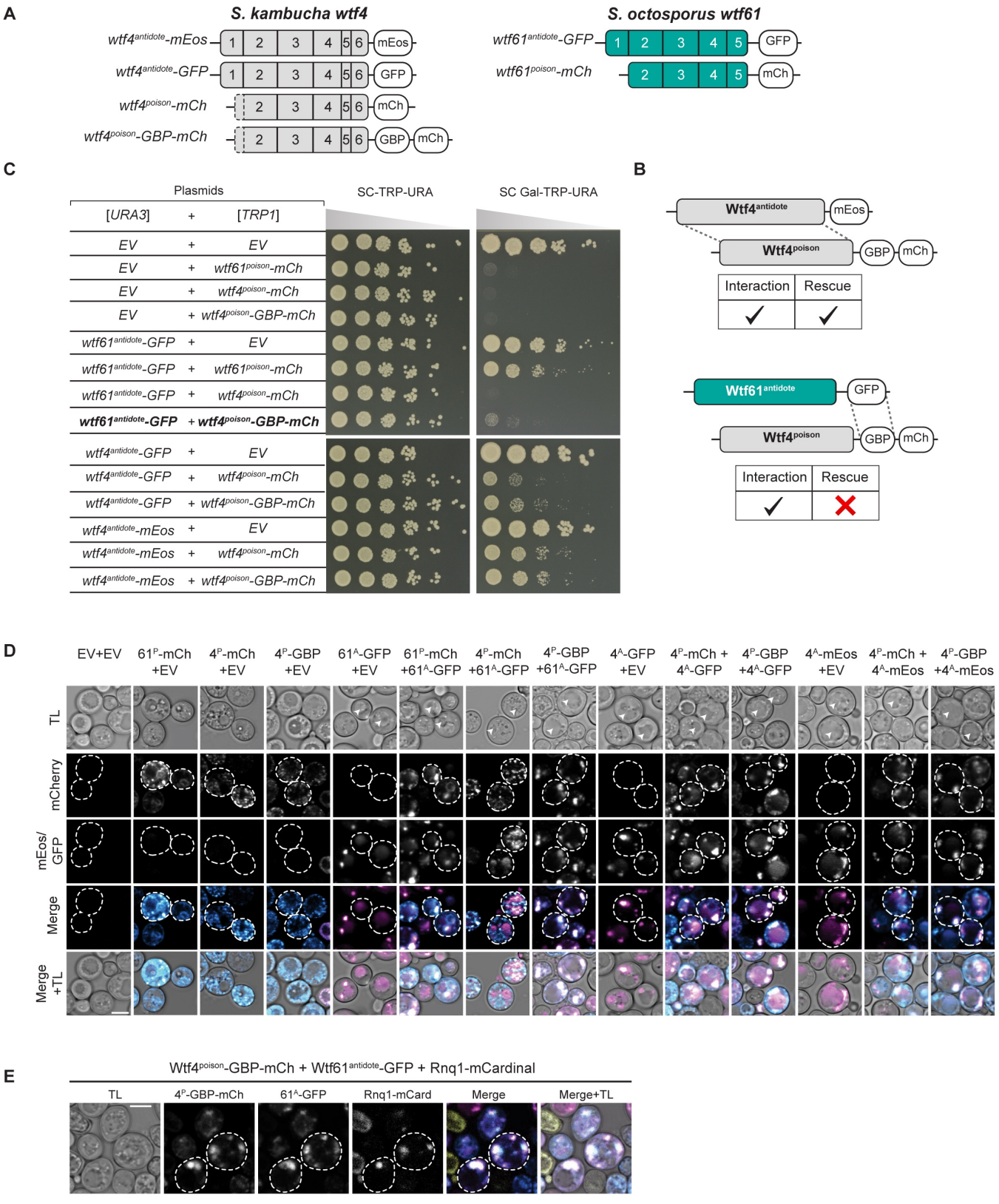
A
S. kambucha wtf4
wtf4antidote-mEos
wtf4antidote-GFP
wtf4poison-mCh
wtf4poison-GBP-mCh
1 2 3 4 5 6
mEos
GFP
mCh
GBP
S. octosporus wtf61
wtf61antidote-GFP
wtf61poison-mCh
1 2 3 4 5
C
Plasmids
[URA3] + [TRP1]
SC-TRP-URA
SC Gal-TRP-URA
EV + EV
EV + wtf61poison-mCh
EV + wtf4poison-mCh
EV + wtf4poison-GBP-mCh
wtf61antidote-GFP + EV
wtf61antidote-GFP + wtf61poison-mCh
wtf61antidote-GFP + wtf4poison-mCh
wtf61antidote-GFP + wtf4poison-GBP-mCh
wtf4antidote-GFP + EV
wtf4antidote-GFP + wtf4poison-mCh
wtf4antidote-GFP + wtf4poison-GBP-mCh
wtf4antidote-mEos + EV
wtf4antidote-mEos + wtf4poison-mCh
wtf4antidote-mEos + wtf4poison-GBP-mCh
B
Wtf4antidote
mEos
Wtf4poison
GBP
mCh
Interaction
Rescue
Wtf61antidote
GFP
Wtf4poison
GBP
mCh
Interaction
Rescue
D
EV+EV
61P-mCh +EV
4P-mCh +EV
4P-GBP +EV
61A-GFP +EV
61P-mCh +61A-GFP
4P-mCh +61A-GFP
4P-GBP +61A-GFP
4A-GFP +EV
4P-mCh + 4A-GFP
4P-GBP +4A-GFP
4A-mEos +EV
4P-mCh + 4A-mEos
4P-GBP +4A-mEos
TL
mCherry
mEos/ GFP
Merge
Merge +TL
E
Wtf4poison-GBP-mCh + Wtf61antidote-GFP + Rnq1-mCardinal
TL
4P-GBP-mCh
61A-GFP
Rnq1-mCard
Merge
Merge+TL

Figure 6

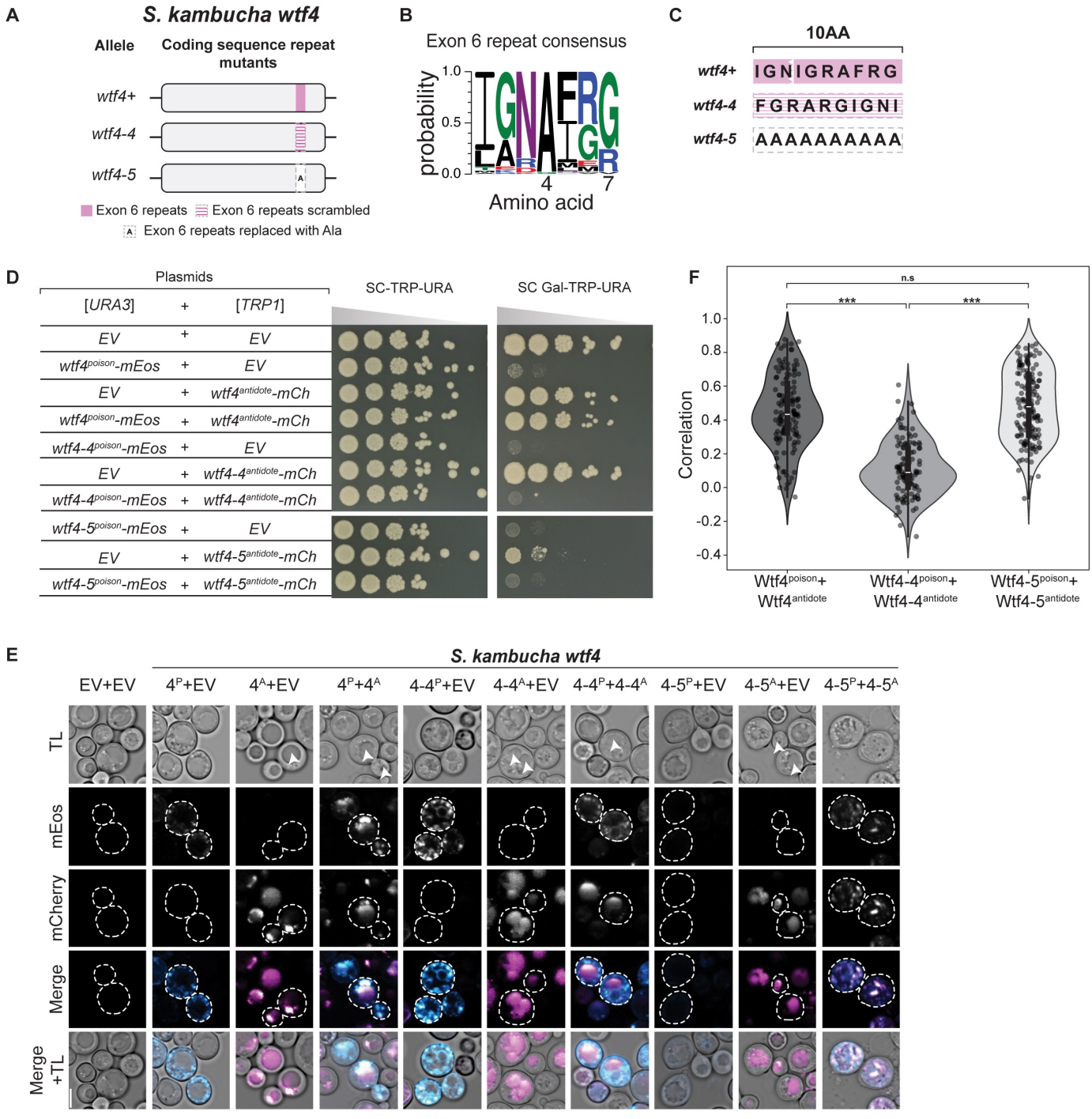
A
S. kambucha wtf4
Allele
Coding sequence repeat mutants
wtf4+
wtf4-4
wtf4-5
Exon 6 repeats
Exon 6 repeats scrambled
Exon 6 repeats replaced with Ala
B
Exon 6 repeat consensus
probability
1.0
0.5
0.0
4
7
Amino acid
C
10AA
wtf4+ IGNIGRAFRG
wtf4-4 FGRARGIGNI
wtf4-5 AAAAAAAAAA
D
Plasmids
[URA3] + [TRP1]
SC-TRP-URA
SC Gal-TRP-URA
EV + EV
wtf4poison-mEos + EV
EV + wtf4antidote-mCh
wtf4poison-mEos + wtf4antidote-mCh
wtf4-4poison-mEos + EV
EV + wtf4-4antidote-mCh
wtf4-4poison-mEos + wtf4-4antidote-mCh
wtf4-5poison-mEos + EV
EV + wtf4-5antidote-mCh
wtf4-5poison-mEos + wtf4-5antidote-mCh
F
n.s
***
***
Correlation
1.0
0.8
0.6
0.4
0.2
0.0
-0.2
-0.4
Wtf4poison+ Wtf4antidote
Wtf4-4poison+ Wtf4-4antidote
Wtf4-5poison+ Wtf4-5antidote
E
S. kambucha wtf4
EV+EV
4P+EV
4A+EV
4P+4A
4-4P+EV
4-4A+EV
4-4P+4-4A
4-5P+EV
4-5A+EV
4-5P+4-5A
TL
mEos
mCherry
Merge
Merge +TL

S1 Figure

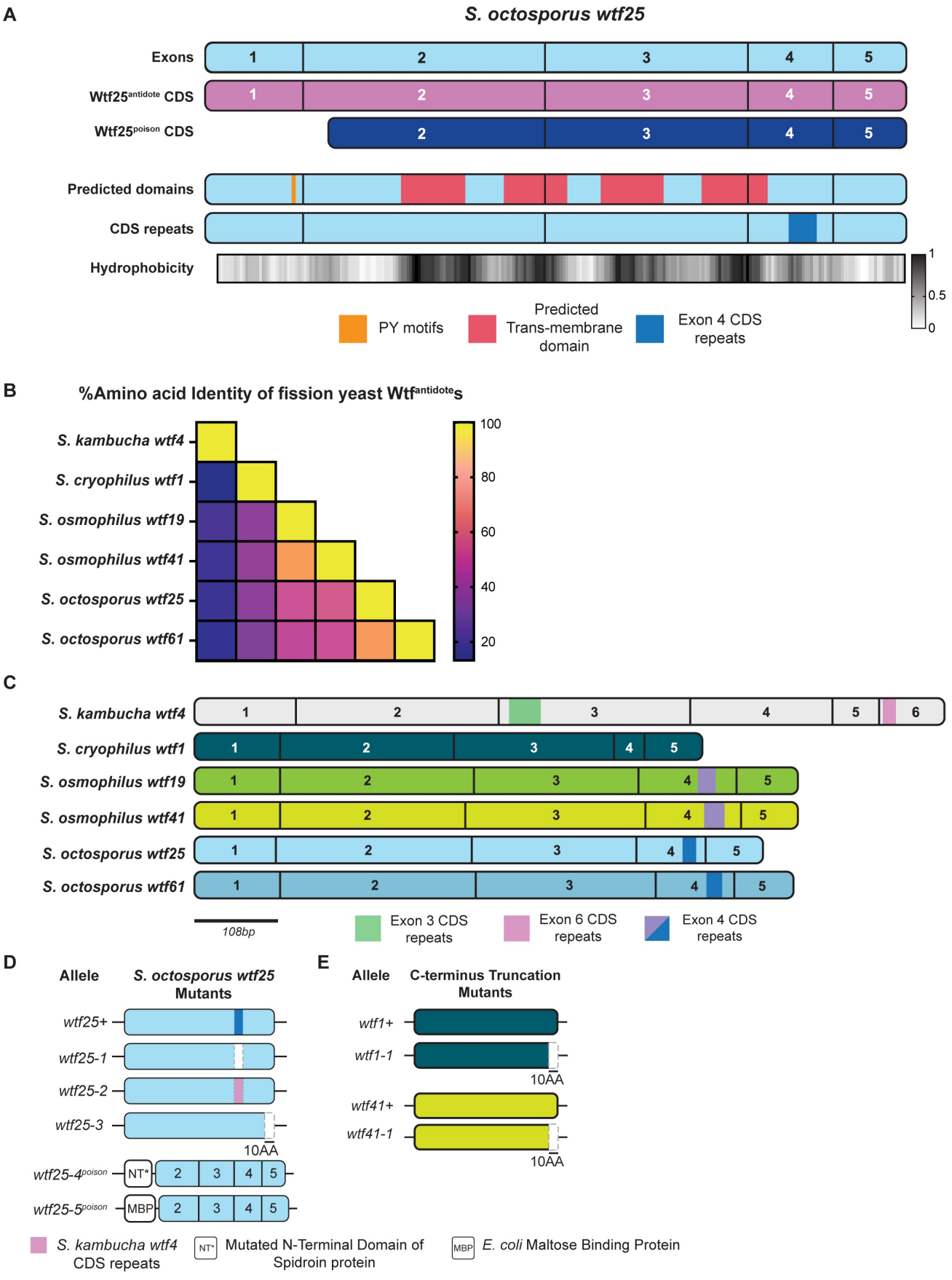
A
S. octosporus wtf25
Exons
Wtf25antidote CDS
Wtf25poison CDS
Predicted domains
CDS repeats
Hydrophobicity
1
0.5
0
PY motifs
Predicted Trans-membrane domain
Exon 4 CDS repeats
B
%Amino acid Identity of fission yeast Wtfantidotes
S. kambucha wtf4
S. cryophilus wtf1
S. osmophilus wtf19
S. osmophilus wtf41
S. octosporus wtf25
S. octosporus wtf61
100
80
60
40
20
C
S. kambucha wtf4
S. cryophilus wtf1
S. osmophilus wtf19
S. osmophilus wtf41
S. octosporus wtf25
S. octosporus wtf61
108bp
Exon 3 CDS repeats
Exon 6 CDS repeats
Exon 4 CDS repeats
D
Allele
S. octosporus wtf25 Mutants
wtf25+
wtf25-1
wtf25-2
wtf25-3
10AA
wtf25-4poison
NT*
wtf25-5poison
MBP
E
Allele
C-terminus Truncation Mutants
wtf1+
wtf1-1
10AA
wtf41+
wtf41-1
10AA
S. kambucha wtf4 CDS repeats
Mutated N-Terminal Domain of Spidroin protein
E. coli Maltose Binding Protein

S2 Figure

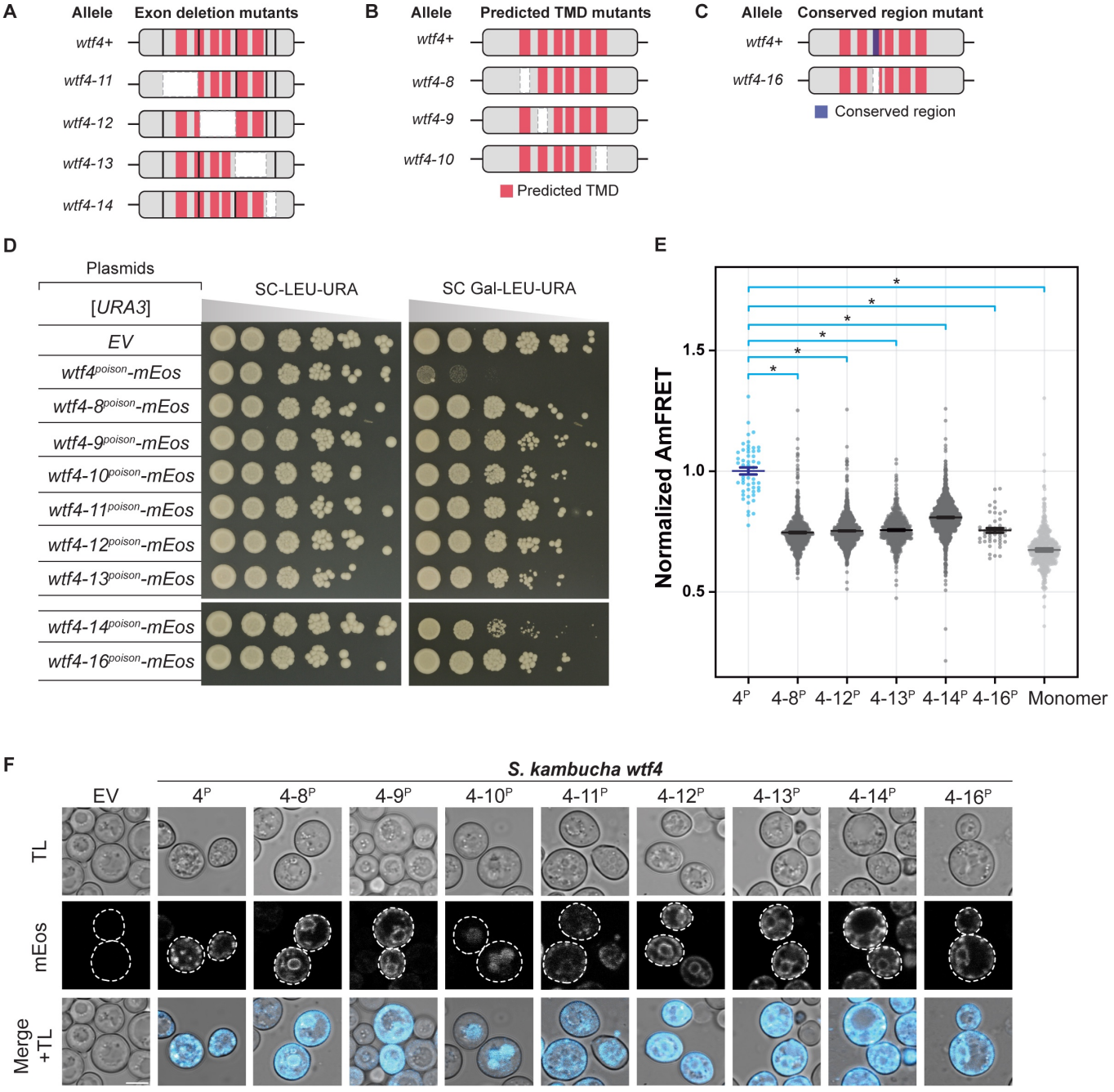
A
Allele
Exon deletion mutants
wtf4+
wtf4-11
wtf4-12
wtf4-13
wtf4-14
B
Allele
Predicted TMD mutants
wtf4+
wtf4-8
wtf4-9
wtf4-10
Predicted TMD
C
Allele
Conserved region mutant
wtf4+
wtf4-16
Conserved region
D
Plasmids
SC-LEU-URA
SC Gal-LEU-URA
[URA3]
EV
wtf4poison-mEos
wtf4-8poison-mEos
wtf4-9poison-mEos
wtf4-10poison-mEos
wtf4-11poison-mEos
wtf4-12poison-mEos
wtf4-13poison-mEos
wtf4-14poison-mEos
wtf4-16poison-mEos
E
Normalized AmFRET
1.5
1.0
0.5
4P
4-8P
4-12P
4-13P
4-14P
4-16P
Monomer
F
S. kambucha wtf4
EV
4P
4-8P
4-9P
4-10P
4-11P
4-12P
4-13P
4-14P
4-16P
TL
mEos
Merge +TL

S3 Figure

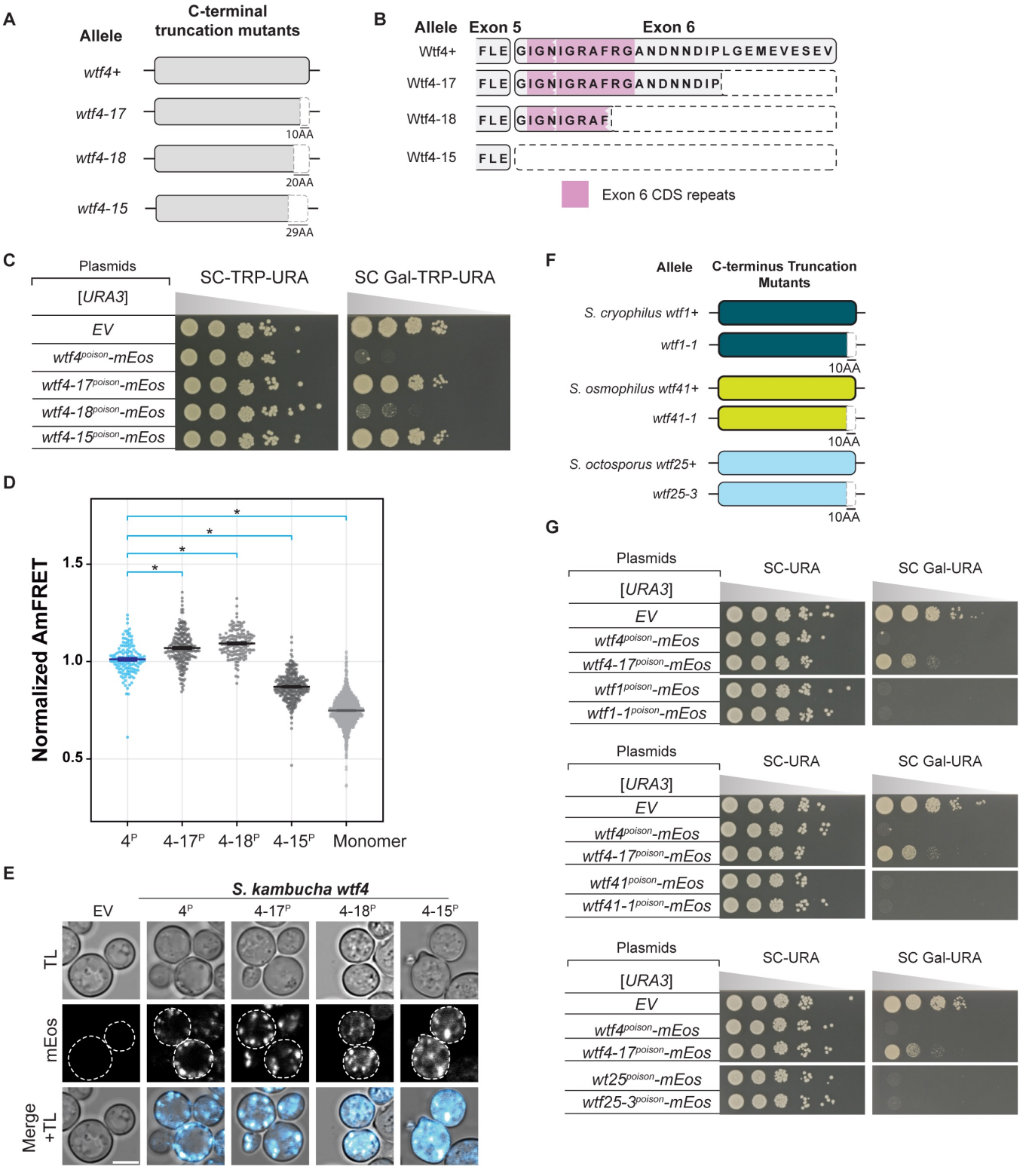
A
Allele
C-terminal truncation mutants
wtf4+
wtf4-17
10AA
wtf4-18
20AA
wtf4-15
29AA
B
Allele
Exon 5
Exon 6
Wtf4+
FLE
GIGNIGRAFRGANDNNDIPLGEMEVESEV
Wtf4-17
FLE
GIGNIGRAFRGANDNNDIP
Wtf4-18
FLE
GIGNIGRAF
Wtf4-15
FLE
Exon 6 CDS repeats
C
Plasmids
SC-TRP-URA
SC Gal-TRP-URA
[URA3]
EV
wtf4poison-mEos
wtf4-17poison-mEos
wtf4-18poison-mEos
wtf4-15poison-mEos
D
Normalized AmFRET
1.5
1.0
0.5
4P
4-17P
4-18P
4-15P
Monomer
E
S. kambucha wtf4
EV
4P
4-17P
4-18P
4-15P
TL
mEos
Merge +TL
F
Allele
C-terminus Truncation Mutants
S. cryophilus wtf1+
wtf1-1
10AA
S. osmophilus wtf41+
wtf41-1
10AA
S. octosporus wtf25+
wtf25-3
10AA
G
Plasmids
SC-URA
SC Gal-URA
[URA3]
EV
wtf4poison-mEos
wtf4-17poison-mEos
wtf1poison-mEos
wtf1-1poison-mEos
Plasmids
SC-URA
SC Gal-URA
[URA3]
EV
wtf4poison-mEos
wtf4-17poison-mEos
wtf41poison-mEos
wtf41-1poison-mEos
Plasmids
SC-URA
SC Gal-URA
[URA3]
EV
wtf4poison-mEos
wtf4-17poison-mEos
wt25poison-mEos
wtf25-3poison-mEos

S4 Figure

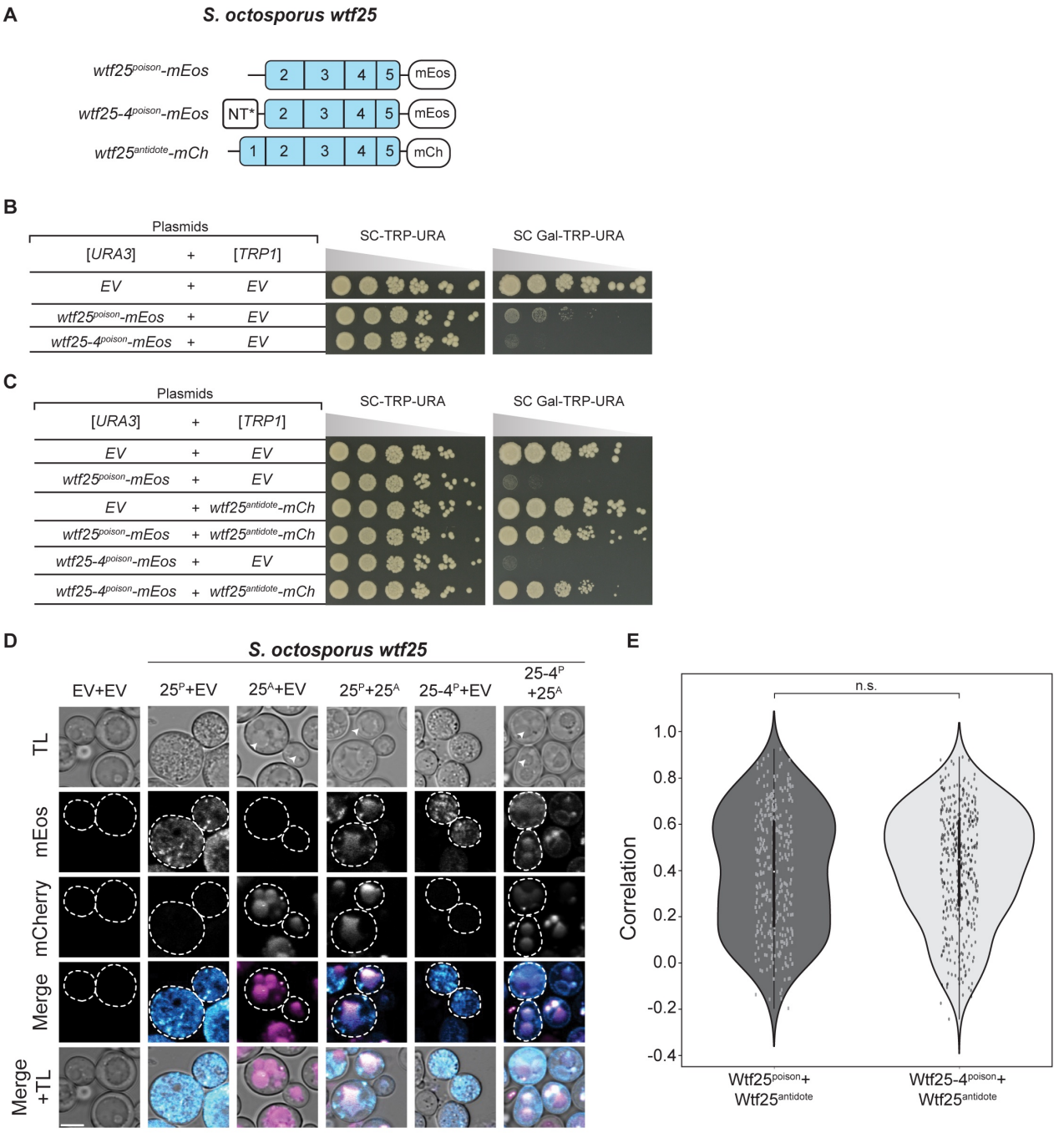
A
S. octosporus wtf25
wtf25poison-mEos
2 3 4 5 mEos
wtf25-4poison-mEos
NT* 2 3 4 5 mEos
wtf25antidote-mCh
1 2 3 4 5 mCh
B
Plasmids
[URA3] + [TRP1]
EV + EV
wtf25poison-mEos + EV
wtf25-4poison-mEos + EV
SC-TRP-URA
SC Gal-TRP-URA
C
Plasmids
[URA3] + [TRP1]
EV + EV
wtf25poison-mEos + EV
EV + wtf25antidote-mCh
wtf25poison-mEos + wtf25antidote-mCh
wtf25-4poison-mEos + EV
wtf25-4poison-mEos + wtf25antidote-mCh
SC-TRP-URA
SC Gal-TRP-URA
D
S. octosporus wtf25
EV+EV
25P+EV
25A+EV
25P+25A
25-4P+EV
25-4P +25A
TL
mEos
mCherry
Merge
Merge +TL
E
n.s.
Correlation
1.0
0.8
0.6
0.4
0.2
0.0
-0.2
-0.4
Wtf25poison+ Wtf25antidote
Wtf25-4poison+ Wtf25antidote

S5 Figure

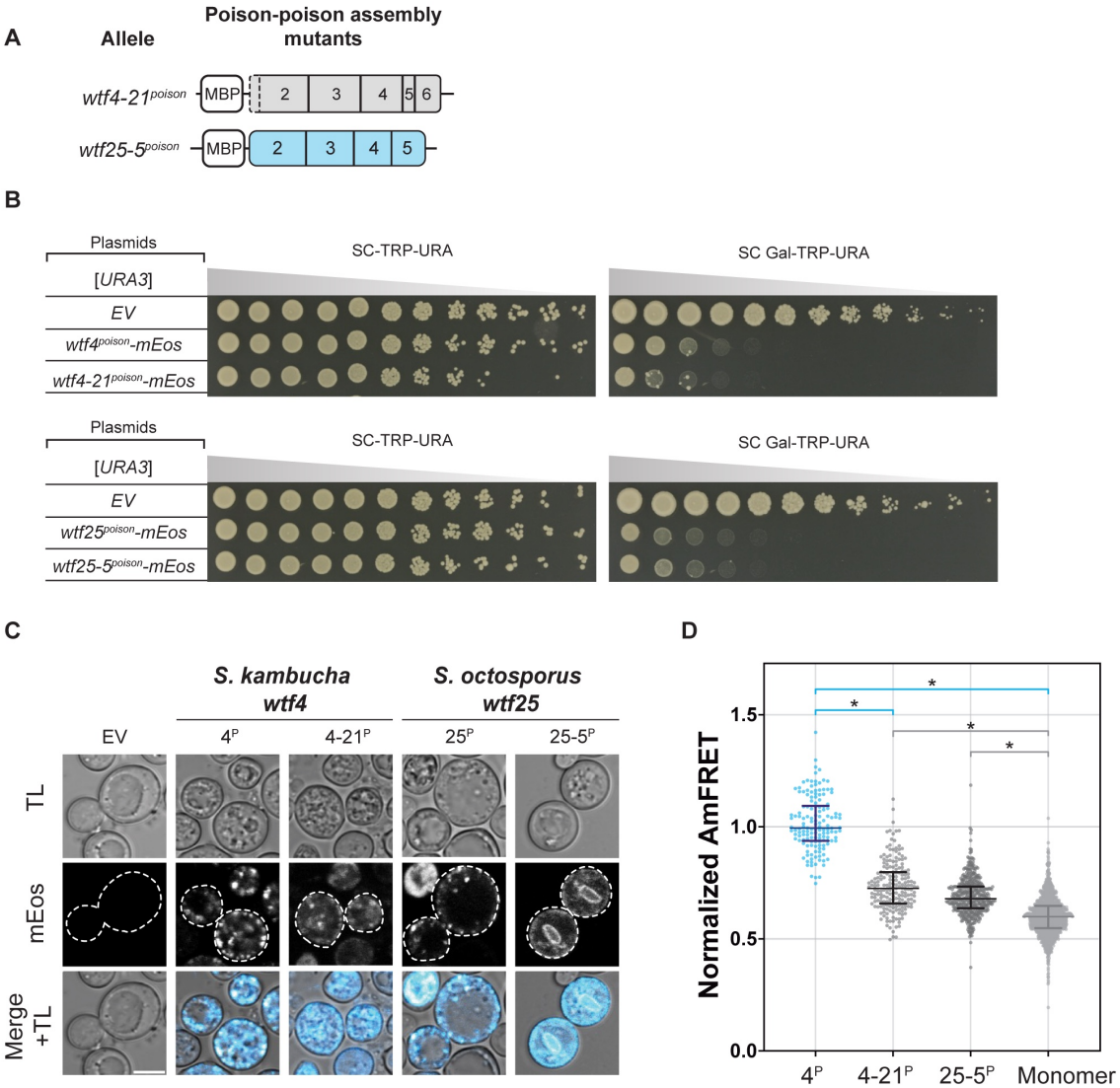
A
Allele
Poison-poison assembly mutants
wtf4-21poison
MBP
2
3
4
5
6
wtf25-5poison
MBP
2
3
4
5
B
Plasmids
[URA3]
EV
wtf4poison-mEos
wtf4-21poison-mEos
SC-TRP-URA
SC Gal-TRP-URA
Plasmids
[URA3]
EV
wtf25poison-mEos
wtf25-5poison-mEos
SC-TRP-URA
SC Gal-TRP-URA
C
S. kambucha wtf4
S. octosporus wtf25
EV
4P
4-21P
25P
25-5P
TL
mEos
Merge +TL
D
Normalized AmFRET
1.5
1.0
0.5
0.0
*
*
*
*
4P
4-21P
25-5P
Monomer

S6 Figure

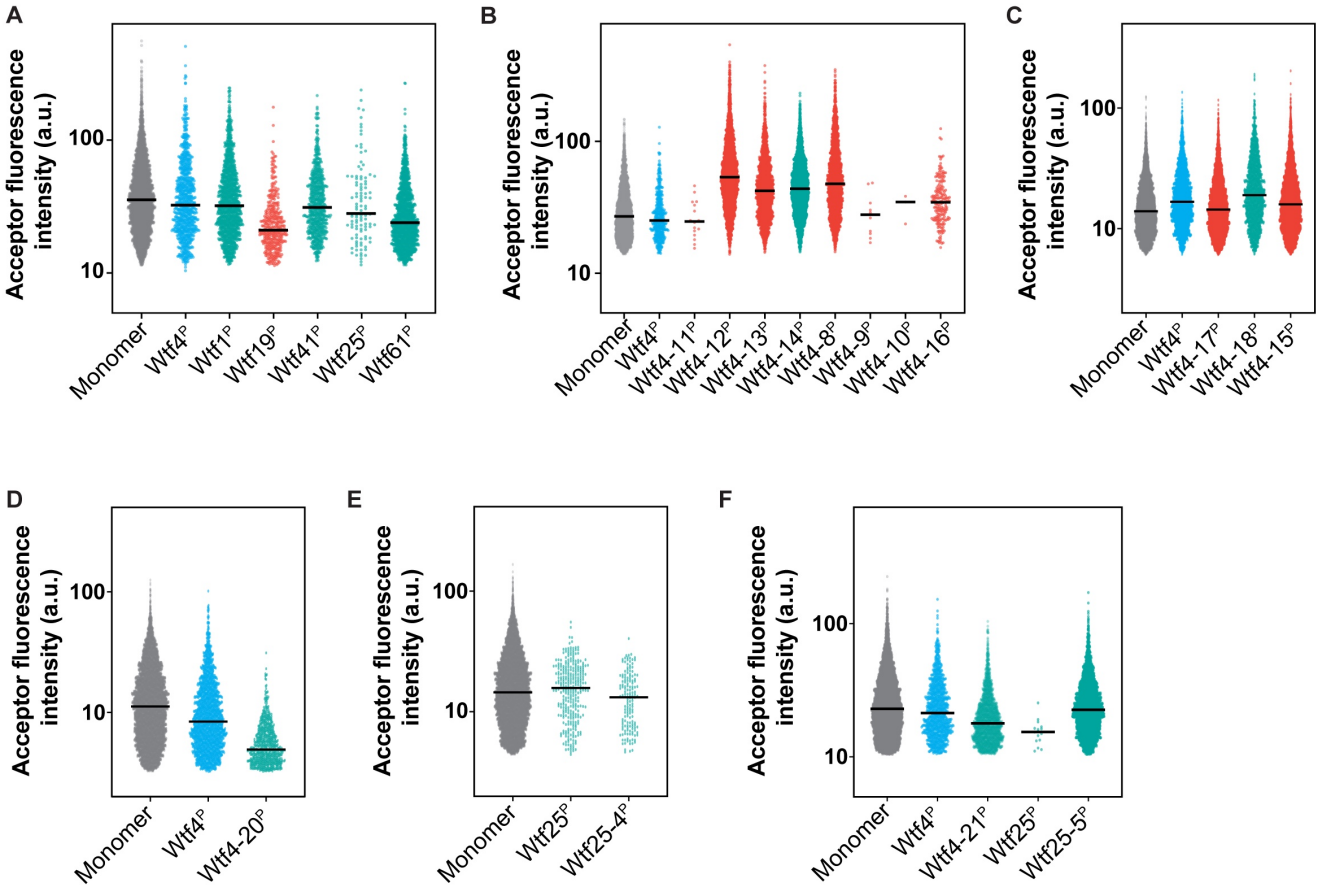
A
Acceptor fluorescence intensity (a.u.)
100
10
Monomer
Wtf4P
Wtf1P
Wtf19P
Wtf41P
Wtf25P
Wtf61P
B
Acceptor fluorescence intensity (a.u.)
100
10
Monomer
Wtf4P
Wtf4-11P
Wtf4-12P
Wtf4-13P
Wtf4-14P
Wtf4-8P
Wtf4-9P
Wtf4-10P
Wtf4-16P
C
Acceptor fluorescence intensity (a.u.)
100
10
Monomer
Wtf4P
Wtf4-17P
Wtf4-18P
Wtf4-15P
D
Acceptor fluorescence intensity (a.u.)
100
10
Monomer
Wtf4P
Wtf4-20P
E
Acceptor fluorescence intensity (a.u.)
100
10
Monomer
Wtf25P
Wtf25-4P
F
Acceptor fluorescence intensity (a.u.)
100
10
Monomer
Wtf4P
Wtf4-21P
Wtf25P
Wtf25-5P

S7 Figure

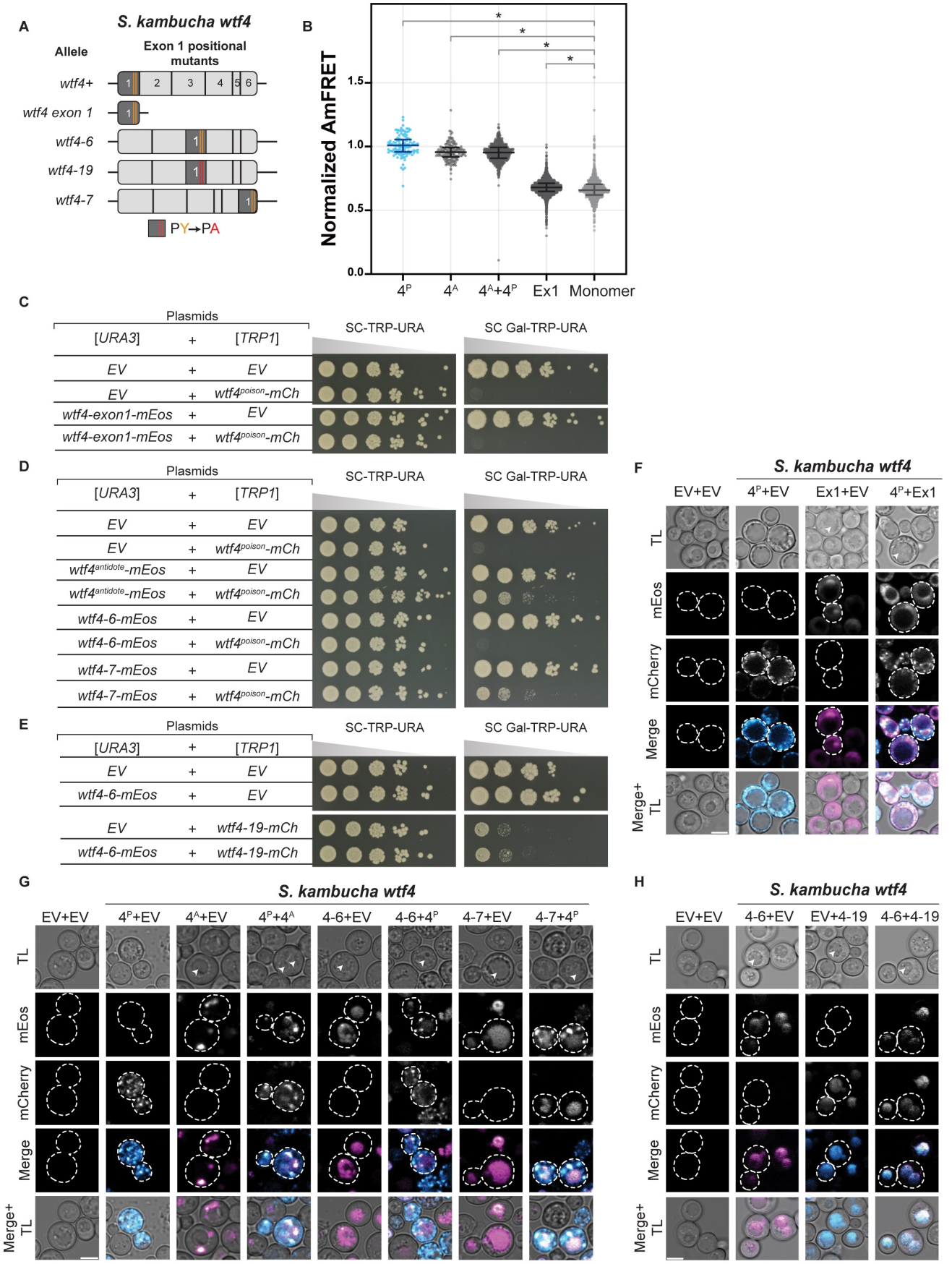
A
S. kambucha wtf4
Allele
Exon 1 positional mutants
wtf4+
wtf4 exon 1
wtf4-6
wtf4-19
wtf4-7
PY→PA
B
Normalized AmFRET
4P
4A
4A+4P
Ex1
Monomer
C
Plasmids
[URA3] + [TRP1]
SC-TRP-URA
SC Gal-TRP-URA
EV + EV
EV + wtf4poison-mCh
wtf4-exon1-mEos + EV
wtf4-exon1-mEos + wtf4poison-mCh
D
wtf4antidote-mEos + EV
wtf4antidote-mEos + wtf4poison-mCh
wtf4-6-mEos + EV
wtf4-6-mEos + wtf4poison-mCh
wtf4-7-mEos + EV
wtf4-7-mEos + wtf4poison-mCh
E
wtf4-6-mEos + EV
EV + wtf4-19-mCh
wtf4-6-mEos + wtf4-19-mCh
F
S. kambucha wtf4
EV+EV
4P+EV
Ex1+EV
4P+Ex1
TL
mEos
mCherry
Merge
Merge+ TL
G
4A+EV
4P+4A
4-6+EV
4-6+4P
4-7+EV
4-7+4P
H
4-6+EV
EV+4-19
4-6+4-19

S8 Figure

A

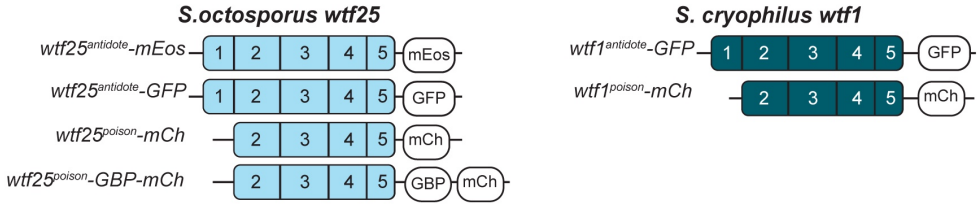

C

Plasmids [URA3]	+	[TRP1]
EV	+	EV
EV	+	wtf25poison-mCh
EV	+	wtf1poison-mCh
EV	+	wtf25poison-GBP-mCh
wtf1antidote-GFP	+	EV
wtf25antidote-GFP	+	EV
wtf25antidote-mEos	+	EV
wtf1antidote-GFP	+	wtf1poison-mCh
wtf1antidote-GFP	+	wtf25poison-mCh
wtf1antidote-GFP	+	**wtf25poison-GBP-mCh**
wtf25antidote-GFP	+	wtf25poison-mCh
wtf25antidote-GFP	+	wtf25poison-GBP-mCh
wtf25antidote-mEOs	+	wtf25poison-mCh
wtf25antidote-mEos	+	wtf25poison-GBP-mCh

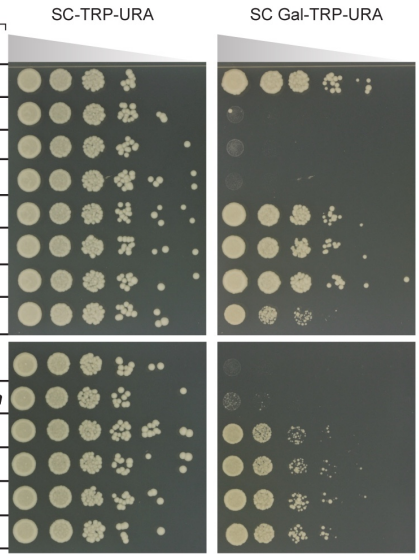

B

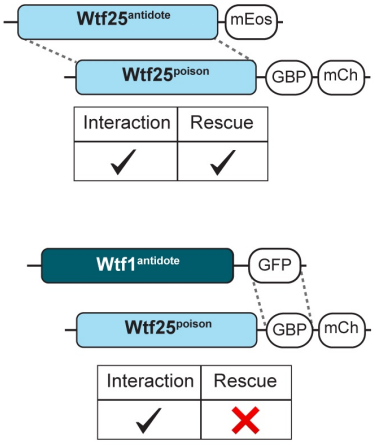

D

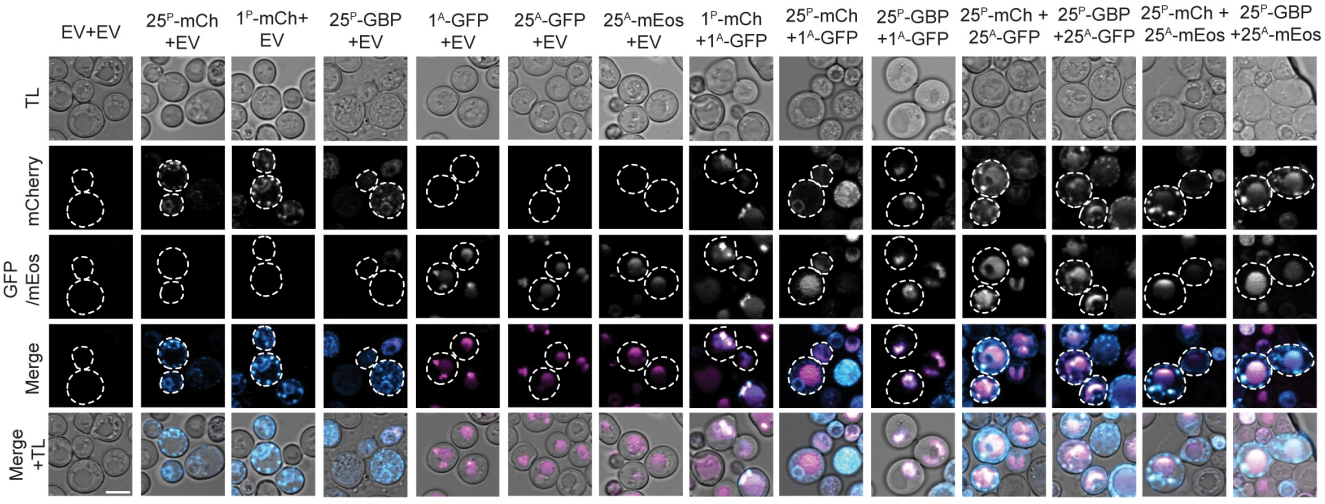

S9 Figure

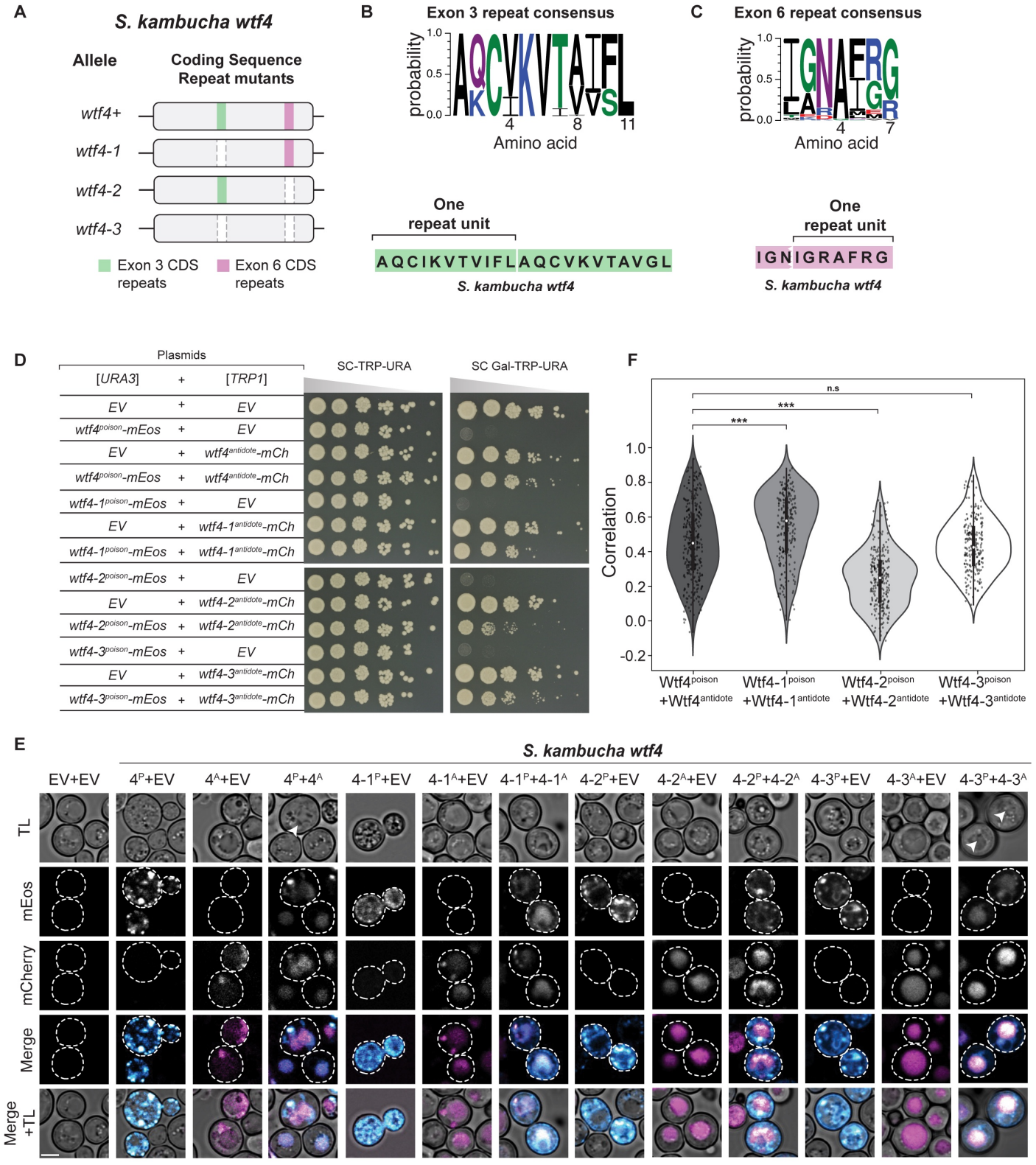
A
S. kambucha wtf4
Allele
Coding Sequence
Repeat mutants
wtf4+
wtf4-1
wtf4-2
wtf4-3
Exon 3 CDS repeats
Exon 6 CDS repeats
B
Exon 3 repeat consensus
probability
Amino acid
One repeat unit
AQCIKVTVIFLAQCVKVTAVGL
S. kambucha wtf4
C
Exon 6 repeat consensus
probability
Amino acid
One repeat unit
IGNIGRAFRG
S. kambucha wtf4
D
Plasmids
[URA3] + [TRP1]
SC-TRP-URA
SC Gal-TRP-URA
EV + EV
wtf4poison-mEos + EV
EV + wtf4antidote-mCh
wtf4poison-mEos + wtf4antidote-mCh
wtf4-1poison-mEos + EV
EV + wtf4-1antidote-mCh
wtf4-1poison-mEos + wtf4-1antidote-mCh
wtf4-2poison-mEos + EV
EV + wtf4-2antidote-mCh
wtf4-2poison-mEos + wtf4-2antidote-mCh
wtf4-3poison-mEos + EV
EV + wtf4-3antidote-mCh
wtf4-3poison-mEos + wtf4-3antidote-mCh
F
n.s
***
***
Correlation
Wtf4poison +Wtf4antidote
Wtf4-1poison +Wtf4-1antidote
Wtf4-2poison +Wtf4-2antidote
Wtf4-3poison +Wtf4-3antidote
E
S. kambucha wtf4
EV+EV
4P+EV
4A+EV
4P+4A
4-1P+EV
4-1A+EV
4-1P+4-1A
4-2P+EV
4-2A+EV
4-2P+4-2A
4-3P+EV
4-3A+EV
4-3P+4-3A
TL
mEos
mCherry
Merge
Merge +TL

S10 Figure

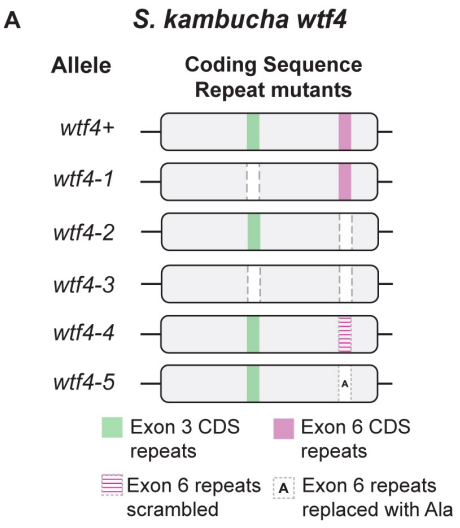
A
S. kambucha wtf4
Allele
Coding Sequence Repeat mutants
wtf4+
wtf4-1
wtf4-2
wtf4-3
wtf4-4
wtf4-5
A
Exon 3 CDS repeats
Exon 6 CDS repeats
Exon 6 repeats scrambled
Exon 6 repeats replaced with Ala

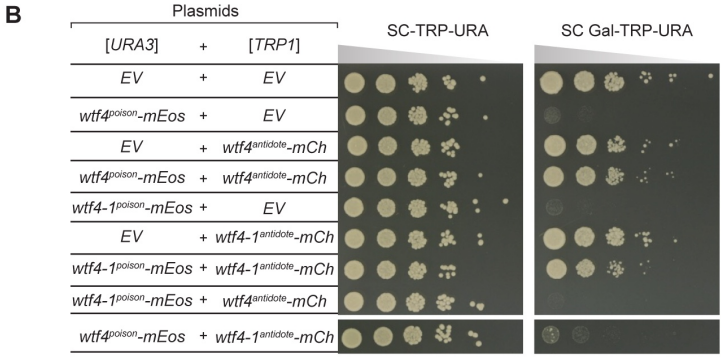
B
Plasmids
[URA3] + [TRP1]
SC-TRP-URA
SC Gal-TRP-URA
EV + EV
wtf4poison-mEos + EV
EV + wtf4antidote-mCh
wtf4poison-mEos + wtf4antidote-mCh
wtf4-1poison-mEos + EV
EV + wtf4-1antidote-mCh
wtf4-1poison-mEos + wtf4-1antidote-mCh
wtf4-1poison-mEos + wtf4antidote-mCh
wtf4poison-mEos + wtf4-1antidote-mCh

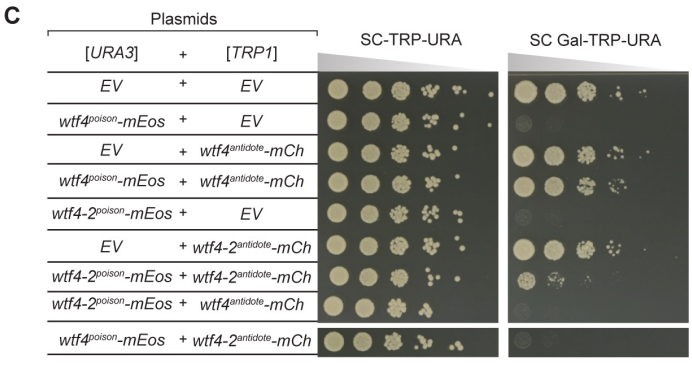
C
Plasmids
[URA3] + [TRP1]
SC-TRP-URA
SC Gal-TRP-URA
EV + EV
wtf4poison-mEos + EV
EV + wtf4antidote-mCh
wtf4poison-mEos + wtf4antidote-mCh
wtf4-2poison-mEos + EV
EV + wtf4-2antidote-mCh
wtf4-2poison-mEos + wtf4-2antidote-mCh
wtf4-2poison-mEos + wtf4antidote-mCh
wtf4poison-mEos + wtf4-2antidote-mCh

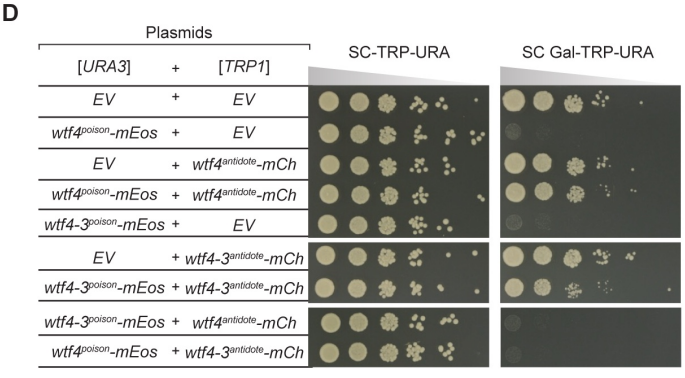
D
Plasmids
[URA3] + [TRP1]
SC-TRP-URA
SC Gal-TRP-URA
EV + EV
wtf4poison-mEos + EV
EV + wtf4antidote-mCh
wtf4poison-mEos + wtf4antidote-mCh
wtf4-3poison-mEos + EV
EV + wtf4-3antidote-mCh
wtf4-3poison-mEos + wtf4-3antidote-mCh
wtf4-3poison-mEos + wtf4antidote-mCh
wtf4poison-mEos + wtf4-3antidote-mCh

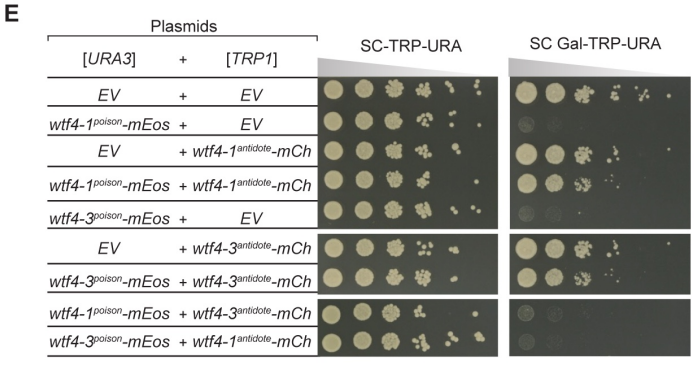
E
Plasmids
[URA3] + [TRP1]
SC-TRP-URA
SC Gal-TRP-URA
EV + EV
wtf4-1poison-mEos + EV
EV + wtf4-1antidote-mCh
wtf4-1poison-mEos + wtf4-1antidote-mCh
wtf4-3poison-mEos + EV
EV + wtf4-3antidote-mCh
wtf4-3poison-mEos + wtf4-3antidote-mCh
wtf4-1poison-mEos + wtf4-3antidote-mCh
wtf4-3poison-mEos + wtf4-1antidote-mCh

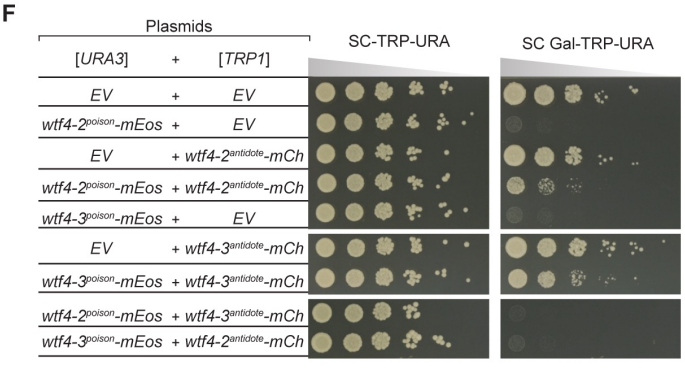
F
Plasmids
[URA3] + [TRP1]
SC-TRP-URA
SC Gal-TRP-URA
EV + EV
wtf4-2poison-mEos + EV
EV + wtf4-2antidote-mCh
wtf4-2poison-mEos + wtf4-2antidote-mCh
wtf4-3poison-mEos + EV
EV + wtf4-3antidote-mCh
wtf4-3poison-mEos + wtf4-3antidote-mCh
wtf4-2poison-mEos + wtf4-3antidote-mCh
wtf4-3poison-mEos + wtf4-2antidote-mCh

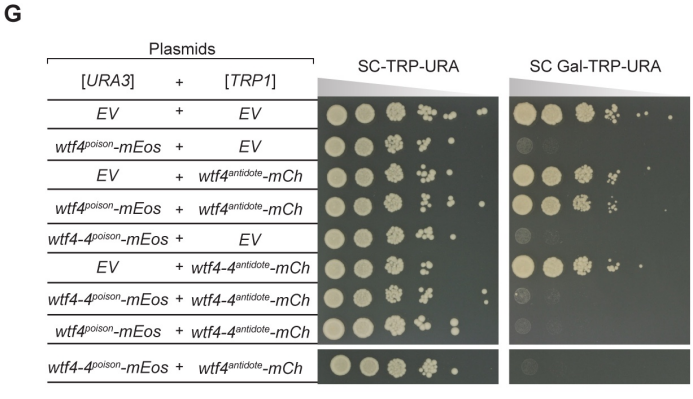
G
Plasmids
[URA3] + [TRP1]
SC-TRP-URA
SC Gal-TRP-URA
EV + EV
wtf4poison-mEos + EV
EV + wtf4antidote-mCh
wtf4poison-mEos + wtf4antidote-mCh
wtf4-4poison-mEos + EV
EV + wtf4-4antidote-mCh
wtf4-4poison-mEos + wtf4-4antidote-mCh
wtf4poison-mEos + wtf4-4antidote-mCh
wtf4-4poison-mEos + wtf4antidote-mCh

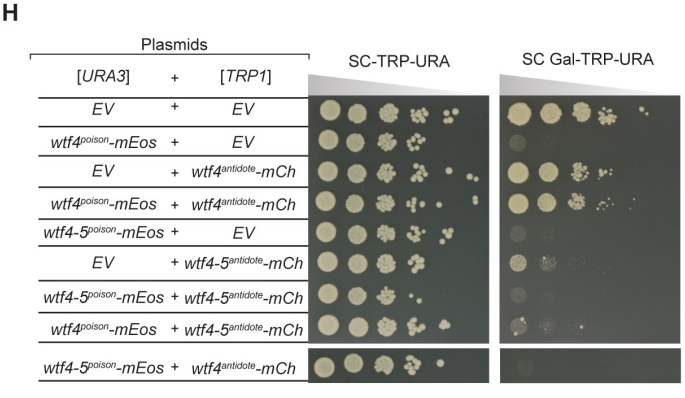
H
Plasmids
[URA3] + [TRP1]
SC-TRP-URA
SC Gal-TRP-URA
EV + EV
wtf4poison-mEos + EV
EV + wtf4antidote-mCh
wtf4poison-mEos + wtf4antidote-mCh
wtf4-5poison-mEos + EV
EV + wtf4-5antidote-mCh
wtf4-5poison-mEos + wtf4-5antidote-mCh
wtf4poison-mEos + wtf4-5antidote-mCh
wtf4-5poison-mEos + wtf4antidote-mCh

S11 Figure

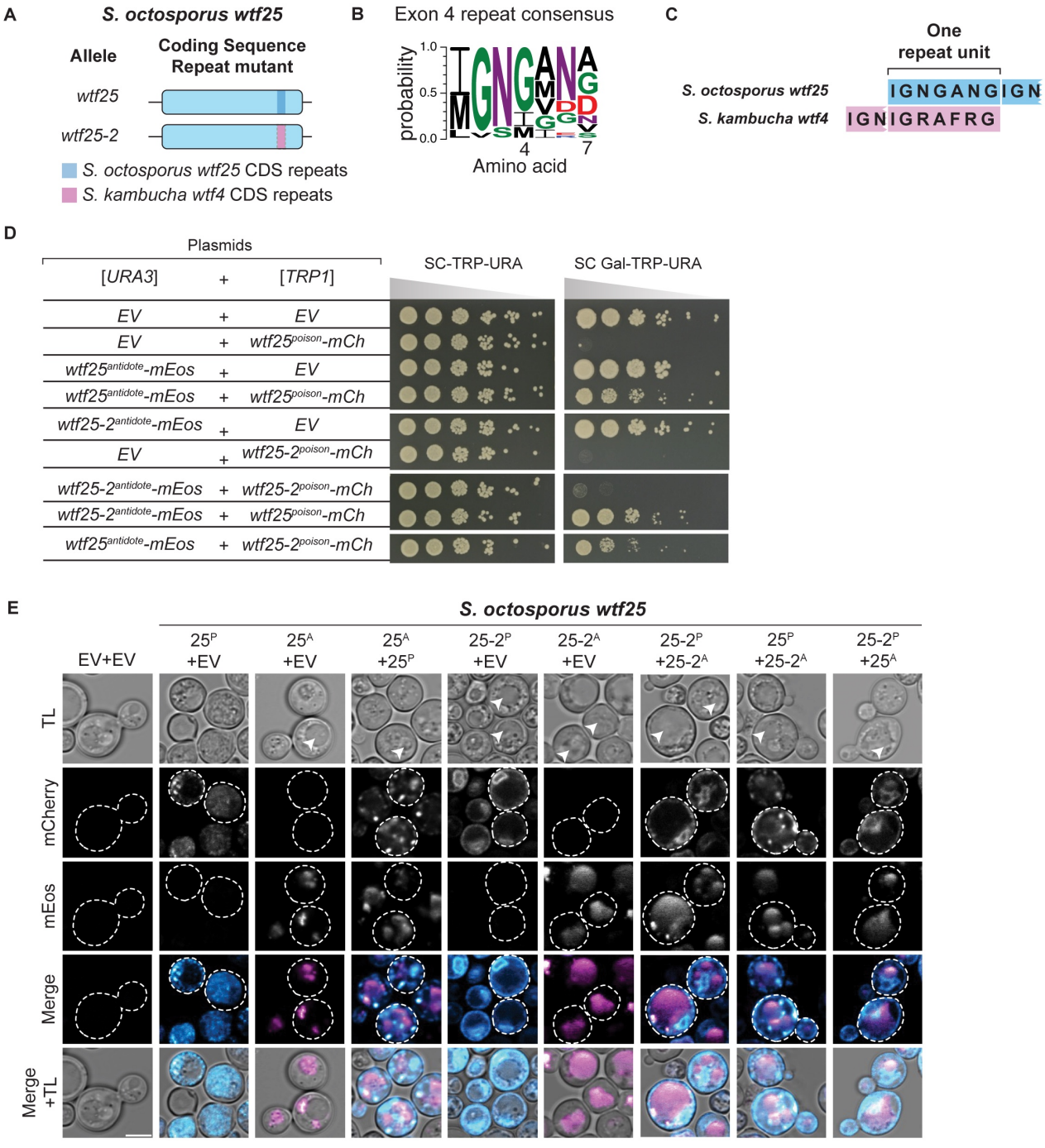
A
S. octosporus wtf25
Allele
Coding Sequence Repeat mutant
wtf25
wtf25-2
S. octosporus wtf25 CDS repeats
S. kambucha wtf4 CDS repeats
B
Exon 4 repeat consensus
probability
1.0
0.5
0.0
4
7
Amino acid
C
One repeat unit
S. octosporus wtf25
IGNGANGIGN
S. kambucha wtf4
IGNIGRAFRG
D
Plasmids
[URA3] + [TRP1]
SC-TRP-URA
SC Gal-TRP-URA
EV + EV
EV + wtf25poison-mCh
wtf25antidote-mEos + EV
wtf25antidote-mEos + wtf25poison-mCh
wtf25-2antidote-mEos + EV
EV + wtf25-2poison-mCh
wtf25-2antidote-mEos + wtf25-2poison-mCh
wtf25-2antidote-mEos + wtf25poison-mCh
wtf25antidote-mEos + wtf25-2poison-mCh
E
S. octosporus wtf25
EV+EV
25P +EV
25A +EV
25A +25P
25-2P +EV
25-2A +EV
25-2P +25-2A
25P +25-2A
25-2P +25A
TL
mCherry
mEos
Merge
Merge +TL

S12 Figure

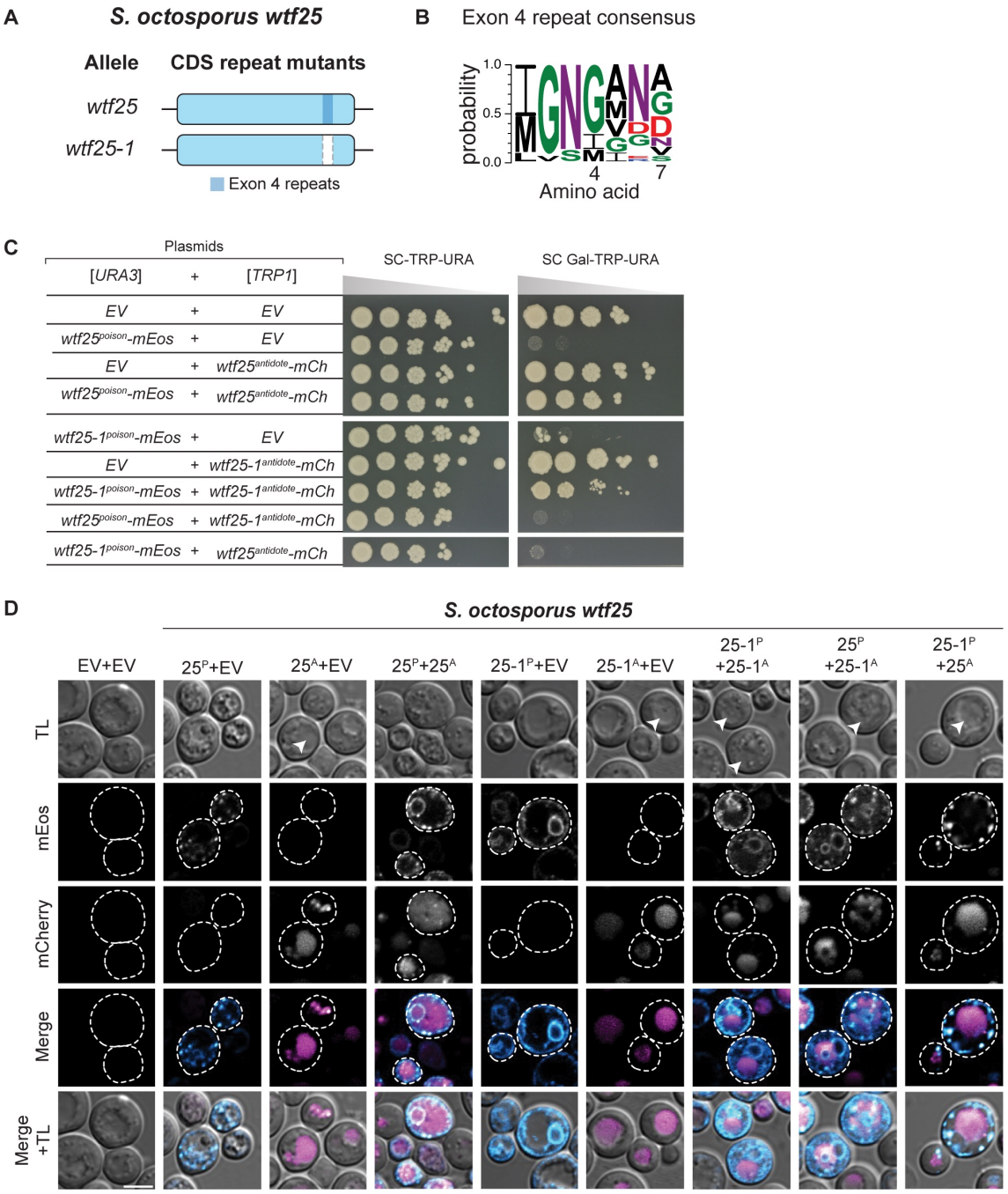
A
S. octosporus wtf25
Allele
CDS repeat mutants
wtf25
wtf25-1
Exon 4 repeats
B
Exon 4 repeat consensus
probability
1.0
0.5
0.0
4
7
Amino acid
C
Plasmids
[URA3] + [TRP1]
SC-TRP-URA
SC Gal-TRP-URA
EV + EV
wtf25poison-mEos + EV
EV + wtf25antidote-mCh
wtf25poison-mEos + wtf25antidote-mCh
wtf25-1poison-mEos + EV
EV + wtf25-1antidote-mCh
wtf25-1poison-mEos + wtf25-1antidote-mCh
wtf25poison-mEos + wtf25-1antidote-mCh
wtf25-1poison-mEos + wtf25antidote-mCh
D
S. octosporus wtf25
EV+EV
25P+EV
25A+EV
25P+25A
25-1P+EV
25-1A+EV
25-1P +25-1A
25P +25-1A
25-1P +25A
TL
mEos
mCherry
Merge
Merge +TL

S13 Figure

A

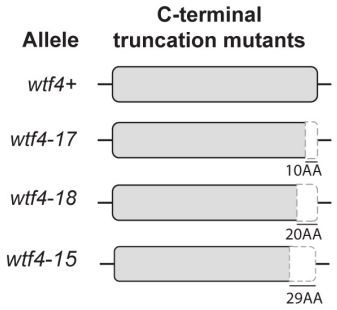

B

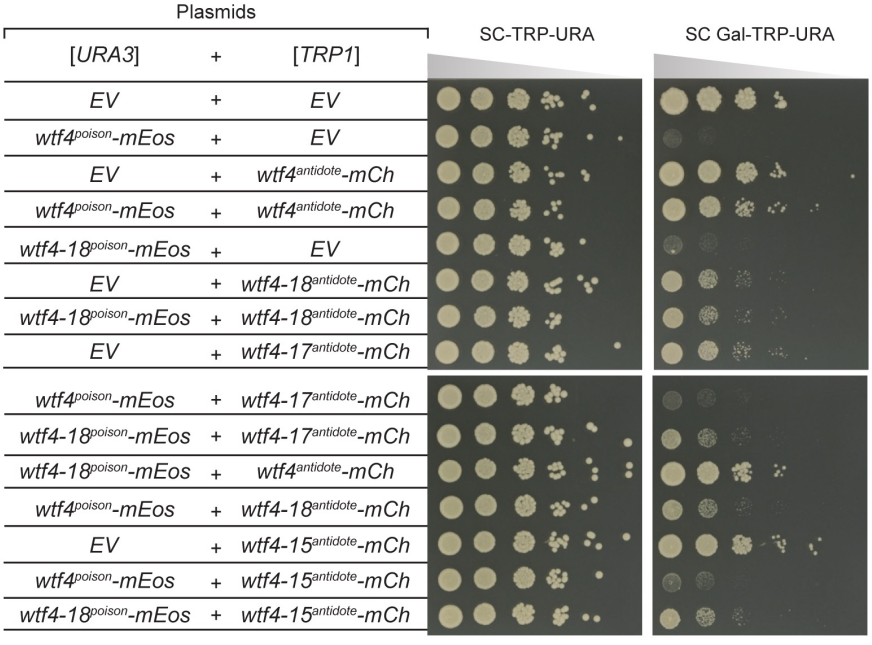

C

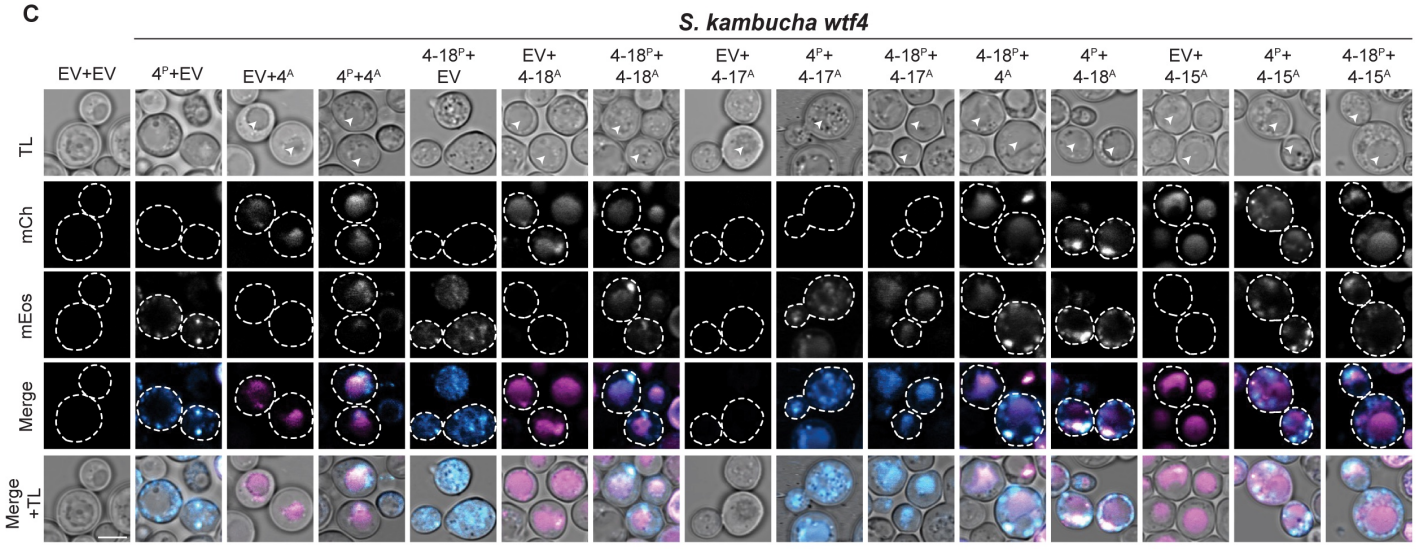

S14 Figure

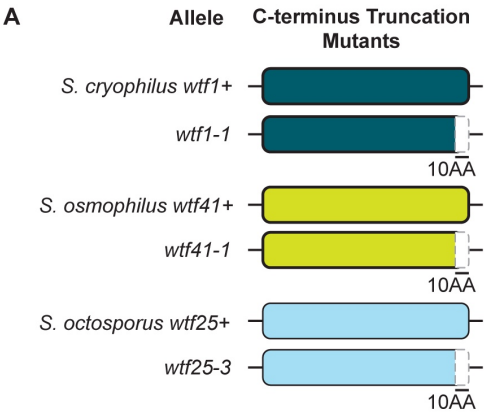
A
Allele
C-terminus Truncation Mutants
S. cryophilus wtf1+
wtf1-1
10AA
S. osmophilus wtf41+
wtf41-1
10AA
S. octosporus wtf25+
wtf25-3
10AA

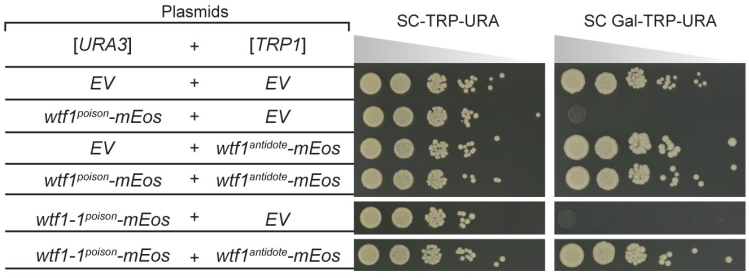
B
Plasmids
[URA3] + [TRP1]
SC-TRP-URA
SC Gal-TRP-URA
EV + EV
wtf1poison-mEos + EV
EV + wtf1antidote-mEos
wtf1poison-mEos + wtf1antidote-mEos
wtf1-1poison-mEos + EV
wtf1-1poison-mEos + wtf1antidote-mEos

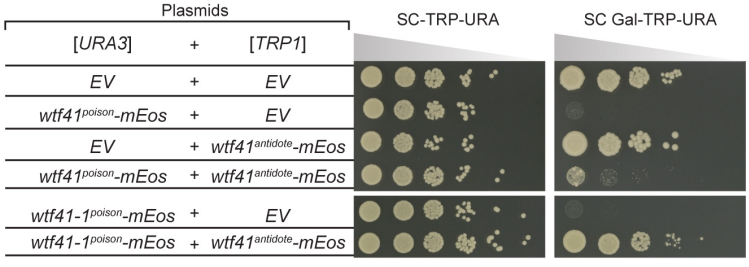
C
Plasmids
[URA3] + [TRP1]
SC-TRP-URA
SC Gal-TRP-URA
EV + EV
wtf41poison-mEos + EV
EV + wtf41antidote-mEos
wtf41poison-mEos + wtf41antidote-mEos
wtf41-1poison-mEos + EV
wtf41-1poison-mEos + wtf41antidote-mEos

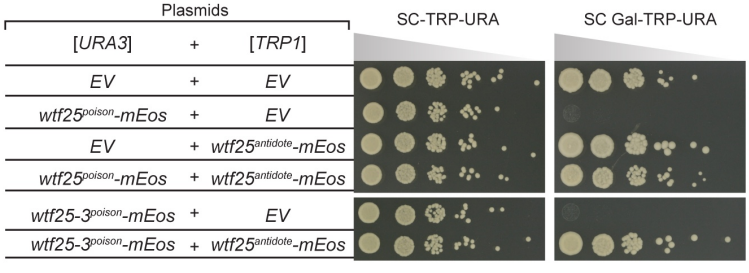
D
Plasmids
[URA3] + [TRP1]
SC-TRP-URA
SC Gal-TRP-URA
EV + EV
wtf25poison-mEos + EV
EV + wtf25antidote-mEos
wtf25poison-mEos + wtf25antidote-mEos
wtf25-3poison-mEos + EV
wtf25-3poison-mEos + wtf25antidote-mEos